Projected Changes in the Seasonality of Rainfall and Temperature over Southern Africa under low mitigation

by

Caroline Reitumetse Mfopa

(1483552)

Dessertation

Submitted in fulfilment of the requirements for the degree

Master of Science

in

Geography and Environmental Management

in the Faculty of Science, University of the Witwatersrand, Johannesburg, South Africa

Supervisor: Prof. Francois A. Engelbrecht

Co-supervisor: Dr. Dawn Mahlobo

20 October 2022

DECLARATION

I declare that this research project is my own, unaided work. It is submitted in fulfilment of the requirements of the degree of Masters of science in the field of Geography, Archaeology and Environmental studies (climate science) in the University of the Witwatersrand, Johannesburg. It has not been submitted before for any degree or examination in any other University.

20 October 2022

ABSTRACT

The single most prominent characteristic feature of southern African climate is its pronounced dry-wet seasonality, as opposed to the warm-cold seasonality that dominates climate of the high latitudes of the Northern Hemisphere. It is thought that the African savannahs, the dominant biome in southern and East Africa, evolved in the presence of fire and dry-wet seasonality over the last 10 million years. Global warming is already impacting on southern African climate, with the interior regions recording a rate of temperature increase almost twice the rate of global warming, over the last several decades. The main aim of this research was to investigate how regional climate change in southern Africa may impact on the seasonality of rainfall and temperature across the region, using the large ensemble of CMIP6 global climate model projections.

Verification of the climate models revealed that they are capable to simulate intra-annual variability (that is, the seasonal cycle) of both rainfall and temperature in southern Africa with remarkable realism. This holds true for regions with diversely different climatic regimes: the winter-rainfall region of South Africa, the larger summer rainfall region of southern Africa, and the bimodal rainfall region of East Africa. There is a single exception, namely the narrow all-year rainfall region of the Cape south coast of South Africa, where the correlation between the model simulations and observations in terms of intra-annual rainfall variability is substantially weaker than for other regions in southern Africa.

The CMIP6 ensemble projects general reductions in rainfall over southern Africa under low mitigation, with corresponding drastic increases in temperature. These results confirm the 2018 classification by the IPCC SR1.5 report, of the southern African region being a climate change hotspot: when a warm and dry region becomes even warmer and likely also drier, the options for adaptation are limited. There are some important exceptions, in terms of the general pattern of change projected by the CMIP6 ensemble. The first is the northernmost parts of southern Africa, located in the tropical savannah zone, where increases in rainfall are projected. This pattern of change relates to the expansion of the humid tropical belt in a warmer climate. The second is the eastern escarpment areas of South Africa where increases in rainfall are similarly projected, driven by an increase in specifically summer rainfall. This implies an increase in the nature of rainfall – namely more intense rainfall events in summer and an increase in the amplitude of dry-wet seasonality. For most of the southern African region, however, general drying is projected, in conjunction with drastic warming. In fact, the CMIP6 ensemble projects staggeringly large temperature increases over the interior regions of southern Africa under low mitigation relative to 1979-2014. Over large regions of the interior, and across all seasons, this change is in the order of 5 °C by the end of the century. Such drastic increases in temperature, which translates to enhanced evaporation from soils, in combination with projected reductions in rainfall effectively suggests a longer burning season, and a shorter growing season (through reductions in soil moisture). The results point to the need for the region to focus strongly on climate change adaptation actions, in addition to its efforts on fairly contribute to greenhouse gas mitigation.

ACKNOWLEDGEMENT

I would like to thank the following people and organizations for assisting in completing this research project:

My supervisor and co-supervisor from the University of the Witwatersrand's, Global change Institute (GCI), Professor Francois Engelbrecht, and Dr. Dawn Mahlobo, for their continued technical assistance in developing this manuscript.

The National Research Foundation (NRF) Earth System Science Research Programme, through Grant 118604 deals with "The Origin of Southern African Seasonality", for funding me throughout my MSc studies.

The National Research Foundation (NRF), South African Earth Observation Network (SAEON). The entire data science team, and HR team for giving me some time off from work to be able to channel my efforts towards completing this dissertation.

Jesus, for giving me supernatural strength throughout this process.

And finally, my mother, Maria Mfopa, for releasing me from all household chores during the writing and compilation process.

TABLE OF CONTENTS **PAGE**

CHAPTER 1: INTRODUCTION

CHAPTER 2: LITERATURE REVIEW

CHAPTER 3: VERIFICATION OF MODEL SIMULATIONS OF PRESENT-DAY SEASONALITY OVER SOUTHERN AFRICA

CHAPTER 4: PROJECTIONS OF FUTURE CLIMATE CHANGE OVER SOUTHERN AFRICA USING THE CMIP6 ENSEMBLE CLIMATE

LIST OF ABBREVIATIONS

AAO: Antarctic Annular Oscillation

AOGCMs: Atmosphere-Ocean Coupled General Circulation Models

AR4: Assessment Report Four

AR6: Assessment Report Six

AWI: Alfred Wegener Institute

BCC: Beijing Climate Centre

C4: Four Carbon Grass Ecosystems

CAMS: Chinese Academy of Meteorological Sciences

CAS: Chinese Academy of Sciences

CCCma: Canadian Centre for Climate Modelling and Analysis

CFS-R: Climate Forecast System Reanalysis

CH_4: Methane

CMIP5: Coupled Model Inter-comparison Project Phase Five

CMIP6: Coupled Model Inter-comparison Project Phase Six

CNRM: Centre National de Recherches Météorologiques

CO_2: Carbon Dioxide

COLs: Cut-off Lows

CRU TS4.04: Climatic Research Unit (CRU) Time-Series (TS) version 4.04

CRU: Climate Research Unit

CSIRO: Commonwealth Scientific and Industrial Research Organization

DJF: December January February

E: East

ECMWF: European Centre for Medium-Range Weather Forecasts

EEC: European Community Earth Consortium

ENSO: El Niño Southern Oscillation

ESA: Eastern Southern Africa

GCMs: Global Climate Models

GDP: Gross Domestic Product

GPCP: Global Precipitation Climatology Project

HADCRU: Met Office Hadley Centre Observations Datasets

INM: Institute for Numerial Mathematics

IPCC: Intergovernmental Panel on Climate Change

IPSL: Institut Pierre-Simon Laplace

ITCZ: Inter-Tropical Convergence Zone

JAMS: Japan Agency for Marine-Earth Science

JJA: June July August

MAM: March April May

MIROC: Model for Interdisciplinary Research on Climate

MOHC: UK Met Office Hadley Centre

MRI: Meteorological Research Institute

N: North

NCAR: National Centre for Atmospheric Research

NCC: Norwegian Climate Centre

NCEP: National Centres for Environmental Prediction

NDVI: Difference Vegetation Index

NESA: North-eastern South Africa, South Zimbabwe, and South Mozambique

NUIST: Nanjing University of Information Science and Technology

OND: October November December

RCMs: Regional Climate Models

RCP: Representative Concentration Pathway

RMSE: Root Mean Square Error

S: South

SICZ: South Indian Convergence Zone

SIOCZ: South Indian Ocean Convergence Zone

SON: September October November

SRZ: Summer Rainfall Zone

SSP: Shared Socio-economic Pathways

SSTs: Sea Surface Temperature

TTTs: Tropical-Temperate Troughs

USAID: United States Agency for International Development

W: West

WCRP: World Climate Research Programme

WRZ: Winter Rainfall Zone

YRZ: Year-Round Rainfall Zone

LIST OF TABLES **PAGE**

LIST OF FIGURES **PAGE**

LIST OF SYMBOLS

Symbol	**Name of symbol**
°C	Degree Celsius
mm	Millimeters
m	Meters
hPa	Hectopascal
>	Greater than
<	Less than
%	Percentage
°	Degrees
+	Addition/plus
CH_4	Methane
CO_2	Carbon dioxide

CHAPTER 1: INTRODUCTION

1.1 Background

Seasonality is the characteristic of a climatic time series in which the data displays troughs and peaks that reoccur periodically every calendar year, and is associated with the cycle in solar radiative forcing (Micheels et al., 2007). In the case of rainfall, seasonality is typically defined in terms of the start and end dates of the rainy and dry seasons. Seasonality in temperature is typically defined as the difference in average temperature between the hottest and coldest months of the year (Lee., 2017).

The mid and high latitudes of the Northern Hemisphere experience pronounced hot-cold seasonality, but in the subtropical landmasses of the Southern Hemisphere, including southern Africa, wet-dry seasonality is the main signature of the annual cycle in solar radiation (Engelbrecht et al., 2015a). Wet-dry seasonality may be defined as the occurrence every year of a predominantly dry season (precipitation greater than potential evaporation for at least 3 months' duration), and a predominantly wet season (precipitation greater than or close to potential evaporation for at least 3 months) (Engelbrecht et al., 2015a; Hoegh-Guldberg et al., 2019).

southern Africa can be divided into three distinctly different regions in terms of rainfall seasonality. A recent objective classification of these rainfall zones is provided by (Roffe et al., 2019), who estimated the boundaries of the summer, winter, and year-round rainfall zones. Within each of these zones, the seasonality of rainfall is more or less homogeneous. The winter rainfall region is largely confined to the south-western Cape. This is a region of pronounced dry-wet seasonality, with the rainfall peak in mid-winter (Engelbrecht et al., 2009). Along the Cape south coast, more or less between Mosel Bay in the west and East London in the east, an all-year (year-round) rainfall exists (Engelbrecht et al., 2015a). The remainder of the southern African region, here defined as Africa south as 10 °S, is a summer rainfall region.

Southern Africa is expected to grow much hotter and drier as a result of future climate change (Engelbrecht et al., 2015a; Hoegh-Guldberg et al., 2019). Climate change is expected to have an increasing impact on many sectors in southern Africa, including agriculture (Tadross et al., 2005), water security, human health (Garland et al., 2015), vector-borne disease spread (Mabaso et al., 2007), tourism (Fitchett et al., 2017), and conservation. If climate change has a significant influence on climatic seasonality in southern Africa, particularly through variations in rainfall and temperature, it might have far-reaching repercussions in a variety of industries (Van Wilgen et al., 2016).

This research seeks to investigate changes in the seasonal cycle of rainfall and temperature in southern Africa, by making use of a large ensemble of climate model projections. The models are first verified in terms of their ability to represent present-day seasonality before they are applied to obtain projections of change in the near-term (2021-2040), mid-term (2041-2060), and long-term (2081-2099).

1.2 Seasonality and the southern African landscape

The occurrence every year of a predominantly dry season is a dominant feature of the present-day climate in southern Africa. Wet-dry seasonality began in southern and East Africa within the past 10 Ma (ten million years) (Archer., 2017). This wet-dry seasonality is fundamentally different from the much better-studied hot-cold seasonality which dominates the climate and ecology of high latitude and is caused by the inclination of the Earth's axis relative to the plane of the orbit around the sun (Engelbretch et al., 2015).

Wet-dry seasonality over the millions of years had a pronounced influence on the southern African biomes. The regular occurrence of a dry season long enough to force plants to adopt xerophytic strategies, coupled with a wet season long enough to generate significant production and thus fuel loads - but not long enough to support a closed cover of mesophytic trees - is correlated with the occurrence of savannahs - mixed tree and C4 (4 carbon) grass ecosystems- in the Southern Hemisphere (Archibald et al., 2009). New guilds of plants, herbivores, and carnivores evolved into this novel ecosystem. Given the strong correlation between wet-dry seasonality and contemporary savannah distribution, it is critical to understand how future climate change may impact this seasonality of climate (Brooke., 2014). It may be noted that dry-wet seasonality does not exist as a function of axial tilt alone, since the tilt has existed for billions of years with minor variation (and yet dry-wet seasonality is a relatively recent feature) (Engelbretch et al., 2015).

Of particular importance in this regard, is the seasonality of future fire regimes in southern Africa. Currently, wet-dry seasonality favours a pronounced fire season in southern Africa during the dry season, with implications for the delicate balance between trees, grasses, fire, and CO_2 in the savannahs (Archibald et al., 2009). Changes in seasonality, for example, a longer dry season associated with higher temperatures; (Engelbretch et al., 2015) may favour a longer and more intense meteorological fire season in the savannahs, with implications on both biodiversity and agriculture.

1.3 Study area

In terms of latitude, Africa's position is relatively unique in that it has near mirror images of climate zones north and south of the equator (Africa’s Climate Report., 2016). Africa's six major climate zones are; equatorial, humid tropical, tropical, subtropical, Mediterranean, and desert (Murumbwa., 2019). The following prominent factors influence the climate of various locations on the African continent (Figure 1): latitude, altitude, distance from the sea, prevalent pressure belts (atmospheric circulation), and the effect of ocean currents (Quagraine., 2019). The tropical savannah climate region is located 15° to 20° north and south of the equator, with the subtropical savannahs stretching from about 20° to 30° north and south. The subtropical high-pressure belt is a prominent feature of these latitudes in winter that produces pronounced dry-wet seasonality. In subtropical North Africa, the Sahel is an important transition zone between the tropical savannahs to the south and the African Sahara Desert to the north, the intertropical convergence zone (ITCZ), which advances north into the Sahel during the boreal winter, is responsible for the Sahel's rainfall (Murumbwa., 2019).

The humid tropical region lies between the equatorial and tropical savannahs (Jury et al., 2013). This region has year-round rainfall, but it is heaviest in the summer about the position of the ITCZ. Temperatures are high given the tropical location. The Mediterranean climatic region of North Africa is located between 30° and 40° north and south of the equator (Dedekind et al., 2016), and in southern Africa is limited to the south-western Cape region (Murumbwa., 2019) Winter rainfall brought on by cold fronts characterizes this region. Finally, the desert regions are located between 18° and 36° north and south of the equator in the western parts of the southern African continent, but across the Sahara in North Africa (Lee., 2017). This region's climate is characterized by subtropical highs in both summer and winter, and it is strongly influenced by the cold Canary and Benguela currents.

This research project is focused on seasonality in southern Africa, here defined as Africa south of 10 °S, following (Engelbrecht et al., 2009). This region is surrounded by oceans, with the Atlantic Ocean with the cold Benguela current to the west, the Indian Ocean with hot Agulhas current to the east, and the Southern Ocean to the south. Topographically, the region is characterized by a broad plateau, with a generally narrow coastal plain. The southern and eastern escarpments are steep, with mountain peaks of the Drakensberg in the east reaching altitudes of more than 3000 meters. In the west, the Cape Fold Mountains stretch from the south to the north, merging into the western escarpment. The coastal plain broadens significantly in Mozambique (Dedekind et al., 2016).

Most of southern Africa is located in the subtropics and is constantly influenced by subtropical highs, notably the South Atlantic and South Indian Anticyclones (Preston-Whyte & Tyson., 1988; Mahlobo et al., 2018; Roffe et al., 2019). southern Africa has a mainly continental climate, with cold and dry winters and hot, wetter summers, due to the interplay of various weather systems and orography. The region, in other words, has a distinct dry-wet seasonally. Very large portions of central and western southern Africa are classified as semi-arid (Engelbrecht & Engelbrecht., 2016), with wetter climates prevailing in the east, resulting in a general west-east gradient in rainfall (Preston-Whyte & Tyson., 1988; Dedekind et al., 2016). Along the most northern edges of the study domain, wetter climates prevail under the direct influence of ITCZ (Engelbrecht et al., 2009). Over the most southern edges of the domain, along the South African west and south coasts, weather systems from the mid-latitudes prevail resulting in winter rainfall (Preston-Whyte & Tyson., 1988; Wolski et al., 2018).

1.4 Seasonality of southern African climate

As mentioned southern Africa is characterized by three prominent rainfall zones, namely a summer rainfall zone, winter rainfall zone, and the all-year rainfall zone (Engelbrecht et al., 2015a; Roffe et al 2019). These regions exist as a result of their distinctive geographical location in southern Africa (Roffe et al., 2019).

Due to the strong subsidence that prevails over most of subtropical southern Africa in winter, which occurs in association with the ITCZ being displaced to the north of the equator, winters are generally dry and sunny (Mahlobo et al., 2018). Southern Africa is consequently largely a summer rainfall region (Engelbrecht et al., 2009; Jury et al., 2013). About 80% of the region’s rainfall occurs in the form of thunderstorms, which often form within tropical-temperate cloud bands that link the tropics to the oceanic regions of South Africa (Hart et al., 2013). The majority of the rain falls from December to February when the ITCZ reaches the southern African areas, at times as far south as central Zimbabwe (Preston-Whyte & Tyson., 1988; Jury et al, 2013; Nicholson., 2020).

Southern Africa’s winter rainfall region is confined to the most southern parts of South Africa, where mid-latitude cyclones sweep through and the subtropical highs are not blocking their movement (Bates et al., 2008). These systems reach their equator-most latitudes during the winter months of June to August, and that is when the bulk of winter rainfall occurs (Jury et al., 2013; Roffe et al., 2019). South Africa’s winter rainfall region is confined to the south-western Cape, but frontal rainfall also occurs along the Cape south coast, which is an all-year rainfall region (Engelbrecht et al., 2015a).

The all-year rainfall region also receives rainfall in summer, autumn and spring, with small bimodal peaks in autumn and spring (Engelbrecht et al., 2015a; Roffe et al., 2019). These rainfall peaks have been shown to occur in association with peaks in the frequencies of cut-off low-pressure systems and ridging highs (Favre et al., 2013; Engelbrecht et al., 2015a).

There are several methodologies available through which southern Africa’s summer, winter, and all-year rainfall regions can be identified objectively, although the different methodologies result in slightly different geographical regions being associated with the main rainfall zones (Roffe et al., 2019). Three widely applied methodologies are the delineation of rainfall regions are discussed by (Engelbrecht et al., 2015a) and involve the metrics of the ratio of the month of minimum rainfall to the month of maximum rainfall, the number of months for which the mean monthly rainfall total contributes 5% or more to the mean annual rainfall and the average fluctuation of monthly rainfall from the monthly mean rainfall. Most recently, (Roffe et al., 2020) demarcated rainfall regions using a metric formulated in terms of percentile-based wet-season start- and end dates for southern Africa.

1.5 Inter-annual variability

Although the focus of this research is on the long-term changes in the seasonality of southern Africa’s climate, within the context of continued global warming, it is important to note that the region is characterized by pronounced inter-annual rainfall variability. The main driver of this variability is the El Niño Southern Oscillation (ENSO), with El Niño events typically causing below-normal summer rainfall, and La Nina events typically causing above-normal rainfall (Malherbe et al., 2016; Gore et al., 2020). Links between the global modes of variability (such as ENSO) to rainfall variability over the winter and all-year regions are significantly weaker (Engelbrecht & Landman., 2015). Regional sea-surface temperatures play a secondary role in inter-annual rainfall variability in southern Africa (Hoell et al., 2017).

1.6 Future climate change

In a future climate where increasing levels of CO_2 and other greenhouse gasses are projected to lead to continued global warming, it is plausible to expect that changes may occur in rainfall, temperature, and fire seasonality over South Africa. In fact, given that global warming is estimated to have already reached a value of 1.1°C for the period 2011-2020 relative to a pre-industrial baseline (Lee., 2017), climate change can already be detected also in South Africa (Kruger & Nxumalo., 2016). The availability of homogeneous time-series data spanning periods of 30 years or longer is limited in many southern African countries, however, and this constrains the identification of trends that may already have occurred in climate and its seasonality. Annual temperatures are rising drastically in the interior regions of southern Africa, at about twice the global rate of temperature increase (Engelbrecht et al., 2015b). (Kruger & Nxumalo., 2016) reached a similar conclusion for the western and eastern interior regions of South Africa but found somewhat smaller trends over the central interior regions. The analysis of seasonal trends showed that in general temperature trends are the strongest in summer, followed by autumn, winter, and spring.

Unlike temperature trends, rainfall trends in South Africa are in general not locally statistically significant, as pointed out by (Akinsanola et al., 2017). Annual rainfall totals show statistically significant trends only over the Karoo region stretching from the eastern part of the Western Cape interior to the western part of the Eastern Cape interior (positive trends) and over the northern parts of the Limpopo Province (negative trends). In the former case, the annual trends are largely driven by increases in summer precipitation, and in the latter case largely by decreases in autumn precipitation (Kruger & Nxumalo., 2017).

As global warming strengthens it is expected that the climate change signal over southern Africa will strengthen and that the region will become generally drier (even under high mitigation measures) (Niang et al., 2014; Engelbrecht et al., 2015b; Hoegh-Guldberg et al., 2019). Such a change is likely to occur in association with the strengthening of the Hadley Cell over southern Africa, and consequently, with continued drastic increases in the regional temperatures (Engelbrecht et al., 2009; Engelbrecht et al., 2015b; Bates et al., 2008).

These changes in regional circulation may lead to changes in the seasonality of climate. For example, over the summer rainfall region of South Africa, the onset of rainfall may occur later due to the enhanced subsidence of a stronger Hadley Cell. Further to the north, over

Mozambique, climate change may result in a lengthening of the “tropical cyclone season”, potentially with the landfall of systems both earlier and later in the season. Existing studies have already indicated that changes in tropical cyclone tracks and frequencies are likely above the southwest Indian Ocean (Malherbe et al., 2013; Tadross et al., 2005). Over the most southern parts of South Africa, on the other hand, the winter rainfall season may become shorter due to the poleward displacement of cold fronts (Engelbrecht et al., 2013). Of particular importance, in this case, are increases in the length of the burning season and decreases in the length of the growing season (Engelbrecht et al., 2015b).

The main aim of this research endeavour is to assess how the seasonality of rainfall and temperature may change in southern Africa as global warming continues (as a function of different climate change mitigation scenarios). Projected changes in the occurrence of seasonality over South Africa under climate change are available from dynamic global climate models (GCMs) and regional climate models (RCMs). These models have become the main tools towards understanding how the Earth System is likely to respond to increased anthropogenic forcing (primarily through the continued emission of CO_2 into the atmosphere). The latest global projections of future climate change are those of the Coupled Model Inter-comparison Project Phase Six (CMIP6) and will form the baseline data set for the research to be undertaken. The CMIP6 simulations of seasonality over southern Africa will be verified against observations, followed by an analysis of the CMIP6 projected changes in seasonality.

1.7 Aim and Objectives

1.7.1 Aim

This research aims to assess how future climate change may impact dry-wet seasonality in southern Africa under low mitigation, through the use of objective model projections of future climate change.

1.7.2 Objectives

a) To statistically analyse how climate change may impact the seasonal cycle of temperature over southern Africa using multi-model ensemble projections of future climate change.
b) To statistically analyse how climate change may impact the seasonal cycle of rainfall over southern Africa using multi-model ensemble o projections of future climate change.

The focus of the research is on low mitigation futures, given that these present the greatest risks to the southern African environment and society. The southern Africa region is highly vulnerable to the impacts of anthropogenic induced climate change. The area has an economy which is sustained by subsistence farming and relies heavily on rain fed crops, in a climate system that exhibits such a great deal of variability. As such, this research is important because it allows us to be able to prove the reliability of future climate simulations, to provide a background for planning and mitigation measures

1.8 Structure of the report

The subsequent chapter is the literature review, where an in-depth review of previous studies on seasonality and changing seasonality in southern Africa is presented. In Chapter 3 the CMIP6 model simulations will be verified against observations, to determine their ability in representing the present-day seasonality of southern Africa. Chapter 4, deals with the CMIP6 model projections of changes in rainfall and temperature in southern Africa. Finally, we will be closing with key findings and the conclusion of the study in chapter 5.

CHAPTER 2: LITERATURE REVIEW

2.1 Introduction

The southern African climate is affected by four major components (Davis-Reddy & Vincent., 2017). Firstly, the subcontinent's position in relation to the southern hemisphere's principal circulation patterns (quasi-stationary high-pressure systems) (Nicholson., 2000). Secondly, the Inter-Tropical Convergence Zone (ITCZ) movement has an impact on the timing and intensity of rainfall (Davis-Reddy & Vincent., 2017). Thirdly, peaks in the Drakensberg which exceed 3000 m in altitude (Nicholson., 2000). Finally, influence by the hot Indian Ocean in the east coast, and by the cold Atlantic Ocean in the west coast, resulting in increases/decreases in rainfall received over the region (Nicholson., 2000).

The southern African region has two distinct rainfall seasons (Tyson & Preston-Whyte., 2000). There is a wet season in the summer season, from November to March, and a dry season in the winter, from April to October (Tyson & Preston-Whyte., 2000). Rainfall for this region is highest in the tropics around the equator, where it reaches a maximum of 3100 mm annually (Akinsanola et al., 2017). Tropical cyclones occasionally make landfall on the shores of Mozambique and South Africa, causing rain and flooding in Mozambique, northern South Africa, western Madagascar, and Zimbabwe (Akinsanola et al., 2017). The southern African regions has a semi-arid climate, with a bulk of the region receiving average annual temperatures of more than 17°C (Davis-Reddy & Vincent., 2017).

The predominant rainy season in southern Africa is during the austral summer (October to March) (Richard et al., 2001), except for a few countries in southwest Africa and certain southern African coastal locations. Furthermore, the late summer season (January – March) accounts for more than 40% of the yearly total rainfall received by the region, except for a few isolated areas in South Africa's Lowveld (Hoegh-Guldberg et al., 2019).

Throughout the years, variations in the southern African rainfall were caused by changes in solar insolation and the Hadley cell's north-to-south movement (Mahlobo et al., 2018). During the summer season moisture is brought from the Southwest Indian Ocean and the hot Agulhas Current, while winter brings dry air from the South Atlantic Ocean and the cold Benguela Current (Jury et al., 2013).

The intensity and extent of climate signals within a specific region can be determined by conducting regular examinations of previous and anticipated regional climate trends. Regular investigations of historical and anticipated regional climate patterns are useful in identifying the size and the scope of climate signals within a specific region (Dedekind et al., 2015). Regular explorations into past and projected trends of regional climate are informative in determining the magnitude and extent of climate signals within any given region. Global climate observations, reanalysis, and coupled numerical models are constantly improving, One-third of Africans live in arid regions, which are vulnerable to climatic change impacts which are harmful to their health. As a result, it is critical to correctly understand and predict climate patterns.

In this chapter, we will be discussing various literature studies that have researched the seasonality of temperature and rainfall in the southern Africa region. Firstly, starting with understanding southern Africa's climate landscape and its synoptic overview. Secondly, the effects of dry and wet seasonality on the sub-continents climate. Followed by model performance in projecting future climate and the biased related. Lastly, we will be looking at the effects of climate change at different rates of warming and the related threats.

2.2 Regional climate overview

The Southern African region incorporates ten African countries namely: Angola, Botswana, Lesotho, Malawi, Mozambique, Namibia, South Africa, Swaziland, Zambia, and Zimbabwe. These countries span over four different climate zones. The first climate zone we will be discussing is the South-western dry climates, followed by the Central/South-eastern hot temperate climates with dry winters and hot summers; and the Tropical Savannah, and lastly the tropical Coastal, coastal climates (Africa's Climate Report., 2016).

In terms of latitude, Africa's position is relatively unique in that it nearly mirrors the climate zones to the northern and southern regions from the Equator (Tyson & Preston-Whyte., 2000). To the north and south of the equator, Africa's six major climate zones are; equatorial, humid tropical, tropical, semi-desert (Sahel), Mediterranean, and desert (Africa's Climate Report, 2016). The following prominent factors influence the climate of various locations on the African continent: latitude, altitude distance from the sea, prevalent pressure belts, and the effect of ocean currents (Nicholson., 2000). The tropical savannah climate region is located 15° to 20° N and S of the equator, is characterized by subtropical high-pressure cells over the region in winter, and is primarily a summer rainfall region prone to droughts and tornadoes (Africa's Climate Report., 2016). A tropical rainforest climate, humid tropical climate or equatorial climate is a tropical climate sub-type usually found within 10 to 15 degrees' latitude of the equator (Kruger & Nxumalo., 2017). The intertropical convergence zone (ITCZ) moves north in this region, resulting in summer rainfall, primarily due to a continental effect (Kruger & Nxumalo., 2017).

The humid tropical region lies between the equatorial and tropical savannahs (Africa's Climate Report., 2016). This region has year-round rainfall, but it is heaviest in the summer (Jury et al.., 2013), and because of its tropical location, it has high temperatures. The Mediterranean climatic region is located between 30° and 40° N and S of the equator (Africa's Climate Report., 2016). The Mediterranean region is located on the African continent's northern and southernmost margins. Winter rainfall brought on by cold fronts characterizes this region (Africa's Climate Report., 2016). Finally, the dessert region is located between 18° and 36° north and south of the equator. This region's climate is characterized by a subtropical high-pressure zone, and it is located in the cold Canary and Benguela Currents (Kruger & Nxumalo., 2017). See figure 1 below outlining Africa's climate regions (figure 1.1).

2.3 Southern Africa Rainfall Regions

The duration and intensity of rainfall throughout the summer and winter seasons in southern Africa are critical in agricultural productivity and water resource management (Roffe et al., 2020). While there are several definitions for the rainfall season's start and end dates, majority of them rely on threshold values chosen for local-scale applicability (Roffe et al., 2019).

During the austral winter months (June–August), the subtropical high-pressure system is positioned over southern Africa, imposing large-scale subsidence thus causing rainfall (Dedekind et al., 2015). This high-pressure belt blocks cold front, preventing it from sweeping across larger areas of the subcontinent (Dedekind et al., 2015). Only the south-western Cape and the Cape south coast of South Africa receive winter rains during JJA (June, July and August) months The high-pressure band shifts southward during summer, while a broad continental trough deepens at lower altitudes (Jury et al., 2013).

Southern Africa receives majority of its rainfall throughout the summer half of the year (October to March) (Tyson & Preston-Whyte., 2000). During sprig, tropical-temperate troughs (TTTs) generate the majority of the rain (about 60%) (Harrison., 1984). The cut-off low is another important rain-producing mechanism (D'Abreton., 1996; Taljaard, 1996). Despite being characterized as upper westerly cold-core depressions that develop to generate closed circulations extending to the surface, these systems get the majority of their moisture from the tropics (D'Abreton., 1996; Taljaard., 1996).

COLs are powerful rain-and-flood-producing systems that commonly occur across South Africa's central interior, as well as the south and east coastlines. They're most frequent throughout the transitional seasons of Autumn and spring (Tyson., 1986).

Southern Africa contains the eastern escarpment which is about 3 kilometres in height in Lesotho's Maluti Mountains (Engelbrecht et al., 2002). The eastern escarpment, which receives a bulk of rain each year, is susceptible to convection rainfall. This is caused by complex mesoscale circulation patterns that arise across the region as a result of synoptic-scale circulation forcing and the topographical driving force (Tyson., 1986).

2.3.1 Winter Rainfall Zone

The winter rainfall zone is located southwest of southern Africa's southernmost region (Roffe et al., 2019), which is 30 degrees south of the equator, making it the southern hemisphere's smallest rainfall zone (Roffe et al., 2020). From April to September, the winter rainfall zone is dominated by frontal produced rainfall systems brought on by westerly derived mid-latitude storms.

2.3.2 Summer Rainfall Zone

The summer rainfall zone, which spans the interior and eastern sections of the southern Africa region, receives predominantly convective rainfall from October to March (Crétat et al., 2012). As a result, the southern Africa region is mostly a summer rainfall zone (Engelbrecht et al., 2009; Jury et al., 2013). Thunderstorms account for around 80% of the region's rainfall, and they frequently originate inside tropical-temperate cloud bands that connect the tropics to southern Africa's maritime areas (Roffe et al., 2019). When the ITCZ reaches the southern African region, sometimes as far south as central Zimbabwe, the majority of the rain in this zone, falls between December and February (Preston-Whyte & Tyson, 1988; Jury et al., 2013; Nicholson, 2020).

2.3.3 All-Year Rainfall Zone

Summer, winter, autumn, and spring provide rain to the all-year rainfall zone, with a slight bimodal maximums during autumn and spring (Roffe et al., 2019). The frequency of cut-off low-pressure systems and ridging highs have been shown to coincide with these rainfall peaks (Favre et al., 2013; Engelbrecht et al., 2015a). The Cape south coast of South Africa and Madagascar's eastern area have year-round rainfall (Kruger & Nxumalo., 2017).

The Cape south coast is located to the east of the Western Cape's coastline area. Cold fronts, west-wind troughs, cut-off lows (COLs), and ridging high-pressure systems are all mid-latitude weather patterns that bring rain to the Cape south coast (Roffe et al., 2020). According to (Engelbrecht et al., 2015a), ridging high-pressure systems account for 46% of annual rainfall, tropical–temperate troughs for 28%, and cut-off lows (COLs) associated with ridging highs and tropical–temperate troughs account for 16% of the annual rainfall total in this region.

Furthermore, COLs have been linked to large rainfall occurrences along the Cape south coast area in South Africa. The October rainfall peak is connected to ridging high-pressure systems from the southwest, tropical–temperate troughs, and high-pressure systems southeast of the subcontinent (Roffe et al., 2020).

2.4 Rainfall trends

(Jury et al., 2013) examined the observed and anticipated changes in the climate of southern Africa between 1900 and 2100. Changes in surface air temperature, rainfall, air pressure, winds, ocean currents, and sea surface height were investigated using ten observed, reanalysed, and model-simulated climatic data sets. The assessment of two coupled model simulations (IPSL, MIROC) based on the A1B emission scenario was based on the investigation of geographical and temporal climate trends from historical data.

Rainfall patterns in the ECMWF, GPCP, and model data sets were inconsistent and mainly negative throughout maritime latitudes (35–40°S) south of Africa. Over the Congo, the NCEPe and GPCP trends were downward, while the ECMWF and CFS-R trends were upward (Jury et al., 2013). In the equatorial West Indian Ocean, all data sets showed increasing trends, whereas NCEPe and model simulations predicted growing rainfall in the mid-latitudes. Over the tropical Atlantic Ocean, the ECMWF and CFS-R rain trends were upward, as were IPSL and MIROC A1B models (Jury et al., 2013). The GPCP data set revealed a diminishing trend over Madagascar, which was confirmed by the CFS-R data, whereas the ECMWF data showed a declining rainfall trend in eastern South Africa (Jury et al., 2013). Except for the wet (north) and dry (south) trend pattern, there was limited consensus among the various data sets about rainfall (Jury et al., 2013).

There was an overall drop of -0.6 mm/day and much higher inter-annual variability when the model simulated and predicted rainfall over southern Africa (Jury et al., 2013). Even though rainfall trends were limited in many data sets throughout the satellite period due to a drought in the early 1980s, the IPSL simulation showed a substantial decrease of 0.013 mm/day in the annual rainfall trend over the region (Jury et al., 2013). This will cause stress in water resources availability, necessitating adaptation and conservation techniques such as relocating agriculture to higher land and enhancing water usage and recycling, as proposed in the previous study. One of the most important findings stated here is that observed trends are consistently lower than model estimates, except coastal sea level, which translates to beach recession implications (Jury et al., 2013).

2.5 Temperature trends

Across the previous two decades, research on historical climate trends has steadily increased, and great progress has been achieved in understanding climate change over southern Africa (Tyson & Preston-Whyte., 2000). Over the last century, observational data have shown signs of a changing global climate. Since 1880, the global average annual temperature has risen by 0.85°C (IPCC., 2021), and this trend is expected to continue under low SSP mitigation scenarios (IPCC., 2021). Climate change governance will be supported by continued monitoring through extended observational networks across the continent. Degree temperature increases are not uniform/standard across the southern Africa region, with some areas experiencing more change than others. Over the Western Cape, the biggest trend, of 3°C per century, is observed (IPCC., 2007). The temperature rate of heating in the Northern Cape and Limpopo province of South Africa is 2°C per century (IPCC., 2007).

According to the (IPCC., 2021), since 1960, the annual temperature increased by 1.5°C. Southern Africa has experienced significant temperature increases, with more pronounced surges within the dry inland areas of the sub-continent (Hoegh-Guldberg., 2019). Across all seasons, both maximum and minimum daily temperatures have increased. Temperature extremes have also increased dramatically in number (e.g. heat waves, field fire, vector borne disease, drought etc.) (IPCC., 2021). Notably, the pace of temperature change has varied, with the largest rates of temperature increases recorded from the mid-1970s to the early 1980s, and then again from the late 1990s to the mid-2000s. Furthermore, since 1901, 2019 holds the record for the year with the highest mean annual temperature in southern Africa (IPCC.,2021).

Across all data sets, changes in surface air temperature were positive, and they were more significant in recent years (Jury et al., 2013). Over the twentieth century, the NCEPe and NCDC heating trends were +0.01 °C/year (comparable to HADCRU), with the lowlands and marine environment warming the most. In the second half of the twentieth century, both the ECMWF and CFS-R data sets indicated quicker heating in the sub-tropical Indian Ocean, southern Congo, and the coastal plains (+0.03 °C/year), and weaker trends in the South Atlantic mid-latitudes (Jury et al., 2013).

For the period 1900–2100, IPSL and MIROC model simulations indicated rapid heating across the southern plateau and Kalahari, as well as an extension south of Cape Town. The smallest data set (CFS-R) found rapid heating in the Agulhas outflow area, which was likely caused by upstream heating in the West Indian Ocean as well as changes in regional currents. In contrast to model simulations, none of the observed temperature changes were greatest in the inner highlands and plateau (Jury et al., 2013).

2.6 Controls on the Diversity in Climate Model Projections of Early Summer Drying Projections in Climate Models across southern Africa

(Dieppoise et al., 2015) observed this in their research of the controls and diversity in climate model forecasts for identifying early summer dryness across southern Africa. In the twenty-first century, a wide number of climate models forecast a decline in rainfall over subtropical southern Africa due to rising world temperatures (Engelbrecht et al., 2015a; Shongwe et al., 2009; Stocker et al.,2013). As a result, simulations demonstrate robust indicators only after 2°C of global warming and by the mid-twentieth century, dryness is noticeable in certain models (Dieppoise et al., 2015).

The early summer season (OND), which represents more than 60% of annual rainfall in large areas of subtropical southern Africa, including Botswana, Zimbabwe, and South Africa, has a very high drying signals (Dieppoise et al., 2015).

The Coupled Model Inter-comparison Project (CMIP5) estimates a 42 mm season drop in rainfall over subtropical southern Africa by the end of the century under the (RCP8.5) mitigation scenario under high carbon forcing (IPCC., 2007). Several studies in southern Africa have done this for regional and global climate models, providing a useful starting point for evaluating confidence in estimations (Shongwe et al. 2009; Engelbrecht et al. 2013; Cook & Vizy 2013; Lazenby et al. 2018; Pinto et al. 2018).

Early summer rainfall declines are as a result of the significance of the south Indian Ocean convergence zone (SIOCZ) advancing north-eastward in combination with a stronger thermal low and weaker subtropical high, according to (Pinto et al., 2018). Reports from the IPCC outline that annual mean drying trends in four CMIP5 models are connected to an increase in the frequency of high-pressure systems over southern Africa as a result of continental and mid-latitude lows (IPCC., 2007). These studies are important because they relate rainfall change estimates to specific climatic processes, allowing the models practicality to be evaluated in comparison to observations (Lazenby et al., 2018).

According to (Dieppoise et al., 2015) results, the amount of rainfall across models is similarly connected to changing patterns in tropical sea surface temperatures. Precipitation change across subtropical southern Africa is negatively related to the relative heating of northern tropical SSTs compared to tropical mean oceanic heating (Cook & Vizy., 2013). When compared to the tropical mean, high-magnitude drying models predict much greater heating in the northern tropics, whereas low-magnitude drying models simulate more spatially uniform SST heating across the tropics (Dieppoise et al., 2015).

The significance of SST change patterns indicate that dynamic change processes are critical for understanding uncertainty in future rainfall projections, which is corroborated by research on rainfall change in the tropics (Engelbrecht et al., 2013; Fauchereau et al., 2003; Stocker et al.,2013). Large current precipitation biases that remain over subtropical southern Africa might affect future rainfall decrease estimates. Models that predict high-magnitude drying over subtropical southern Africa have more precipitation biased than models that project low-magnitude drying, and these biases are connected to a distortion of the structure of uplift/subsidence across subtropical southern Africa (Stocker et al.,2013).

2.7 Inter-annual variability

Although the focus of this research is on the long-term seasonality of southern Africa's climate, it is important to note that the region is characterized by pronounced inter-annual variability in rainfall. Links between the global modes of variability such as ENSO to rainfall variability over the winter and all-year regions are significantly weaker (Engelbrecht & Landman., 2015). Regional sea-surface temperatures play a secondary role in inter-annual rainfall variability in southern Africa (Hoell et al., 2017). Seasonal forecasting is an important tool for managing climate risks (Klutse et al., 2016). Seasonal forecasting data helps with security-related planning and decision-making, such as water resource management, disaster prediction and prevention, health planning, and agriculture management (Klutse et al., 2016).

The El Nino-Southern Oscillation (ENSO) is a natural climate phenomenon that occurs regularly and has severe weather consequences, including extreme floods and droughts in various parts of the world (Schreck & Semazzi., 2004). While origination is largely unexpected over long time scales, it may be predicted up to six months ahead of time and occurs every two to seven years on average (Schreck & Semazzi., 2004). Across the equatorial Pacific, the ENSO cycle is characterized by regionally consistent and significant changes in sea-surface temperatures SST, rainfall, air pressure, and atmospheric circulation.

El Nino is the hot phase of the cycle when above-average SSTs form in the east-central tropical Pacific Ocean and below-average SSTs form over the western Pacific Ocean due to a change in wind patterns (Landman & Beraki., 2012). The ENSO cycle's La Nina phase is the polar opposite, with below-average SSTs forming in the western tropical Pacific Ocean (Landman & Beraki., 2012. Each phase lasts one to two years, with certain occurrences being more pronounced and lasting longer than others (Fauchereau et al., 2009). In southern Africa's summer rainfall regions (Landman & Beraki., 2012), El Nino events are commonly connected with below-average rainfall years, whilst La Nina events are frequently associated with above-average rainfall years (Vigaud et al., 2009). In the Limpopo region, located north of South Africa, frequent floods and droughts are experienced (Reason et al., 2005). The frequency and start date of summer dry spells are linked to ENSO through changes in regional circulation (Reason et al., 2005). Therefore, during the 1979–2002 period, El Nino sea surface temperature (SST) anomalies seemed to have a strong association with dry spell frequency (Reason et al., 2005). Anomalies in the rainy season starting dates from 1979 to

2002 appear to be negatively connected to El Nino SST, with the link growing after 1986 (Reason et al., 2005).

2.7.1 ENSO effects on southern Africa Climate and Seasonality

During El Nino episodes, droughts have favoured the southern African area, notably since the late 1970s (Richard et al., 200).

Interactions between the inter-annual and synoptic timescales influence El Nino's impacts on summer rainfall in southern Africa (Pohl et al. 2007; Fauchereau et al. 2009). Variations in the Walker circulation produce low-level divergence over the region during El Nino episodes (Vigaud et al., 2009; Ratnam et al., 2013a). During the El Nino season, an unusual lower-level divergence across the continent obstructs maritime moisture transfer to South Africa, limiting synoptic disturbances and seasonal rainfall.

El Nino causes the Santa Helena and Indian Ocean subtropical highs to move northward (Cook et al, 2004; Vigaud et al., 2009). Mid-latitude wind flow across the region due to low-pressure anomalies and cyclonic circulation in the south, as well as high-pressure anomalies across the continent, resulting in less rainfall (Vigaud et al., 2009). ENSO causes atmospheric waves in the southern hemisphere, according to (Cook., 2001) and (Ratnam et al., 2014), which may be responsible for an eastward shift of the South Indian Convergence Zone (SICZ), which is where the majority of the synoptic-scale bearing systems affect southern Africa (Todd & Washington 1999; Hart et al. 2013).

SST anomalies in the Indian Ocean, according to (Nicholson., 1997), may shift air convection and rainfall eastward during El Nino events. In recent decades, significant progress has been made in replicating ENSO dynamics and related teleconnections inside Atmosphere-Ocean coupled general circulation models (AOGCMs). Severe El Nino episodes, for example, in 1982/83 and 2015/16, coincided with below-average rainfall and droughts in many parts of the region (Reason et al., 2005). ENSO has an influence on rainfall in South Africa's winter rainfall zone, with El Nino/La Nina years being associated with higher/lower than usual rainfall amounts during May, June, and July.

2.7.2 The influence of ENSO on winter rainfall in South Africa

The southern Africa region receives the bulk of its rainfall during the austral summer, with the exception of a tiny region in the southwest that receives rain during the austral winter (Rouault & Richard., 2003). This region receives the highest rainfall from May to August, when temperate weather systems such as extratropical cyclones, cold fronts, and cut-off lows migrate northward (Rouault et al., 2009). The south-western region, which includes parts of the Western and Northern Cape provinces of South Africa, is defined by the cold Benguela upwelling system to the east and the hot Agulhas Current to the south. The climate in this area is heavily influenced by orography (Rouault et al., 2009).

Although rainfall anomalies and SST in the Pacific have a statistically significant link (Rouault et al., 2009), the relationship between ENSO and regional rainfall is not linear (Rouault et al., 2009). Severe droughts occurred during the El Nino mature period, with wetter summers happening during the La Nina phase (Rouault & Richard 2003). Winter rainfall in South Africa's Western Cape is affected by the Antarctic Annular Oscillation system (AAO).

South Africa endured the worst drought since 1995 during the Austral summer of 2015/2016. There was also a severe drought in 2014/2015. The drought of 2014/2015, which severely depleted water reserves, was the most significant factor in South Africa's GDP decline in 2015. At the same time, during the austral summer of 2014/2015, the Pacific Ocean was hotter than typical. In 2015, the Pacific heat significantly, culminating in one of the strongest El Nino occurrences ever recorded.

2.8 Fire in southern Africa

Savannah and woodland vegetation predominates 10 degrees south of the equator, transitioning to forest or desert shrub lands at the wet and dry boundaries of the rainfall range (Archibald et al., 2009). Fires have consumed a large area of the southern African subcontinent (resulting in 34 percent of the region being burnt at least once in the last 8 years)

(Archibald et al., 2009). Furthermore, during the rainy season, the extent and frequency of burning are affected by vegetation tree cover (biophysical vegetation traits), rainfall seasonality (amount and intensity), and human land-use activities (Archibald et al., 2009; Van Wilgen & Scholes., 1997).

Fire has an important role in terrestrial ecosystems, particularly in the savannah and grassland biomes. Long-term field studies in the African savannahs show that the area burned by wildfires varies from 0% to 80% of the landscape from year to year (Balfour & Howison, 2001; Van Wilgen et al., 2004), which can be attributed to variations in the amount of grass fuel available, which are driven by highly variable rainfall patterns (Archibald et al., 2009). The geographical spread of burning in the savannah and grassland ecosystems is determined by a variety of human, environmental, and climatic factors (Van Wilgen & Scholes, 1997; Archibald et al., 2009). Fire-dominated habitats were more common globally in the late Cenozoic, according to temperature and plant changes (Beerling & Osborne., 2006).

2.8.1 Fire and rainfall seasonality

From November to April and May to October, wildfires rage over Africa's seasonal tropics, particularly in the north and south of the equator, respectively (Van Wilgen & Scholes, 1997). Burning occurs during May-June during the high grasses of the savannah woodland mosaic in the Congo basin's southern border, then moves south and east throughout the subcontinent (Archibald et al.,2009). According to an examination of the geographical distribution of active fires and the spatial distribution of the Normalised Difference Vegetation Index (NDVI) values, the cyclical pattern of vegetation drying out following the end of the yearly rains in the region are closely paralleled by burning (Archibald et al.,2009).

The quantity and seasonal spatial distribution of rainfall in the region varies by distribution of rainfall fluctuating significantly between years and within countries. Year-to-year variations in the yearly burnt area fraction are hence likely to be dominated by climate variability (Van Wilgen & Scholes, 1997). The amount of rainfall has a direct impact on fuel loads, and rainfall seasonality has a direct impact on the availability of dry fuels, resulting in a high fire hazard; meteorological variables have all been verified to influence the extent of fire in savannah and grassland ecosystems (Archibald, et.al 2009).

While all of these climatic variables in southern Africa may shift substantially from year to year, rainfall is frequently seen as the most limiting factor, and the one that causes inter-annual fire regime variations (Archibald, et.al 2009). A measure of cumulative rainfall, according to many studies, may explain up to 60% of the variance in burnt area between years (Balfour & Howison, 2001; Van Wilgen et al., 2004). Early research utilizing remotely sensed data discovered connections between fire and the El Nino/Southern Oscillation (ENSO), with increased fire incidence linked to above-average rainfall periods (Archibald et al.,2009: Anyamba et al., 2003; Riano et al., 2007; Van der Werf et al., 2008).

Seasonality and fire weather have been demonstrated to play a key part in fostering fires in Australia and Africa (Archibald et al., 2009), which is backed by the fact that grass fuels can become combustible after a few weeks of dry weather. In both Australia and Africa, the duration and harshness of the dry season has been demonstrated to have a key influence in the spread of fires (Archibald et al., 2009).

Rising temperatures paired with prolonged dry spells may cause wildfires to spread across bigger regions and become more intense and severe (Balfour & Howison., 2001). The frequency of high fire danger days is expected to rise in the southern Africa region, with rising heat-wave days (Van Wilgen & Scholes., 1997). The regions extended yearly dry season, combined with relatively fast rates of fuel accumulation, provide excellent conditions for grass fires to occur on a frequent basis. Indeed, fire is assumed to have a significant role in determining the climate and distribution of savannah and grassland plant types in Africa (Van Wilgen & Scholes., 1997; Higgins et al., 2000; Bowman et al., 2003). In southern Africa, human activities (such as land clearing, poor land management, and the spread of invasive alien plants) have a significant impact on fires and are a major controlling factor in fire regimes, while climatic factors (such as wind and temperature) play a role in determining the size and intensity of a fire (Van Wilgen & Scholes., 1997).

2.9 Climate change

Climate change is defined as "a change in the state of the climate that may be determined (e.g., using statistical tests) by changes in the mean and/or variability of its attributes over time, generally decades or more" (IPCC., 2021). Change can take anything from decades to millennia to take place (IPCC., 2021). It can have an impact on one or more seasons (summer, winter, or the whole year) as well as one or more meteorological variables (rainfall, temperature, or wind) (IPCC., 2021). Due to periodic oscillations in the earth's orbit, volcanoes, and solar variability or man-made (due to increased emissions of greenhouse gases such as CO2 and CH4, land-use change, and/or aerosol emissions) climate change will occur (Morishima & Akasaka., 2010). The majority of climate change debates, on the other hand, revolve around anthropogenic-caused atmospheric changes.

A number of methodologies have been used to investigate the consequences of global warming on the environment. While they found no long-term trends in cumulative summertime rainfall anomalies in southern Africa, they did find that rainfall variability has grown considerably in recent decades (Morishima & Akasaka., 2010). Droughts, in particular, have intensified and become more common in recent years (Morishima & Akasaka., 2010). Between 1961 and 2000, there was a decline in average rainfall intensity and an increase in dry-spell length. (New et al., 2006). Furthermore, rainfall levels rose from the equator to tropical eastern Africa from 1901 to 2005 (IPCC, 2007; Morishima & Akasaka, 2010), but declined south of 2000s across the African continent (IPCC, 2007; Morishima & Akasaka, 2010). These trends, however, are not visible between 1979 and 2005. (Morishima & Akasaka., 2010). A rising trend in annual mean surface temperature may be seen throughout the continent's western coast. Annual rainfall on the west coast and in the core of the continent north of 1500s declined dramatically after the mid-1990s, particularly in the region with high annual rainfall (Morishima & Akasak., 2010).

Climate change is already influencing every populated location on the planet, with human-caused changes in weather and climate extremes contributing to many of the documented changes. To prevent the worst consequences of climate change, it is widely agreed that the world must reduce emissions as quickly as feasible and limit warming to 1.5°C for controllable scenarios (IPCC, 2021). Any increase in temperature more than 1.5°C will have essentially permanent consequences.

2.10 Conclusion

In closing, southern Africa is an annually invariable rainfall region. Although trends have been seen to remain relatively stable, the temperature is under constant increases, particularly around the tropical regions, which are mostly dominated by grasslands and forestry plantations. Field fires have erupted over the tropical savannah forest as a result of these sudden seasonal shifts, therefore being able to accurately predict the future climate, particularly rainfall and temperature start and end periods, will aid in the effective management and protection of these places. As a result, model forecasts from the CMIP6 model ensemble, which are the most recent climatology models, must be evaluated in terms of their accuracy in predicting these two key variables.

CHAPTER 3: VERIFICATION OF MODEL SIMULATIONS OF PRESENT-DAY SEASONALITY OVER SOUTHERN AFRICA

3.1 Introduction

The potential of global climate change as a consequence of increased anthropogenic greenhouse gas emissions has long been recognized as a threat to society (Hewitson & Crane., 2002). The latest estimates of global warming are that it has reached a degree of increase at 1.1 °C for the period 2011-2020 relative to 1850-1900 (Lee et al., 2021). Under low mitigation futures, warming degrees may reach as high as 4-5 °C by the end of the century (Lee et al., 2021). As a result, resources are being invested into climate change research by various nations to understand the potential regional and global exhibition and impact of such change.

Dynamic climate models have become the primary tools for projecting future climate change, at both the global and regional scales (Engelbrecht et al., 2011). Climate models including global climate models (GCMs) and regional climate models (RCMs) are based on the Laws of Physics, which when applied to the atmosphere result in a set of partial differential equations (Engelbrecht et al., 2011). Solving the equations require that the equations are discretized on a three-dimensional grid, where numerical techniques can be applied to project a future state of the atmosphere-ocean system, provided that an initial state is known (Engelbrecht et al., 2011). The only additional information climate models require to be marched forward into time is the climate system's historical and future radiative forcing (Engelbrecht et al., 2011). These include changes in incoming solar radiation, and most importantly in the context of anthropogenic induced climate change, changes in greenhouse gas concentrations (Engelbrecht et al., 2011).

Dynamic climate model simulations over southern Africa have been studied extensively. (Shongwe et al., 2009) in a study evaluating RCM simulations of the Coordinated Regional Downscaling experiment (CORDEX) over southern Africa established that the general representation of precipitation patterns is satisfactory, particularly over the northern parts. These RCMs’ correlation with the ERA-Interim reanalysis data was high in southern Africa and biases were not substantial (Shongwe et al., 2009. These rainfall biases over southern Africa are generally positive, and the rainfall estimations are worst over the eastern escarpment areas of South Africa, where rainfall is overestimated (Nikulin et al., 2012). Another recent study in assessing the accuracy of dynamic climate models was performed by (James et al., 2020). This study attempted to seek fundamental understanding for southern Africa climate, by examining model ability to simulate a dominant rainfall producing mechanism known as tropical temperate troughs (TTT), using the Coupled Model Inter-comparison Project Phase Six (CMIP6) models. TTTs form as part of a mid-latitude wave that propagates north-eastward into southern Africa (James et al., 2020). All models analyzed in this study generate TTTs with similar synoptic circulation compared to reanalysis (James et al., 2020). The findings of this paper provide confidence that CMIP6 models can realistically portray a key southern African rainfall system, and thereby inform their applications in adaptation forecasting across the region.

In this chapter, we will be looking at the capability of dynamic climate models to correctly simulate the spatial patterns of rainfall and temperature across the southern African region. Furthermore, a detailed analysis is undertaken of how the CMIP6 climate models simulate the seasonal cycle of rainfall and temperature compared to baseline observation datasets (CRU TS 4.05) and reanalysis data (ERA-interim). Undertaking such an analysis require extensive data pre-processing, for example interpolating the large ensemble of CMIP6 simulations to a common latitude-longitude grid, towards facilitating the comparison to observations and reanalysis. The core purpose of this chapter is to answer one of the core objectives that we have in this research. This is to statistically analyse how realistically climate models can represent temperature and rainfall over southern Africa, and how well these three datasets can correctly simulate these climate variables. The purpose of understanding results from these data products is to inform decision-makers on the quality of the model precipitation and temperature products and also quantify the appropriate level of confidence in their use for different applications in the future.

3.2 Data and methods

3.2.1 Observed datasets

The observations dataset used in this research is from the university of east Anglia’s climatic research unit (CRU)'s Time-Series (TS) version 4.04 high-resolution gridded dataset of the month-by-month variation in climate containing precipitation in mm/month readings and temperature in (°C) from global weather stations across municipalities. The data set is available for the period 1901-2019.

The station data used by CRU TS4.04 was interpolated to a 0.5° latitude-longitude grid. Gridding then simply averages all available station temperatures as anomalies within each grid box for each month (Bowman et al., 2003). The station's elevation or location within the grid box is not taken into account, given that anomalies relative to climatology do not strongly depend on altitude (Bowman et al., 2003). In the case of the research reported on in this chapter, the data was analysed as a subset of the original, only focusing on areas south of 10° S, which is the study area.

The second observed dataset is from the European centre for medium-range weather forecasts (ECMWF) Interim reanalysis. This dataset is a global atmospheric reanalysis that is available from 1 January 1979 to 31 August 2019. The system includes a 4-dimensional variation analysis with a 12-hour analysis window. The resolution of the dataset in the horizontal is approximately 0.75 ° on a standard longitude-latitude grid. ERA-Interim employs 60 levels in the vertical, from the surface up to 0.1 hPa.

The two observed data products (ERA-interim and CRU 4.04) were selected due to the following reasons. Firstly, they are widely used in literature and have been highlighted to be potentially useful in Africa. Secondly, they have relatively high spatial resolution and a long temporal time-span. And lastly, these products are easily accessible, and commonly publicly published as final products on respective organizational websites. The model verification period in the chapter is 1979-2014, given that this is the 'historical' period of the CMIP6 simulations that correspond to the onset of the satellite era in atmospheric observations. That is, satellite data only became available in 1979, implying a substantial improvement in the quality of reanalysis data from 1979 onwards (Tennant & Hewiston., 2002). The historical period in the CMIP6 simulations is 1850-2014 – this is the period for which the models were forced with observed greenhouse gas concentrations, and other forms of radiative forcing. The period 1979-2014 is thus selected as the model verification period.

3.2.2 Model data

The most up-to-date, state-of-the-art, and comprehensive set of projections of future climate change is that of the Coupled Model Inter-comparison Project Phase Six (CMIP6) of the World Climate Research Programme (WCRP) (Eyring et al., 2016). Simulations are available from more than 30 institutes worldwide and have been performed in support of Assessment Report Six (AR6) of the Intergovernmental Panel on Climate Change (IPCC). The ensemble of CMIP6 models is the core data set to be analysed in this research, with a selection of models shown in Table 1. Model selection was entirely informed by data availability at the time of finalizing the analysis in 2021. The simulations are verified in terms of their representation of present-day seasonality over southern Africa (see the section on methods). After averaging the model data to a temporal resolution of one month (across the 1979-2014 period), the model data was interpolated from the native model grids to a 1 ° x 1 ° resolution grid (in latitude and longitude) to allow for inter-comparison across the different GCMs. Bilinear interpolation was used, given the smoothness of monthly means.

Modelling Institute	**Acronym**	**Model name**	**Resolution (degree east)**
1. Atmosphere and Ocean Research Institute (University of Tokyo), National Institute for Environmental studies, and Japan Agency for Marine-Earth Science and Technology	MIROC	MIROC6	1.40625
2. UK Met Office Hadley Centre	MOHC	UKESM1-0-LL	1.25
3. Institute for Numerial Mathematics	INM	INM-CM4-8	2
4. Chinese Academy of Sciences	CAS	FGOALS-f3	1.25
5. Canadian Centre for Climate Modelling and Analysis	CCCma	CanESM5	2.8125
6. Centre National de Recherches Météorologiques - Centre Européen de Recherche ET de Formation Avancée en Calcul Scientifique.	CNRM-CERFACS	CNRM-CM6	1.40625
7. Meteorological Research Institute	MRI	MRI-ESM2-0	1.125
8. European Community Earth Consortium	EC Earth Consortium		0.703125
9. National Centre for Atmospheric Research	NCAR	CESM2-WACCM	1.25
10. Beijing Climate Centre	BCC	BCC-CSM2-MR	1.125
11. Chinese Academy of Meteorological Sciences	CAMS	CAMS-CSM1-0	1.125
12. Institute Pierre-Simon. Laplace	IPSL	IPSL-CM6A-LR	2.5
13. Nanjing University of Information Science and Technology	NUIST	NESM3	1.875

14. Alfred Wegener Institute	AWI	AWI-CM-1-1	0.9375
15. Commonwealth Scientific and Industrial Research Organization/Australia	CSIRO	ACCESS-CM2	1.3
16. Commonwealth Scientific and Industrial Research Organization/Australia	CSIRO	ACCESS-ESMI-5	1.2
17. National Centre for Meteorological Research	CNRM	CNRM-CM6-1-HR	0.5
18. National Centre for Meteorological Research	CNRM	CNRM-ESM2-1	1.4
19. EC-EARTH Consortium/ Europe	EEC	EC-Earth3	0.7
20. EC-EARTH Consortium/ Europe	EEC	EC-Earth3-Veg	0.7
21. Chinese Academy of Sciences/China	CAS	FGOALS-f3-L	1
22. Chinese Academy of Sciences/China	CAS	FGOAL-g3	2.3
23. NOAA Geophysical Fluid Dynamics Laboratory/USA	NOAA	GFDL-ESM4	1
24. Institute of Numerical Mathematics, Russian Academy of Sciences/ Russia	INM	INM-CM4-8	1.5
25. Institute of Numerical Mathematics, Russian Academy of Sciences/ Russia	INM	INM-CM5-0	1.5
26. Japan Agency for Marine-Earth Science and Technology, Atmosphere and Ocean Research Institute, The University of Tokyo, National Institute for Environmental Studies, and RIKEN Centre for Computational Sciences/Japan	JAMS	MIROC-ES2-0	2.8
27. Norwegian Climate Centre/ Norway	NCC	NormESM2-LM	1.9

Table 3.1: List of all institutes and models that contributed to producing the model CMIP6 ensemble.

3.2.3 Data processing

The model verification period stretches from 1979-to 2014, 35 years, starting at the beginning of the satellite era in Meteorology (1979), which makes it ideal for model verification purposes. The verification domain is southern Africa (here defined as Africa south of 10 °).

Gridded observational rainfall and surface temperatures were obtained from the European centre for medium-range weather forecasts (ECMWF) interim reanalysis (ERA-Interim) as well as climatic research unit (CRU) data. The ECMWF data are available at a horizontal resolution of 0.75° × 0.75°, this was then interpolated to a resolution of 1 ° by 1 ° to enable comparison with the CMIP6 model data. The CRU TS4.04 data set has a resolution of 0.5° x 0.5° in the horizontal, and was similarly interpolated onto a 1° x 1° grid for direct comparison to the CMIP6 data.

3.3.4 Model Verification

For each GCM, the simulated seasonal cycle in rainfall and surface temperature was calculated for several climate sub-regions in southern Africa following Engelbrecht et al. (2009). These regions are:

	Region	**Latitude**	**Longitude**
A	South-western Cape	$-35° < \varphi \leq -31°$	$17° < \lambda \leq 20°$
B	Cape south coast	$-35° < \varphi \leq -33.5°$	$20° < \lambda \leq 27°$
C	Eastern South Africa	$-34° < \varphi \leq -27°$	$27° < \lambda \leq 33°$
D	Western subcontinent	$-31° < \varphi \leq -20°$	$12.5° < \lambda \leq 20°$
E	Central subcontinent	$-33.5° < \varphi \leq -20°$	$20° < \lambda \leq 27°$
F	North-eastern South Africa, S Zimbabwe, and S Mozambique	$-27° < \varphi \leq -20°$	$27° < \lambda \leq 36°$
G	N Mozambique and Tanzania	$-20° < \varphi \leq -5°$	$30° \leq \lambda \leq 41°$
H	Northern subcontinent	$-10° < \varphi \leq -0°$	$8.5° \leq \lambda < 30°$

Table 3.2: List of southern Africa climate sub-regions applied in this research study.

The calculation of the seasonal cycle simply involves the calculation of the monthly climatological averages for each of the variables over the period 1979-2014. The simulations were subsequently compared to the observed seasonal cycles of the same variables, as described by the CMIP6 ensemble average, ERA-interim reanalysis and CRU data.

The accuracy of the CMIP6 model ensemble average to simulate seasonal cycle (monthly climatology's) of rainfall and temperature over southern Africa is quantitatively examined by calculating the root mean square error (RMSE), bias, standard deviation and spatial correlation coefficient (pattern correlation) of the simulations compared to the CRU datasets (Engelbrecht et al., 2002). The reanalysis data is separately compared to the CRU data, to serve as a bench mark of model performance. The mentioned statistics are presented using Taylor diagrams (Taylor., 2001), which provide a way of graphically summarizing how closely a pattern (or a set of patterns) matches observations. The pattern can be a physical pattern of rainfall across a region, or it can be a time-series of data and the pattern that it maps out in time. The similarity between two patterns is then quantified in terms of their spatial correlation, the root-mean-square error as scaled by the standard deviation of the observations, and the standard deviation of the model simulations as compared to that of the observations (Taylor., 2001). These diagrams are very effective in summarizing model performance across different considerations, such as for different variables and seasons. (Taylor., 2001).

The RMSE calculates the general magnitude of the difference between simulations and observations, regardless of the sign of the difference. The closer the values of RMSE and bias get to zero, the better the agreement between observed and simulated data is. The RMSE is calculated according to (2),

$$RMSE = \sqrt{\frac{1}{N}\sum_{i=1}^{N}\left(x_i^M - x_i^O\right)^2}$$

Where x^M and x^O represent the model and reanalysis data respectively. N ranges from 1 to 12 and indicates the different monthly climatology's that constitute the seasonal cycle.

The temporal correlation coefficient is given by (3),

$$\rho = \frac{\sum_{I=1}^{N}\left(x_I^M - \overline{x^M}\right)\left(x_i^O - \overline{x^O}\right)}{\sqrt{\sum_{i=1}^{N}\left(x_i^M - \overline{x^M}\right)^2}\sqrt{\sum_{i=1}^{N}\left(x_i^O - \overline{x^O}\right)^2}}$$

3.3 Model verification: Rainfall verification

The spatial plots below (Figures 3.1 to 3.3) indicate the mean annual rainfall (annual totals in mm) from the three rainfall datasets (CRU, ERA-interim, CMIP6), spanning from the verification period 1979-2014. This comparison is undertaken to see how well the models simulate present-day annual rainfall, compared to the observed dataset (CRU).

The CRU dataset (observed) indicates that the highest rainfall totals occur in the northern part of the domain, in the tropical savannah climate zone (Figure 3.1). The western portion of southern Africa, including the Namib Desert and extending towards the Northern Cape of South Africa, is arid with a mean annual rainfall of less than 200 mm. There is a prominent west-east rainfall gradient over South Africa, with rainfall totals peaking at more than 1000 mm over parts of the eastern escarpment. A dry-slot of relatively low rainfall totals stretch from Namibia eastwards through Botswana, and into the Limpopo river basin of South Africa and Zimbabwe (Engelbrecht et al., 2002).

The ERA-interim annual average rainfall (mm) realistically depicts the spatial pattern in rainfall over southern Africa compared to the CRU TS4.04 data. It correctly simulates the rainfall peak over the northern sub-continent, although it overestimates rainfall totals in this region. The ERA-interim data also realistically portray the west-east gradient in rainfall over South Africa, the rainfall peaks over the eastern escarpment, and the Limpopo dry slot. The CMIP6 model ensembles are unable to depict the elevation over the eastern escarpment of southern Africa, and consequently can’t resolve the individual rainfall peaks over the eastern escarpment. However, even at this lower resolution the CMIP6 models correctly simulate the west-east rainfall gradient over South Africa, including the relatively high rainfall totals over Kwa-Zulu Natal and parts of Mpumalanga. The wetter northern subcontinent and Limpopo dry slot are also captured in the CMIP6 simulations.

3.3.1 Mean annual rainfall

The spatial plot below indicates the mean annual rainfall from our three rainfall datasets (CRU, ERA-interim, CMIP6), spanning from our investigated period 1979-2014. This comparison is done to see how well the models simulate present-day annual rainfall, compared to the observed dataset (CRU).

The CRU dataset (observed) indicates moderate rainfall peaks northeast and northwest of the sub-continent. The western portion of South Africa, extending towards the interior of the

Northern Cape is generally dry with a mean annual rainfall of less than 200 mm/year. The ERA-interim annual average correctly depicts the trend in rainfall over southern Africa (compared to CRU), it can correctly simulate the rainfall peak but overestimates it over the northern sub-continent, and indicates some underestimation over the eastern escarpment. Moreover, the CMIP6 model ensembles are unable to depict the elevation over the eastern escarpment of southern Africa, and therefore notes high rainfall totals over Kwa-Zulu Natal and parts of Mpumalanga, extending towards the interior of South Africa.

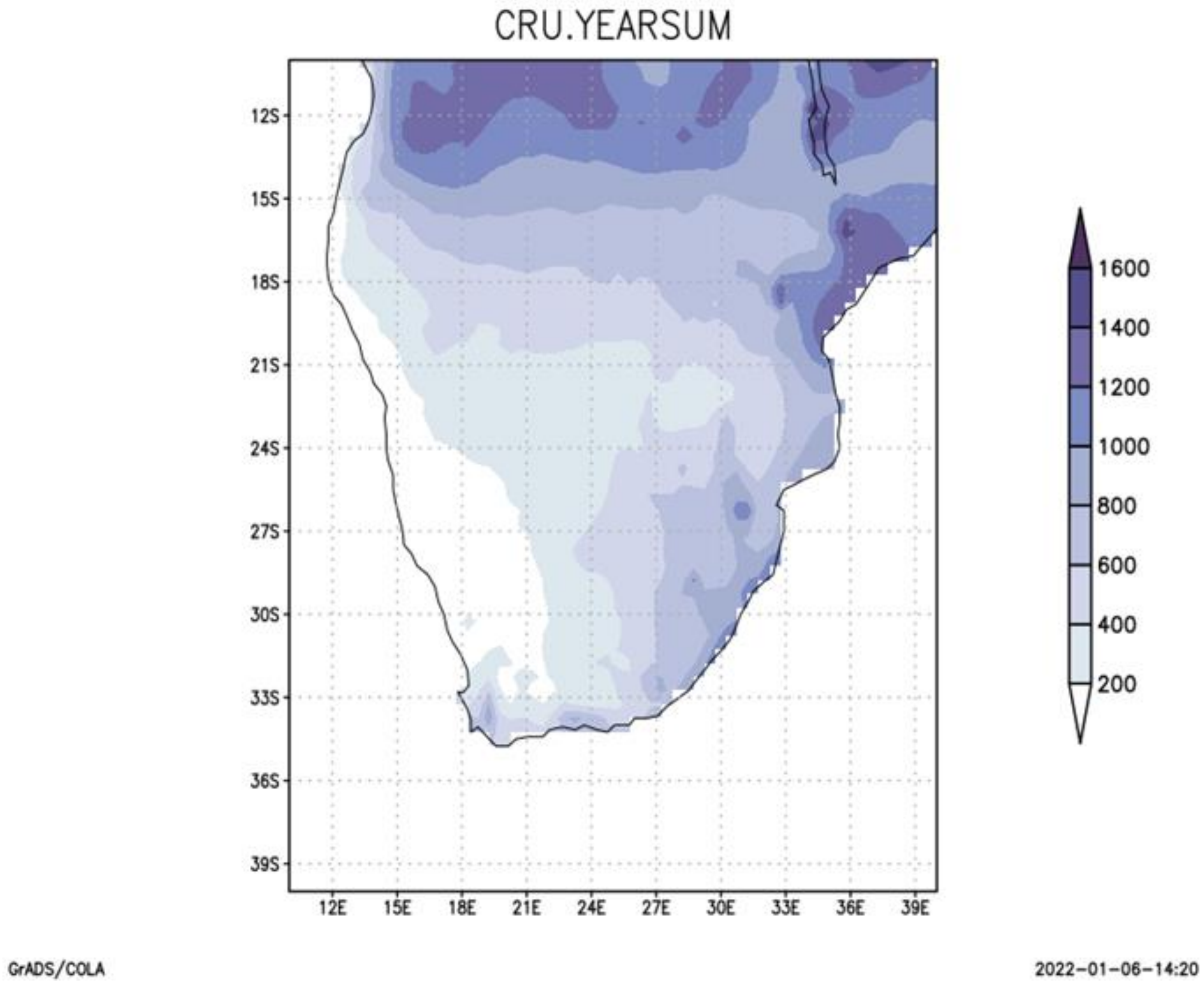

Figure 3.1: Climatology of annual rainfall totals (mm) for the period 1979-2014 as per the CRU TS4.04 dataset.

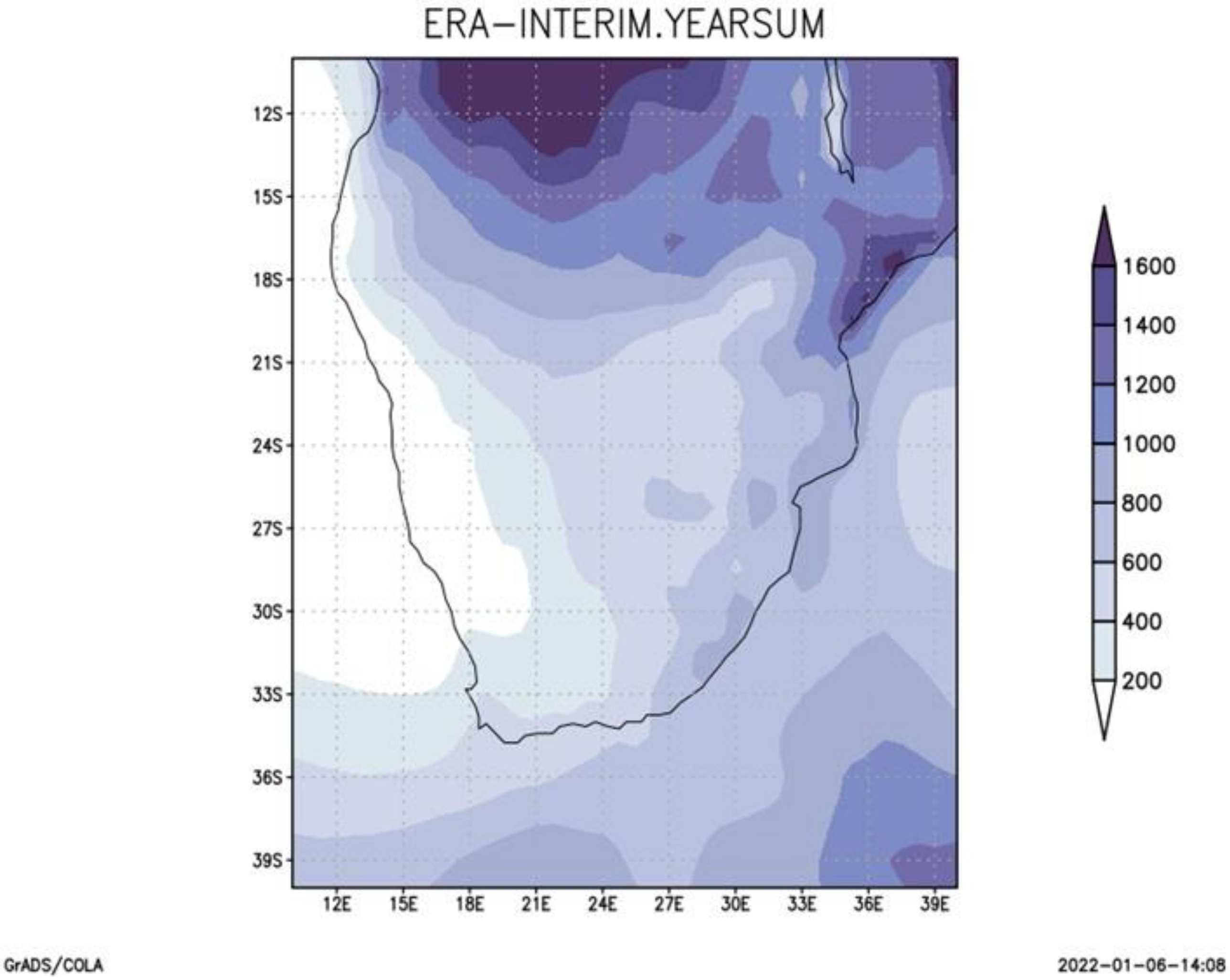

Figure 3.2: Climatology of annual rainfall totals (mm) for the period 1979-2014 as per the ERA-interim dataset.

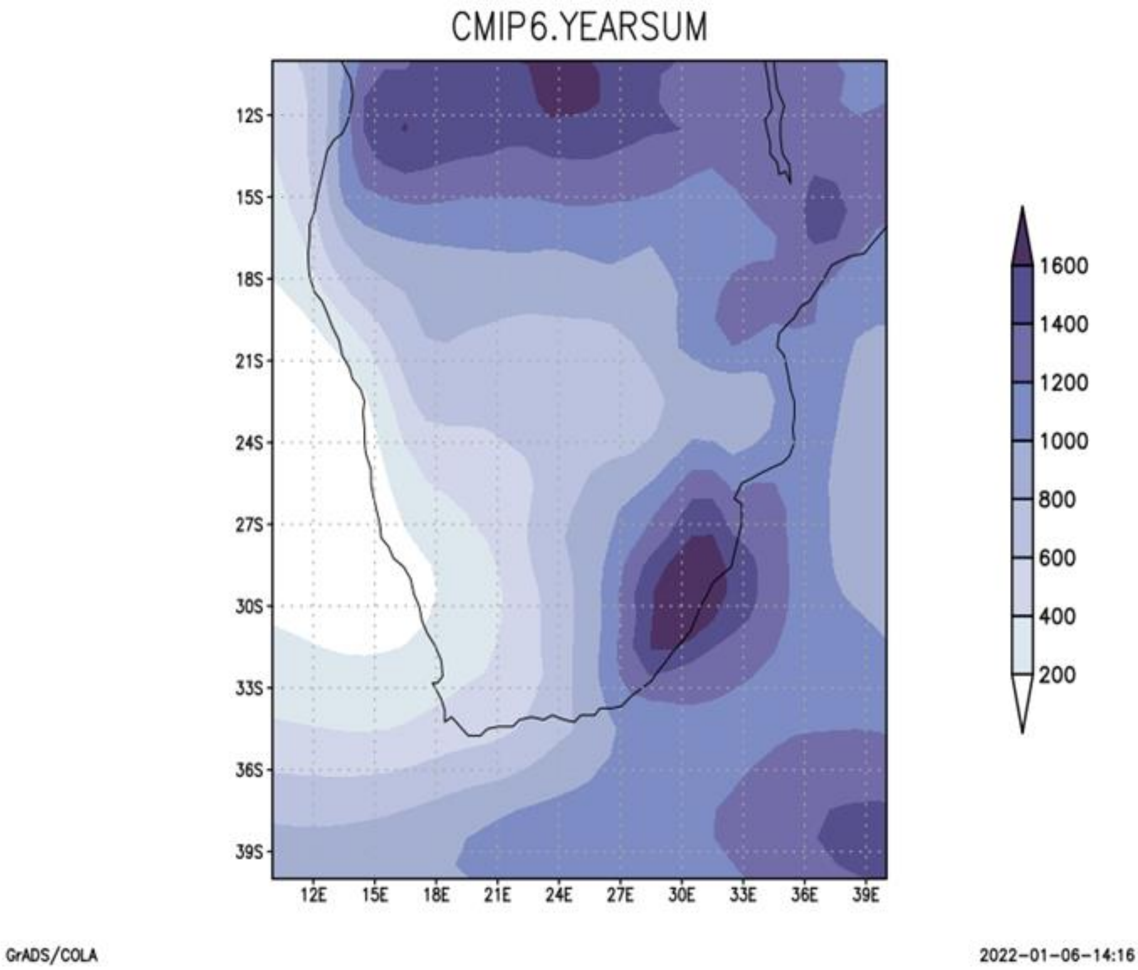

Figure 3.3: Climatology of annual rainfall totals (mm) for the period 1979-2014 as per the CMIP6 dataset.

3.3.2 Mean annual rainfall bias

Figure 3.3 below indicates, the calculated the annual bias for the ERA-interim dataset (model) versus the CRU dataset (observed). The ERA-interim data underestimate rainfall over the eastern escarpment, and also towards north Namibia and some parts of southern Angola. The ERA-interim data also denotes rainfall underestimates over the northern interior of Zimbabwe, and in Malawi bordering Mozambique. The model overestimates rainfall largely over the northern subcontinent and central subcontinent.

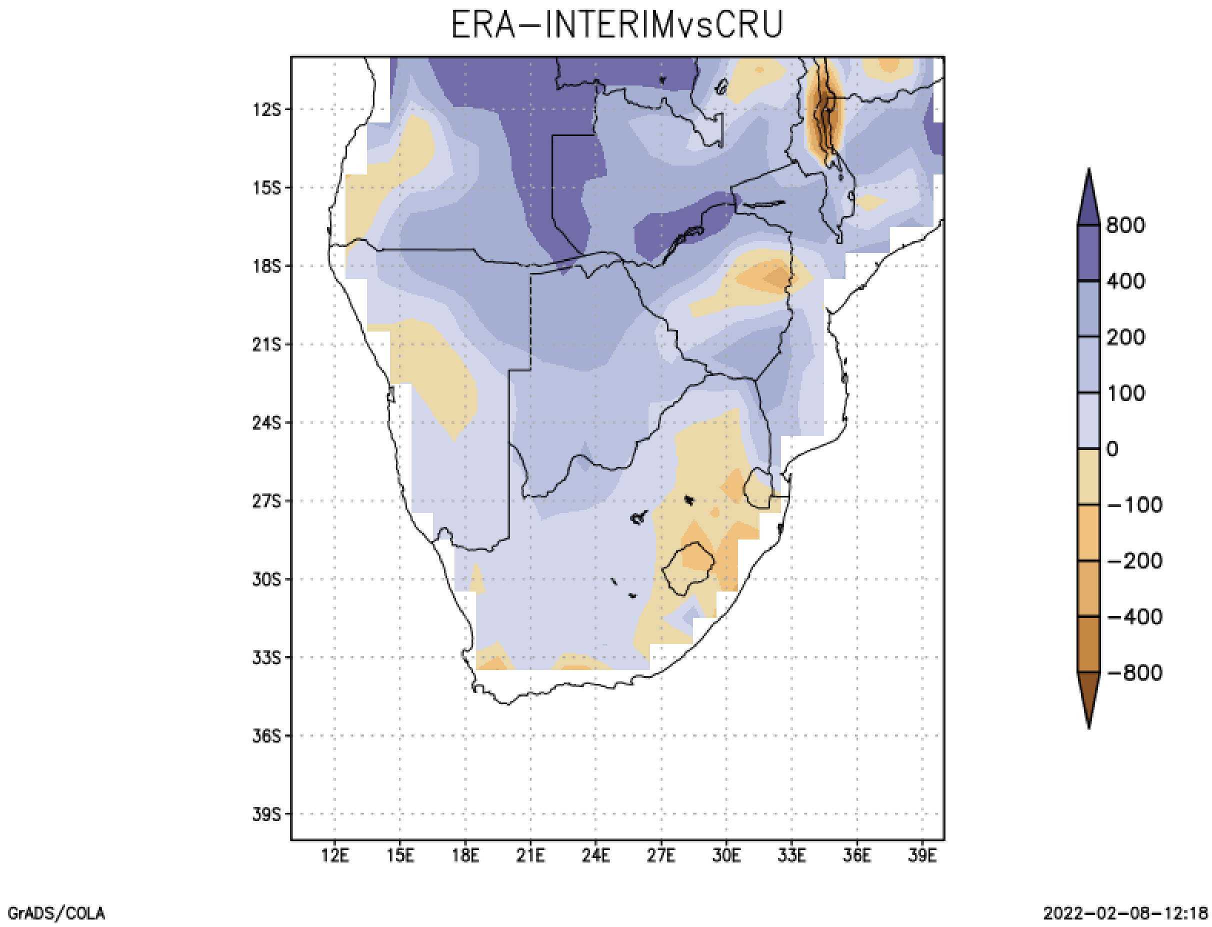

Figure 3.4: Mean annual rainfall bias of the ERA-interim model versus CRU TS4.04 for the period (1979-2014).

Furthermore, bias calculations were also made between the CMIP6 (model) and CRU (observed) in figure 3.4. The rainfall trend is largely different compared to the ERA-interim data results. The CMIP6 model overestimates rainfall by 800mm/year over the eastern portion of South Africa and towards the south of Zimbabwe. There are some underestimates observed towards the coast of Mozambique, and also on the south Western Cape (winter rainfall region).

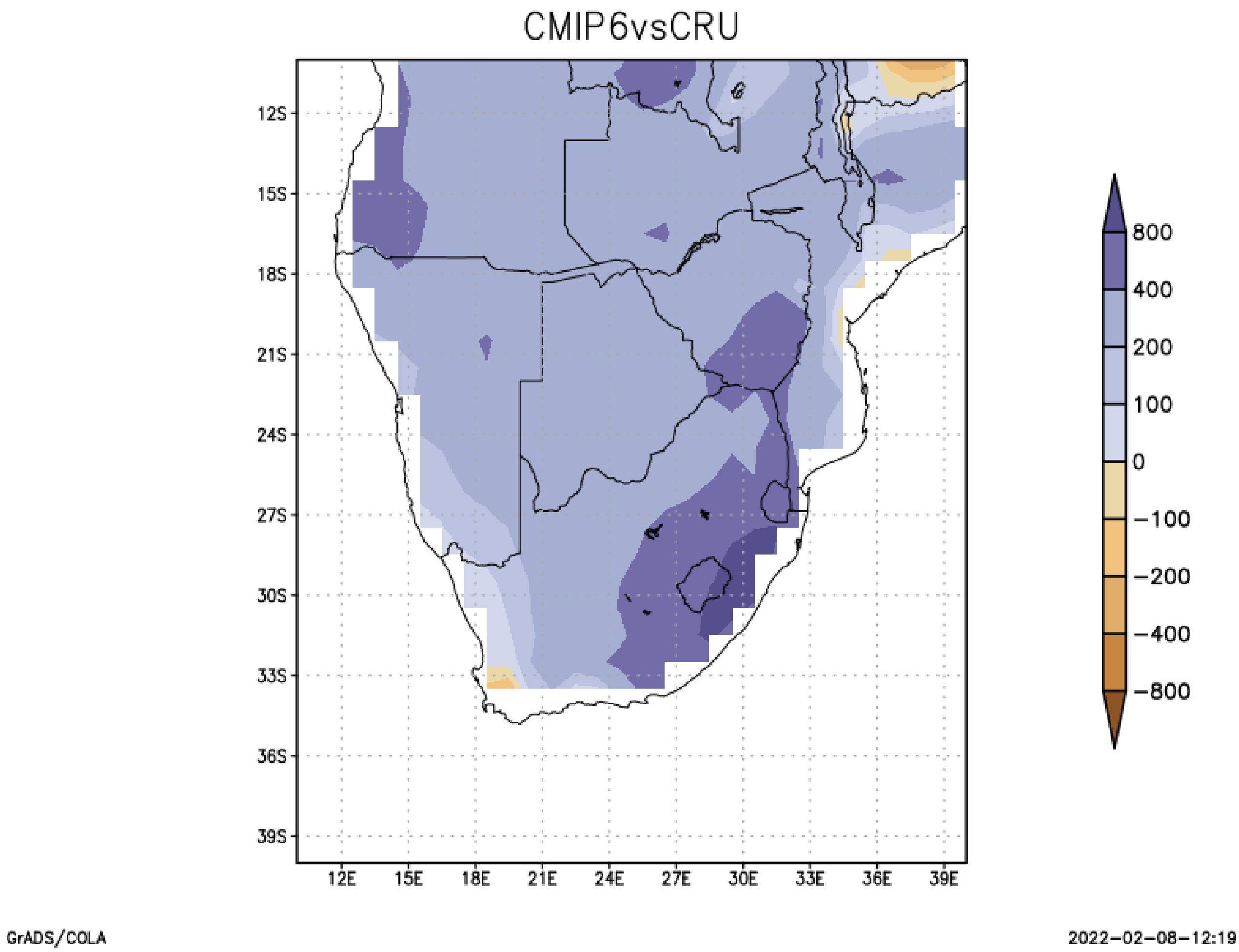

Figure 3.5: Mean annual rainfall bias of the CMIP6 model versus CRU TS4.04 for the period (1979-2014).

3.3.3 Mean seasonal rainfall

Figure 3.5 below indicated mean seasonal rainfall patterns from the CRU TS 4.04 dataset over. Mean seasonal rainfall results, outline southern Africa (Africa south of 10° S) is largely a summer rainfall region (Fauchereau et al. 2009), with the highest season of rainfall being DJF (December-February). During this season mean rainfall maximum with peaks of over 270 mm occur in a zonal band stretching from eastern Angola across Zambia to eastern Mozambique (Figure 3.6). This region of high summer rainfall occurs in association with the poleward displaced ITCZ. The lowest recorded mean seasonal rainfall for DJF occurs over the western parts of the Northern Cape Province, extending northwards to northern Namibia, (JJA; June-August) is a relatively cold and dry season across southern Africa, with the exception of the South Western Cape, which is a winter rainfall region. Frontal rainfall also extends along the Cape south coast in winter (Engelbrecht et al., 2015a).

The JJA rainfall peak ranges from 120-180 mm in the South Western Cape (Figure 3.6). The western interior and central sub-continent are largely dry for JJA, with the lowest mean seasonal rainfall ranging to <30 mm. During the spring season SON (September-November), rainfall peaks are focused over distinct regions; which are central South Africa, coastal Kwa-Zulu natal, Congo, and Angola, with a mean seasonal rainfall peak of 180-220 mm for SON, which is contrary to conditions experienced over the western region (Northern Cape, Namibia, and northern Botswana) which appear to be dry with a mean seasonal rainfall of <30 mm during SON. Moreover, during the autumn season, MAM (March-May) seasonal rainfall peaks are prevalent over eastern Tanzania, coastal Mozambique, and over eastern southern Africa, as the Far East as Angola with some intensified peaks in rainfall reaching over 270 mm.

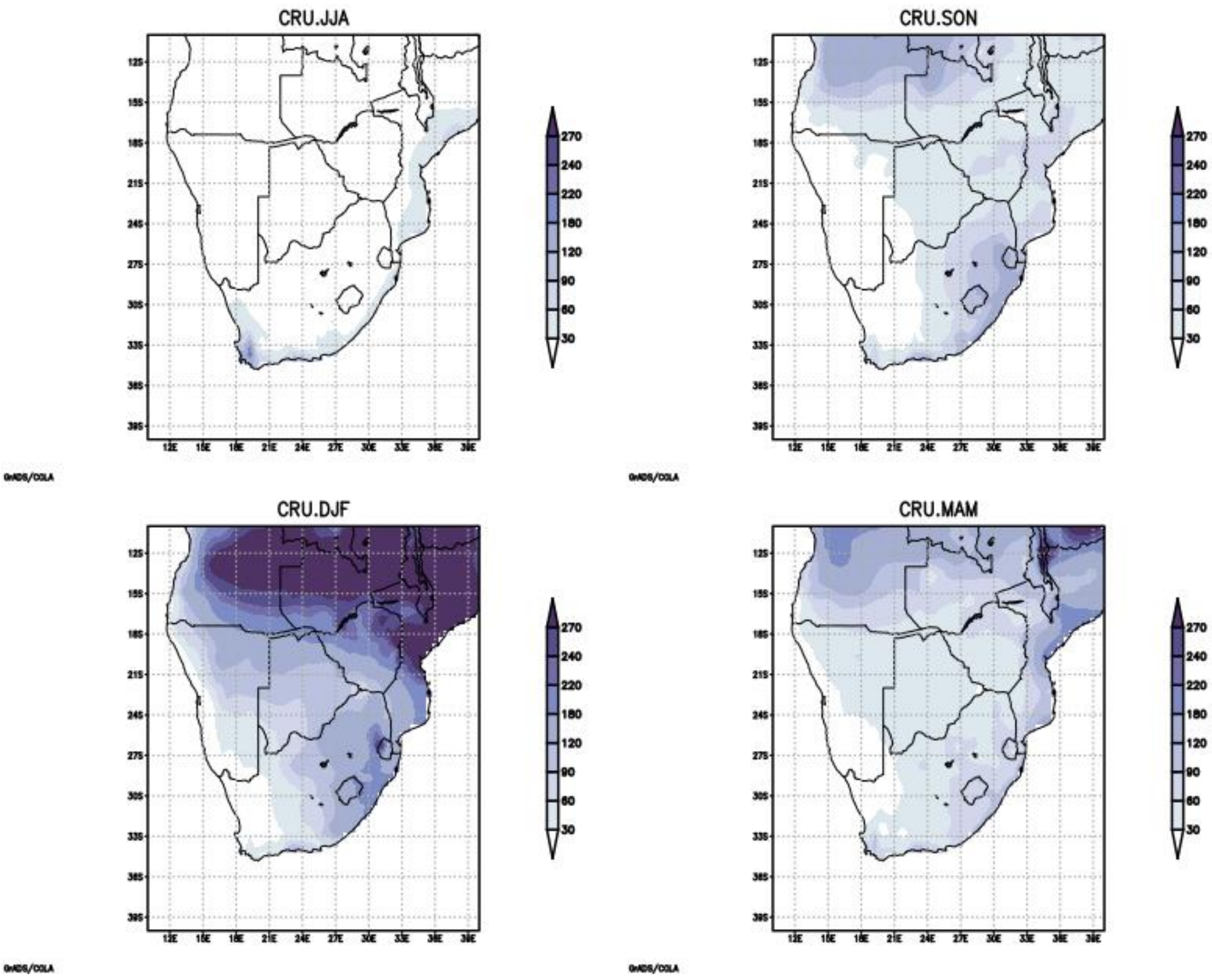

Figure 3.6: CRU TS4.04 observed seasonal rainfall totals (mm) over southern Africa.

Moreover, figure 3.7 below indicates ERA-Interim seasonal rainfall patterns, which indicate that, a bulk of the rain falls during the spring and summer months. The spatial plots below indicate that southern Africa is generally dry during the JJA season, which mirrors the same trend as that of the observed CRU data. During this season (JJA), rainfall peaks occur from the south Western Cape towards the coast reaching Mozambique. The rainfall peak for this season is <60 mm. The DJF season is the season of intense rainfall, observed along the central subcontinent, encompassing countries such as Angola, Zambia, and Botswana. Rainfall peaks for the DJF season > 270 mm, mostly occurring within the regions specified above. During the spring season (SON) there are still moderate amounts of rainfall concentrated on the sub-continent, with peaks occurring in Angola and Zambia at 180-220 mm. Eastern South Africa also experiences rainfall during this season at 120-180 mm during SON. During the autumn months (MAM), rainfall is constant over the entire region with some peaks over the northern subcontinent, at 120-180 mm.

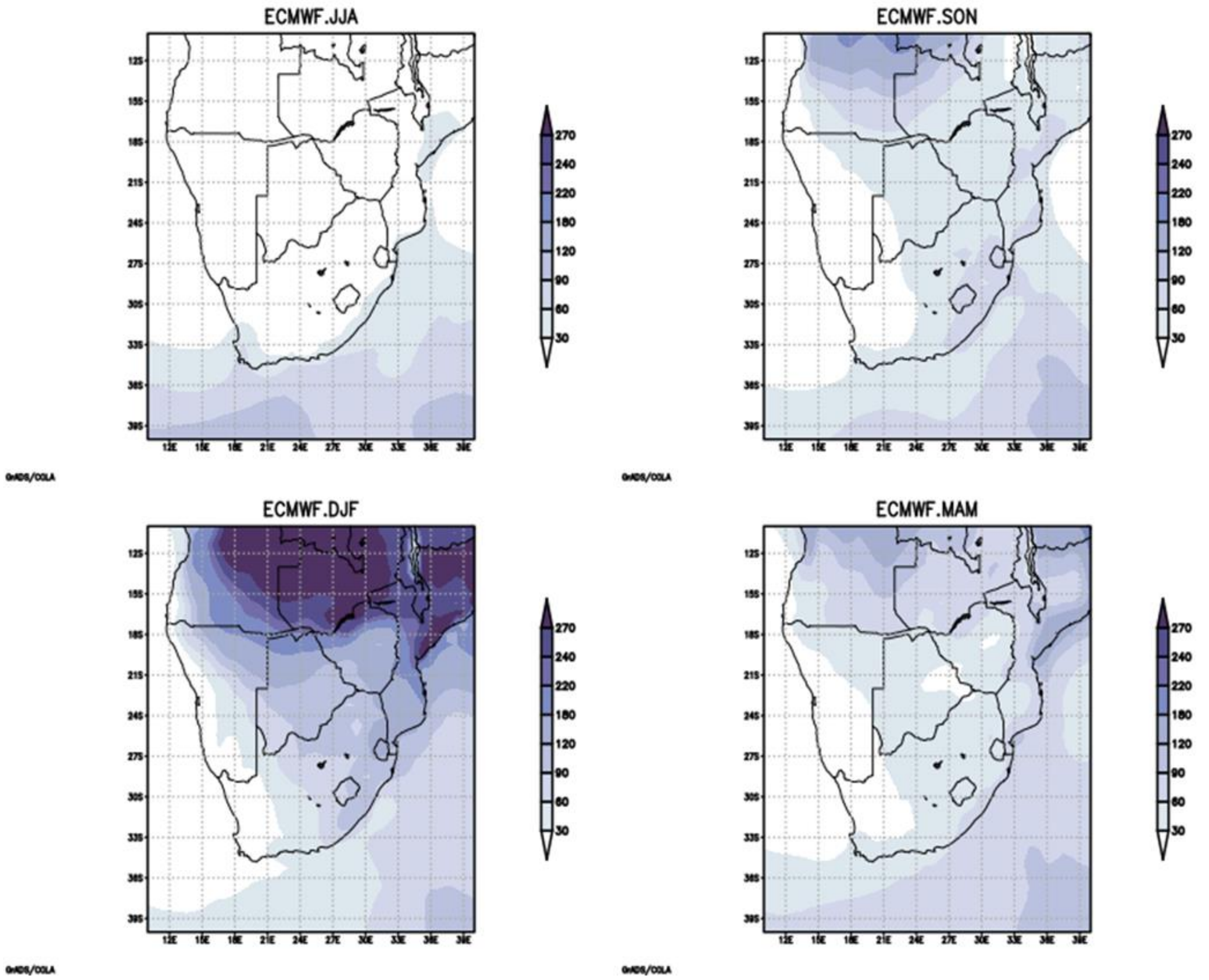

Figure 3.7: Seasonal rainfall totals (mm) over southern Africa as simulated by the ERA-interim ensemble average.

Furthermore, Figure 3.8 below indicates CMIP6 seasonal rainfall patterns, which describe a similar rainfall trend as that of CRU and ERA-Interim data. Because, the CMIP6 data also denotes the fact that southern Africa is a summer and spring rainfall region, and therefore a bulk of the rainfall over the southern Africa region occurs spring and summer months. For the JJA season, CMIP6 notes that this is an overall dry season, but what is significant to note is that it overestimates the rain over eastern southern Africa, which further extends inland into South Africa, however, the observed data CRU limits the rainfall to the coastline. Another noticeable occurrence is that the CMIP6 dataset does not take note of the winter rainfall peak in the south Western Cape. During the summer season (DJF), CMIP6 notes this season as the season of intense rainfall (which is true with the observations), however, the model picks up rainfall peaks over eastern South Africa, and slightly along the coast of Mozambique. The spring season (SON) is also a season of active rainfall according to the CMIP6 model, with some rainfall peaks over the east of South Africa and the northern subcontinent. Finally, the autumn (MAM) season is also a rainfall active season but not to the same extent and intensity as the spring and summer months. Overall, the CMIP6 models correctly represent the overall trend and pattern of rainfall over southern Africa, although with some overestimates and underestimates in particular regions. What I have noticed is that there is always some form of overestimating with the models over the eastern escarpment and general underestimates over the South Western Cape.

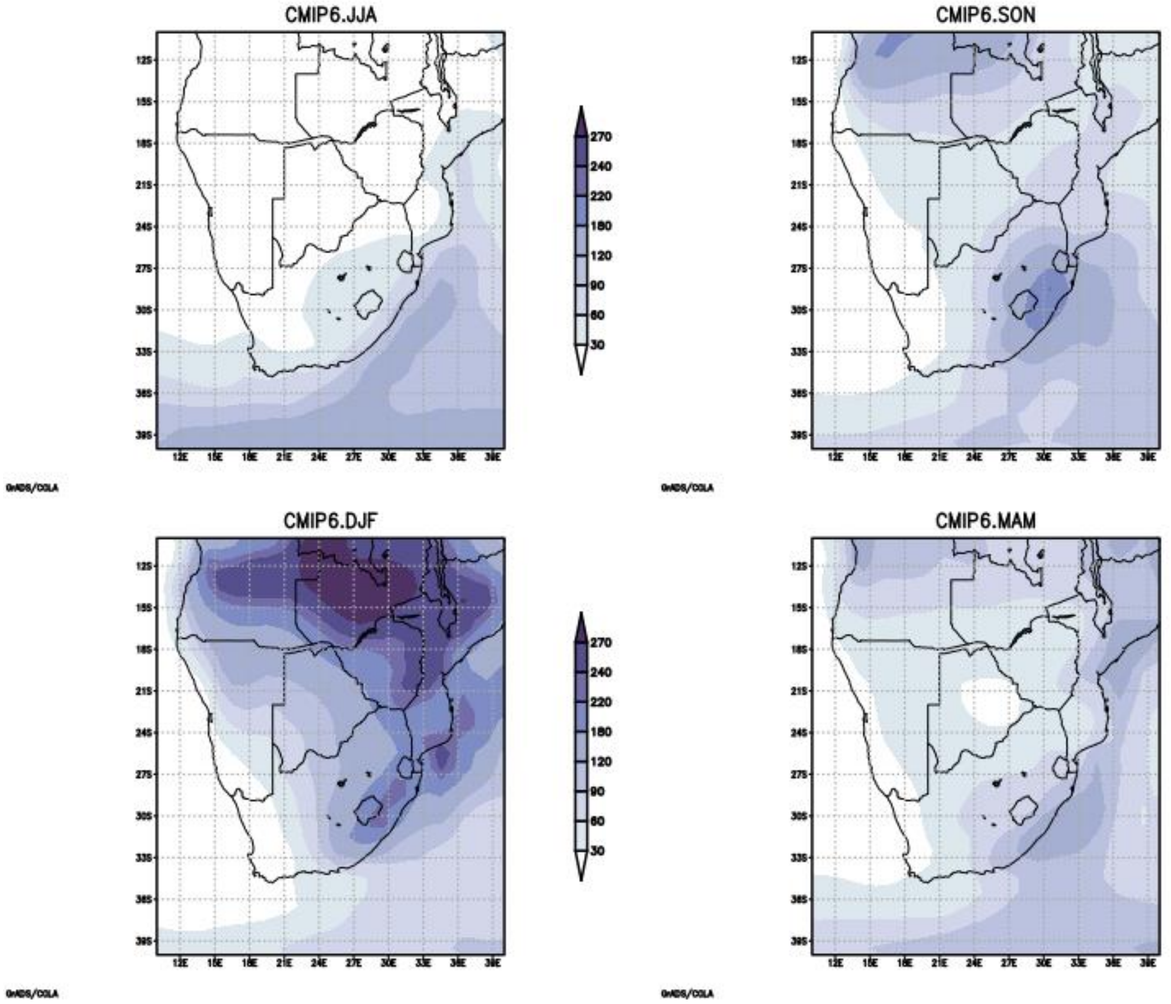

Figure 3.8: Seasonal rainfall totals (mm) over southern Africa as simulated by the CMIP6 ensemble average.

3.3.4 Mean seasonal rainfall bias

The ERA-interim data biases with respect to CRU data are indicative of general rainfall overestimations for all four seasons shown in Figure 3.9. An exception is the underestimations over the eastern escarpment regions of South Africa in summer and autumn for autumn and spring, general rainfall overestimations of rainfall over the central interior regions of southern Africa can be detected (Figure 3.9), the latter may be indicative of too frequent/intense TTT formation in Era-interim.

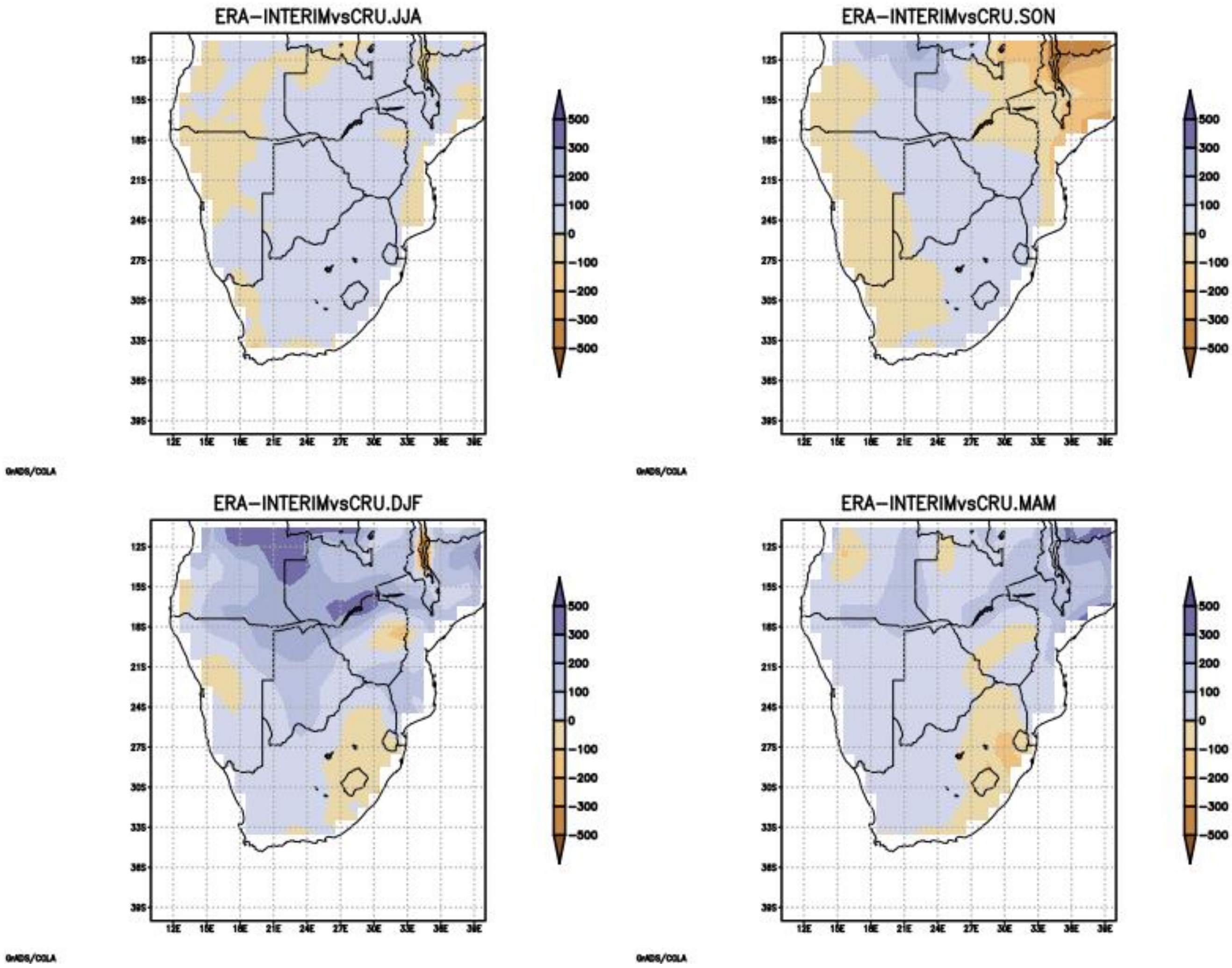

Figure 3.9: ERA-INTERIM ensemble average biases (mm) in simulating seasonal rainfall totals over southern Africa.

Bias calculations for the CMIP6 ensemble average vs CRU in (Figure 3.10) give an overall indication of rainfall underestimates over the northern interior for at least three seasons (SON, DJF, and MAM), meaning that the CMIP6 dataset underestimates the precipitation over this region. However, this underestimation is only by 100 mm, however, the rainfall underestimation intensifies in the summer months. Moreover, bias comparison also outlines an overestimation in the southern interior of South Africa particularly, and on the northern interior for the JJA season.

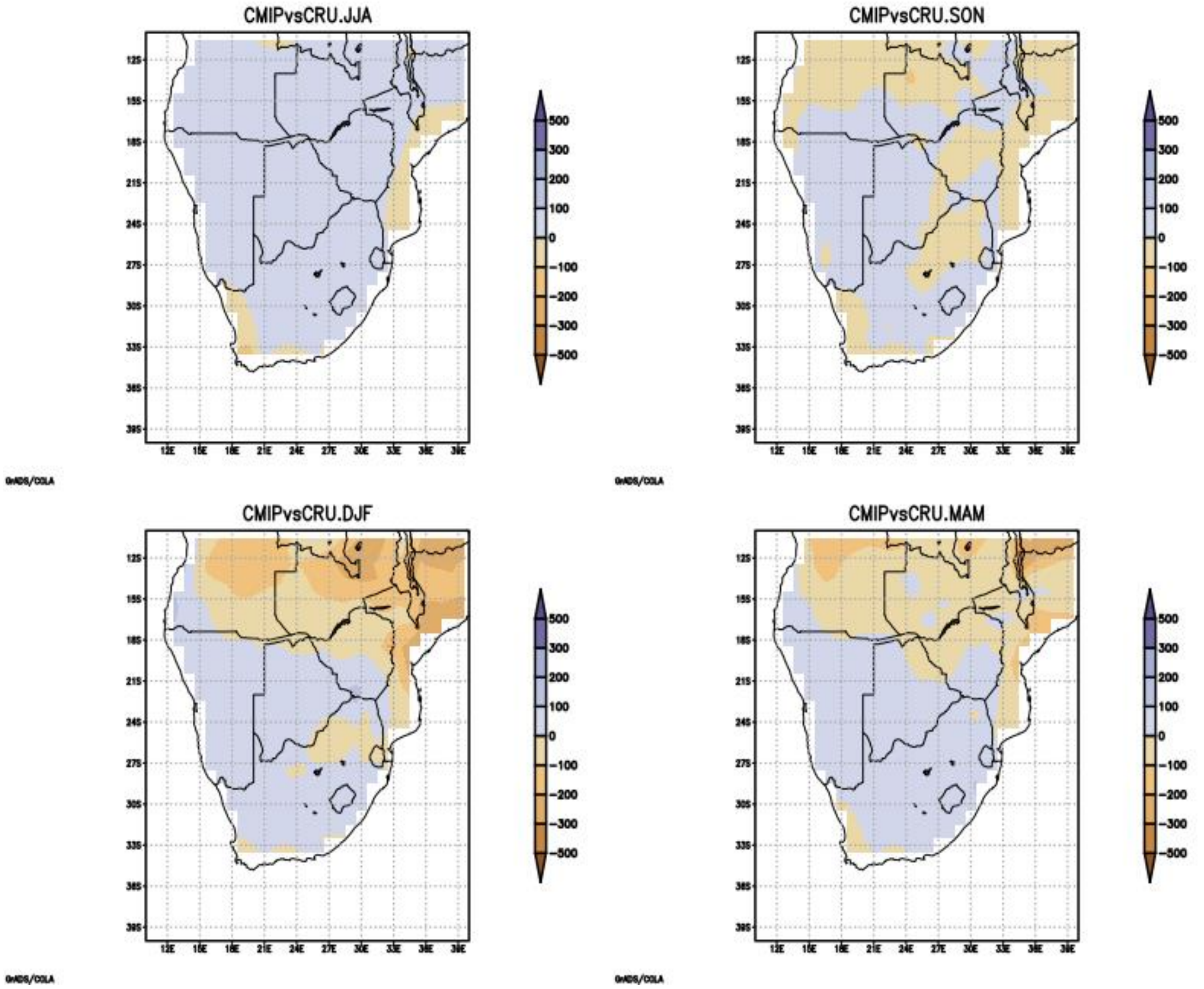

Figure 3.10: ERA-interim seasonal rainfall biases (mm) over southern Africa.

3.3.5 Regional rainfall

Graphs below demonstrate regional rainfall patterns between the observed dataset (CRU) and model ensembles (ERA-interim and CMIP6).

3.3.5.1 Cape South Coast

Observations from the CRU dataset for rainfall during the period 1979-2014, confirm that the Cape south coast is indeed an all-year-round rainfall region, with substantial amounts of rainfall occurring in all seasons. The CRU data also depicts the bimodal monthly rainfall peaks referred to by Roffe et al. (2020). The initial rainfall peak is apparent during April with a mean monthly rainfall of 52 mm and the second rainfall peak is apparent during October with 60 mm of rain (Figure 3.11). The ERA-interim data slightly underestimates the CRU rainfall values for this region (Figure 3.11). The ERA-interim data do capture the bimodal nature of the rainfall, including the April and October peaks, although the amplitude of the second rainfall peak (October) is underestimated by about 10 mm.

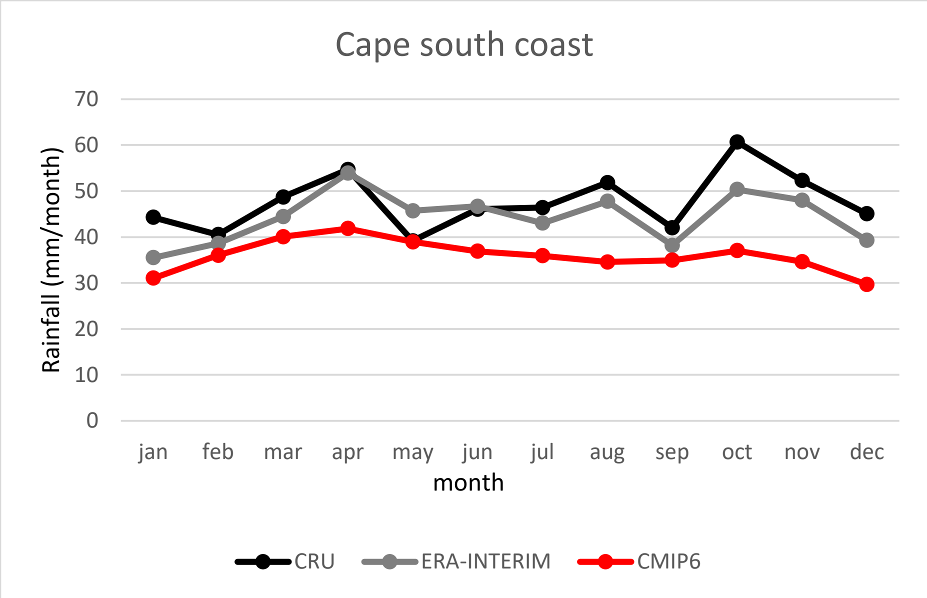

Figure 3.11: Annual cycle in rainfall (mm/month) over the Cape south coast region of Southern Africa.

3.3.5.2Eastern South Africa

Eastern South Africa encompassing Limpopo, Kwa-Zulu natal, Eastern Cape, Mpumalanga, and the interior of South Africa, is a summer rainfall region with peaks of rainfall reaching 120 mm in January and December. JJA has the lowest mean seasonal rainfall for ESA with mean monthly rainfall ranging from 0-20 mm from May until July (figure 3.12). The CMIP6 dataset overestimates rainfall for the winter months by 20mm, beginning April ending September, however, the overall trend follows that of the observation. For the summer months, CMIP6 correctly simulates the rainfall getting the summer rainfall values correct for four of the months (figure 3.12). However, the ERA-interim data underestimates the summer rainfall months, whilst overestimating rainfall for winter, which is the polar opposite of the trend expressed by the CMIP6 dataset (figure 3.12).

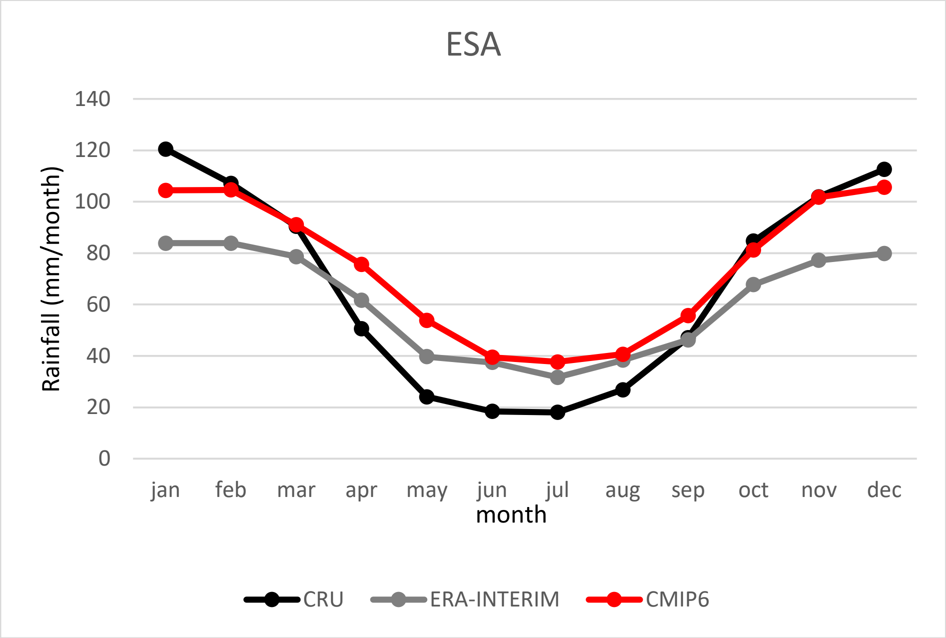

Figure 3.12: Annual cycle in rainfall (mm/month) over the Eastern southern Africa region of southern Africa.

3.3.5.3 Northern sub-continent

Figure 3.13 below, indicates observational results from the northern subcontinent, which include countries such as the Democratic Republic of Congo, some fragments of eastern Gabon, and a small portion of Angola; which are countries southwest of southern Africa. The CRU rainfall curve for the northern sub-continent specifies a high mean monthly rainfall in January at 150 mm, the following month which is February, there is an observed sharp decline in rainfall to below 150 mm, following a peak in rainfall for March; however, the highest rainfall peak is in November with a mean monthly rainfall of 200 mm. The northern sub-continent only experiences two months of below 50 mm rainfall, during June and July, which are winter months (figure 3.13). However, this region clearly distinguishes itself as a heavy precipitation region based on CRU TS 4.04 rainfall results. The two models, ERA-interim and CMIP6 agree with this trend in precipitation, however, these models overestimate and underestimate this trend for specific seasons (Figure 3.13). The CMIP6 data correctly simulates rainfall for this region for winter and slightly overestimates it for the spring and summer months. However, this is just a slight overestimation for these seasons. The ERA-interim data overestimate rainfall for the northern subcontinent by a very large margin of over 250 mm in the summer months and 100 mm for the winter and is nowhere close to feasible with the results outlined by CRU (figure 3.13). The rainfall peak for the CRU dataset is at 120 mm in October, whereas the ERA-interim data notes the rainfall to be 350 mm in October, giving a different margin of over 230 mm for the northern subcontinent.

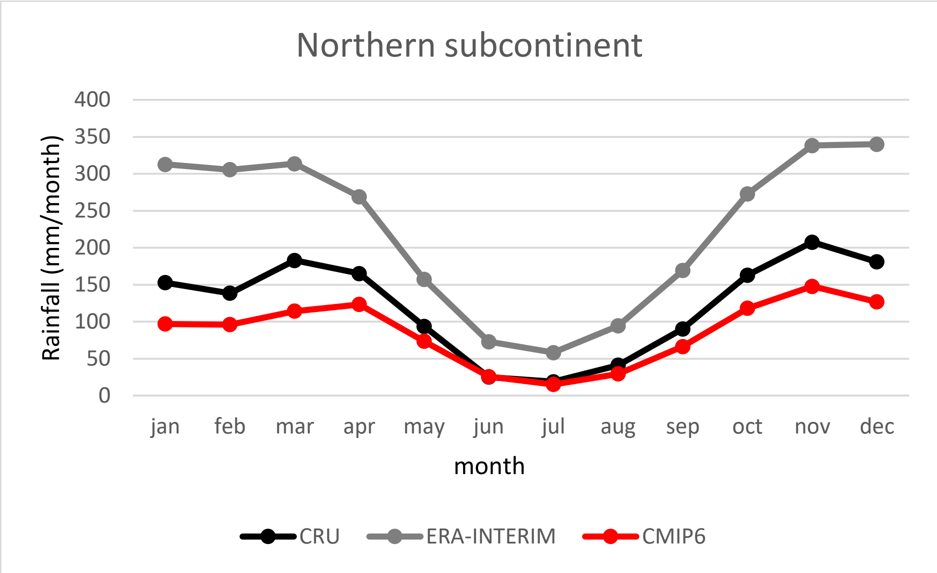

Figure 3.13: Annual cycle in rainfall (mm/month) over the Northern subcontinent region of southern Africa.

3.3.5.4 North-eastern South Africa, S Zimbabwe, and S Mozambique

This region consists of northern and eastern South Africa, southern Zimbabwe, and southern Mozambique. The NESA region, like most of southern Africa, is predominantly a summer rainfall region, however, rainfall concentration is not as high compared to the northern sub-continent (figure 3.14). The highest mean monthly rainfall for this region is <120 mm experienced in January; the winter months which are from May to August experience the lowest recorded mean monthly rainfall with recordings <20mm based on observations from the CRU dataset (figure 3.14). All the models correctly simulate rainfall for this region, however, the ERA-interim data slightly overestimates rainfall for this region from January to April by 10 mm, but for all the months it is strictly traveling in the same trajectory as the CRU dataset and the CMIP6 dataset follows the CRU trajectory from the first to the last month for the NESA region (figure 3.14).

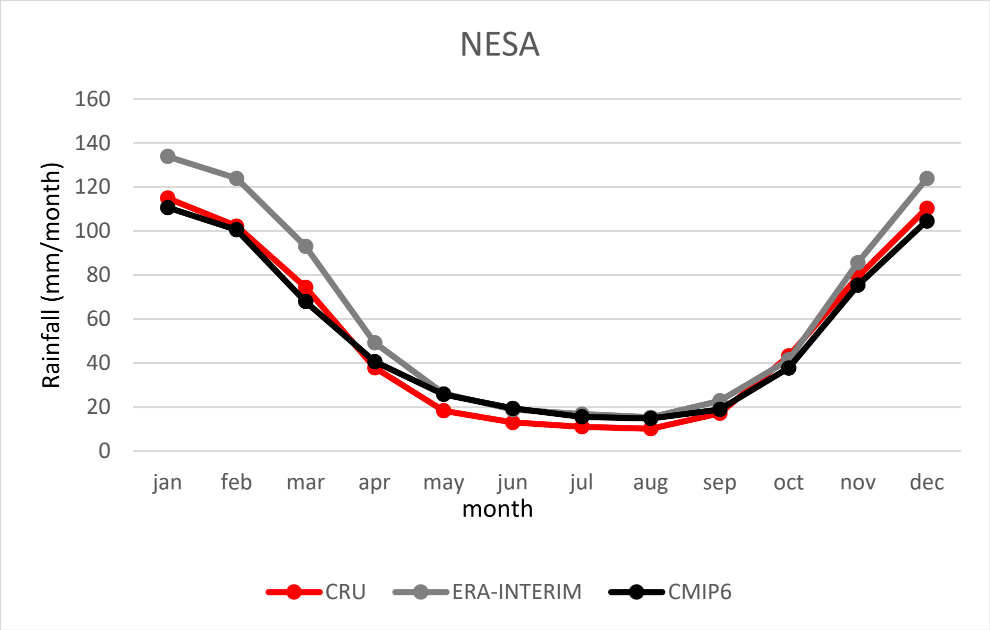

Figure 3.14: Annual cycle in rainfall (mm/month) over the North-eastern South Africa, S Zimbabwe, and S Mozambique region of southern Africa.

. *3.3.5.5 Western subcontinent*

The western subcontinent mainly consisting Northern Cape Province and the horn of Western Cape Province of South Africa. This region distinguishes itself as a usually dry region based on CRU TS 4.04 results. Rainfall peaks are <40 mm during the summer and spring months (figure 3.15). Winter months' experience extremely low rainfall recordings, sometimes reaching below 5 mm of rainfall in each month from May to September based on CRU data (figure 3.15). The CMIP6 and ERA-interim models correctly simulate the rainfall trajectory of the western subcontinent. However, the CMIP6 model overestimates rainfall for the winter season, but the ERA-Interim correctly simulates this season. Moreover, both of the models overestimate the rainfall peak in the summer months, with the ERA-interim data underestimates the peak by 15 mm whereas the CMIP6 overestimates this peak by 5mm (figure 3.15).

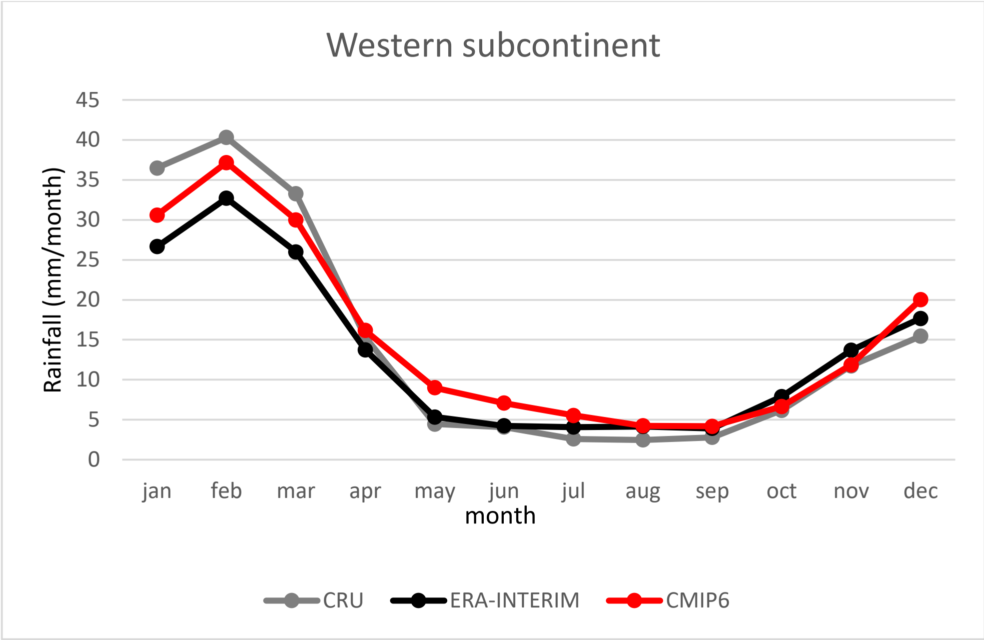

Figure 3.15: Annual cycle in rainfall (mm/month) over the Western subcontinent region of southern Africa.

3.3.5.6 South Western Cape

The winter rainfall region is confined to a relatively small area in the southwest, where gentle rain falls from May to August but the summers are dry. The highest rainfall recorded is in June with over 70 mm based on CRU TS 4.04 results. The lowest recorded rainfall is just over 10mm in January (figure 3.16). Both the models underestimate the rainfall trajectory for this region. The CMIP6 model has the highest rainfall underestimates in the winter months compared to CRU data. The CMIP6 data record the rainfall peak for the south Western Cape to be at 38 mm whereas the CRU data notes it to be just below 70 mm (figure 3.16). The ERA-interim data also underestimates rainfall for the winter season, however not to the greater extent as noted by the CMIP6 dataset, therefore the rainfall peak for this model is 50 mm. The ERA-interim data correctly simulates the summer rainfall. Whereas, the CMIP6 dataset underestimates summer rain over this region (figure 3.16).

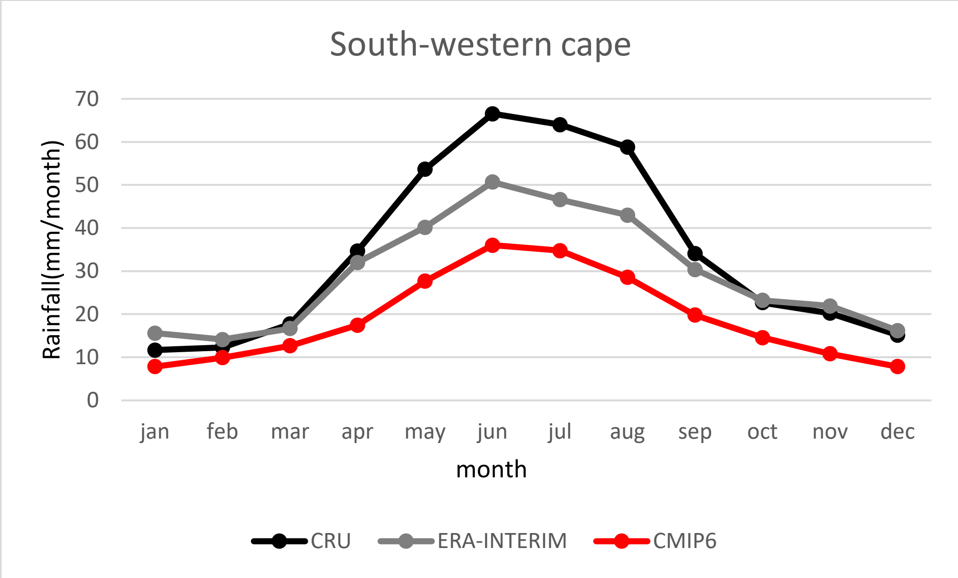

Figure 3.16: Annual cycle in rainfall (mm/month) over the South-western cape region of southern Africa.

3.3.5.7 N Mozambique and Tanzania

CRU data distinguishes northern Zimbabwe and Tanzania as a heavy precipitation region, with a rainfall peak of over 200 mm in January (figure 3.17). The lowest recorded rainfall is from May to September with readings of below 50 mm. CMIP6 and ERA-interim data correctly simulate the low rainfall periods, which are from May to September (figure 3.17). However, from DJFMA the CMIP6 model ensemble underestimates rainfall. The ERA-interim data largely follows the same pattern as CRU, with slight overestimates from DJF.

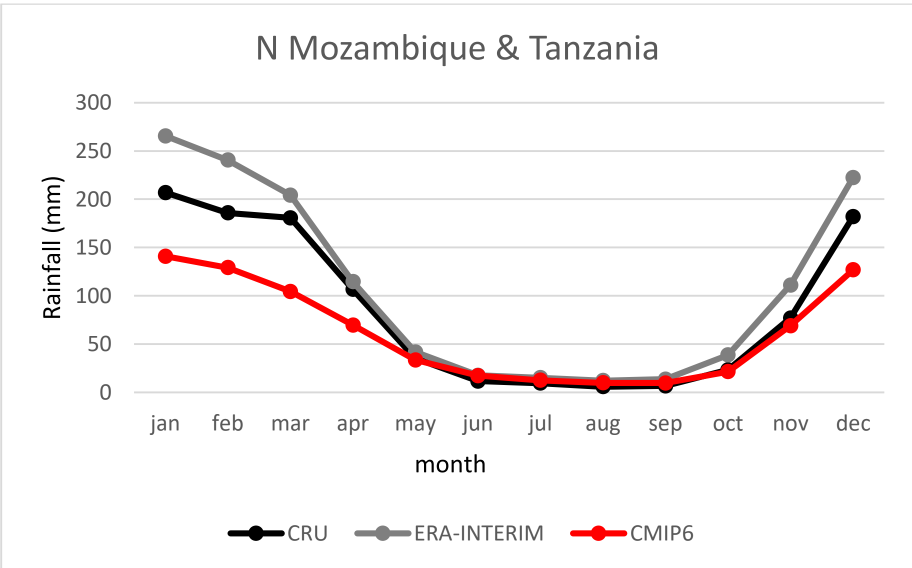

Figure 3.17: Annual cycle in rainfall (mm/month) over the N Mozambique and Tanzania region of southern Africa.

3.3.5.8 Central Subcontinent

The central subcontinent consists of the interior of South Africa and Botswana. The rainfall peak for this region is in January with a monthly rainfall of over 120 mm (figure 3.18). This region is generally dry during JJA, with a monthly rainfall of below 20 mm based on the CRU dataset (figure 3.18). Both models underestimate the summer rainfall, but only the CMIP6 overestimates the winter rainfall, whereas the ERA model correctly simulates winter (figure 3.18).

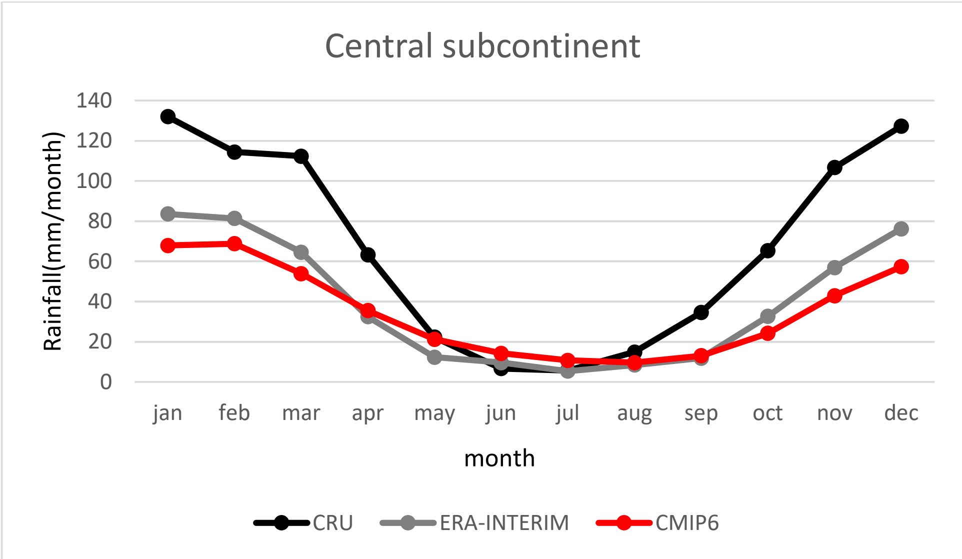

Figure 3.18: Annual cycle in rainfall (mm/month) over the Central subcontinent region of southern Africa.

3.3.5 Statistical Verification

The Taylor diagram, in general, depicts the statistical connection between two fields: a "test" field (ERA-Interim & CMIP6 model data), and a "reference" field (CRU "truth," as determined by observations) (Taylor, 2001 On a Taylor diagram the simulated fields that agree well with corresponding observations are located close to the 'observations' point on the x-axis (Taylor, 2001). These models will have relatively high pattern correlation, and low root mean square error and a standard deviation similar to that of the observations. In the application of Taylor diagrams presented here, the annual cycle of monthly means in rainfall as simulated by ERA-interim and CMIP6 are correlated to the CRU TS4.04 observations.

3.3.5.1 Cape South Coast

The Cape south coast exhibits the lowest Pearson correlation coefficients for all the regions considered, for both the ERA-interim and CMIP6 ensemble data sets (Figure 3.19). This is indicative of models struggling to fully represent the all-year nature of rainfall over this region, including the bimodal peaks. ERA-interim performs best, with a higher Pearson correlation, smaller root-mean-square-error and scaled standard deviation closer to 1 compared to observations.

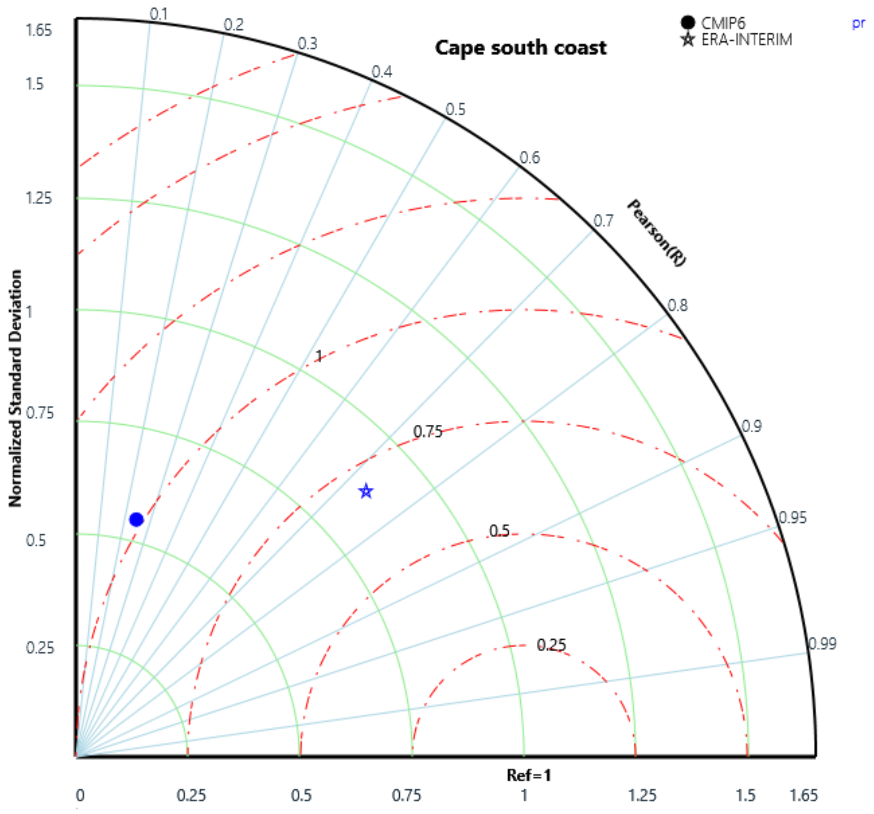

Figure 3.19: Taylor diagram of rainfall in the cape south coast, and how the models (ERA-interim and CMIP6) compared to the observations (CRU TS4.04).

3.3.5.2 Eastern South Africa

For eastern southern Africa, the CMIP6 ensemble average as well as the ERA-interim simulation display high Pearson correlations (Figure 3.20), but lower than for the domain of north-eastern South Africa and Mozambique (Figure 3.22). The root-mean-square-error is smaller for the CMIP6 ensemble average than for ERA-interim. Both simulation data sets have scaled standard deviations less than one, suggesting that the time-series of monthly rainfall totals in this region show less variation compared to reality.

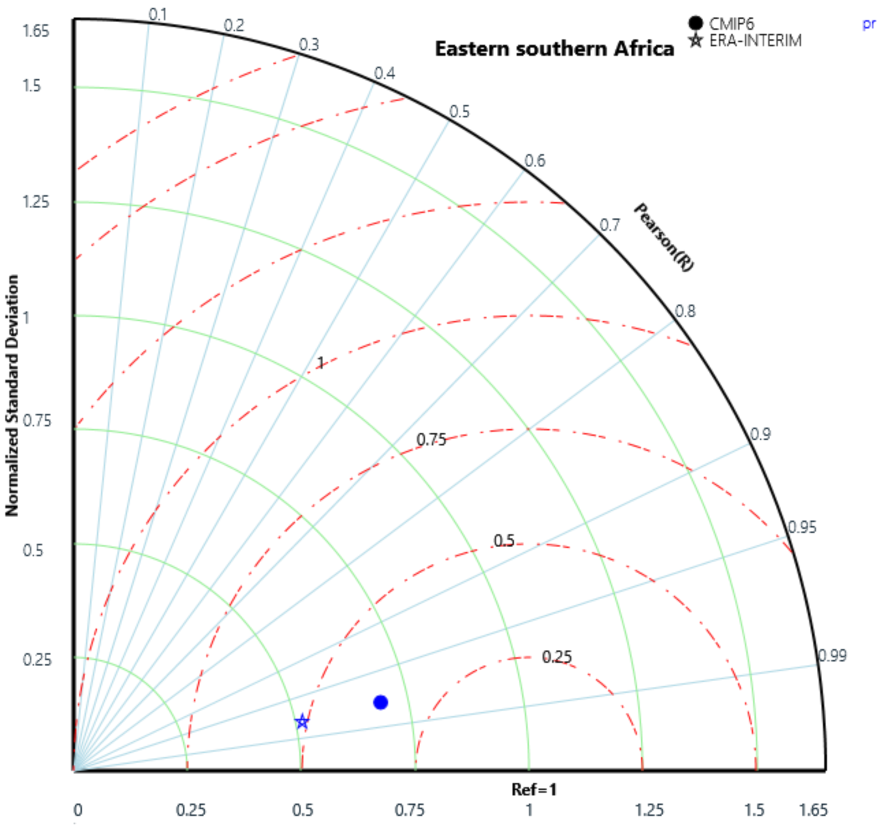

Figure 3.20: Taylor diagram of rainfall in the eastern southern Africa, and how the models (ERA-interim and CMIP6) compared to the observations (CRU TS4.04).

3.3.5.3 Northern subcontinent

For the northern subcontinent, both the CMIP6 and ERA-interim data are closely correlated to the observations in terms of the Pearson correlation (Figure 3.21). However, the CMIP6 model has slightly higher correlations to the observation with a correlation coefficient of 0.99). The scaled root mean-square error of theCMIP6 ensemble average is smaller than that for CRU. For the CMIP6 ensemble, the scaled standard deviation is less than 1, meaning that the data is not as widely dispersed as for the CRU observations. For the ERA-Interim data, the scaled standard deviation is greater than one, implying that the simulated annual cycle shows more variation in time than is observed.

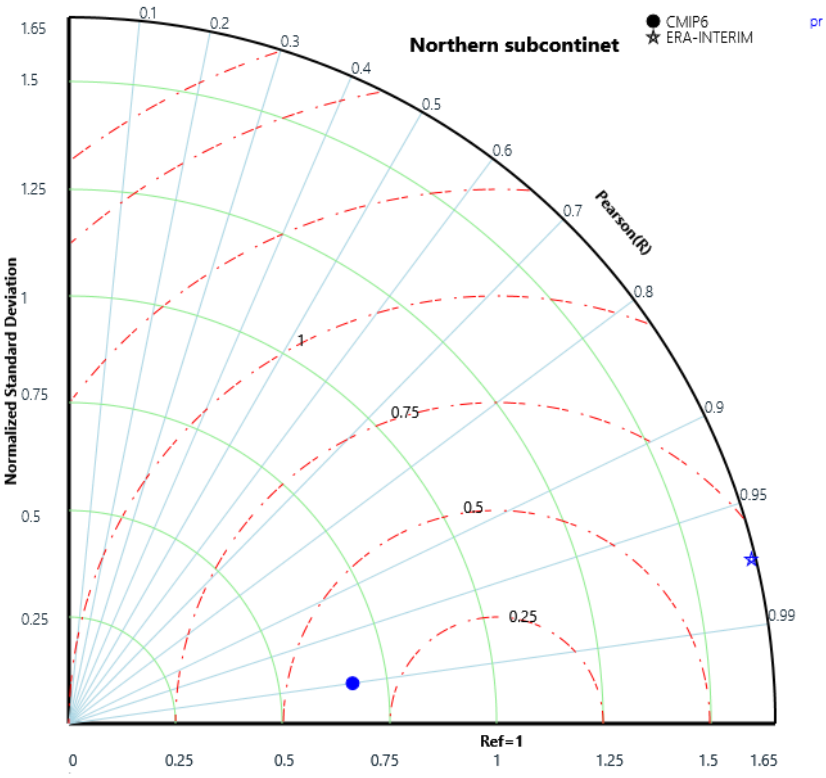

Figure 3.21: Taylor diagram of rainfall in the northern subcontinent, and how the models (ERA-interim and CMIP6) compared to the observations (CRU TS4.04).

3.3.5.4 North-eastern South Africa, S Zimbabwe, and S Mozambique

For this region in the eastern parts of southern Africa, the ERA-interim and CMIP6 annual cycle of rainfall closely resembles reality (CRU), as depicted by the very high Pearson correlations (Figure 3.22). The root-mean-square errors are also low, and the scaled standard deviations are close to 1. For CMIP6 the fields are slightly smoother than reality (scaled standard deviation less than 1) and for ERA-interim the fields are slightly more detailed than reality (Scaled standard deviations slightly greater than one). Overall, the scores are indicative that this is a region where both simulated data sets closely resemble the CRU TS4.04 annual rainfall cycle.

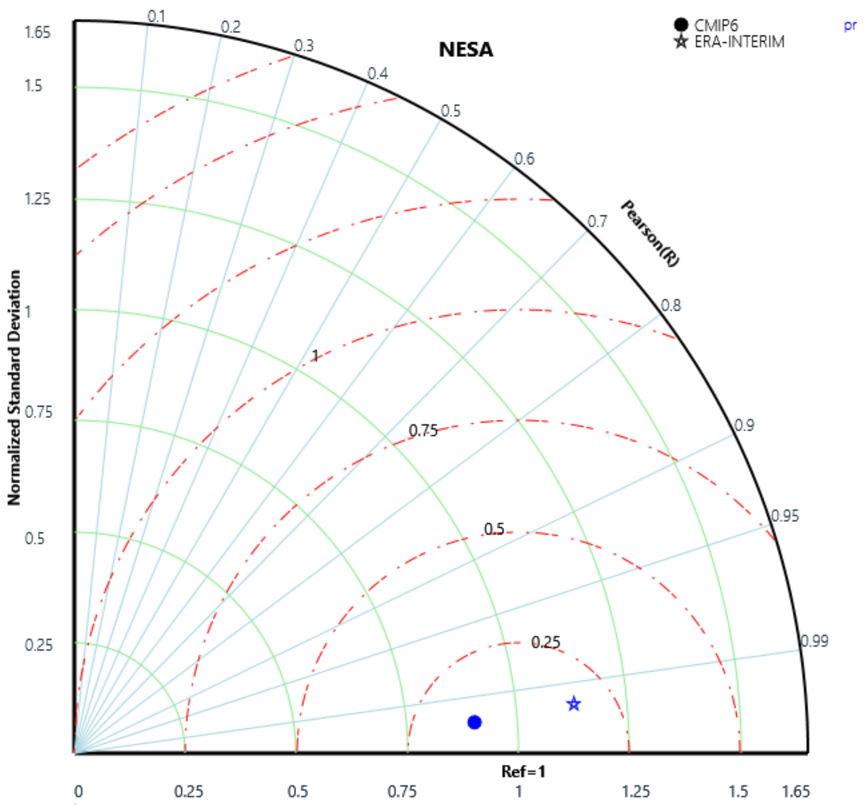

Figure 3.22: Taylor diagram of rainfall in North-eastern South Africa, S Zimbabwe, and S Mozambique, and how the models (ERA-interim and CMIP6) compared to the observations (CRU TS4.04).

3.3.5.5 Western subcontinent

For the Western subcontinent (Figure 3.23). Model performance is very similar than for the Cape South coast. Both the ERA-interim data and CMIP6 ensemble average show small root-mean-square errors and high Pearson correlations. The standard deviations are close to but less than 1, suggesting underestimations of the observed intra-annual variability.

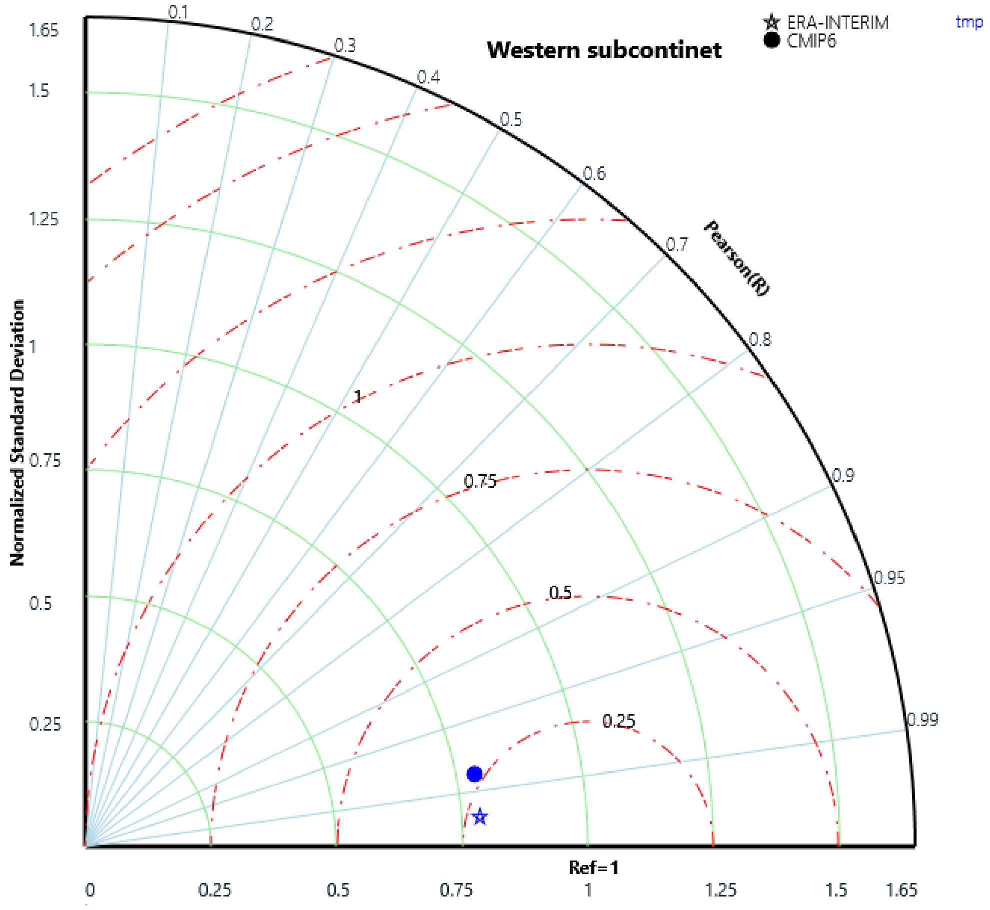

Figure 3.23: Taylor diagram of rainfall in western subcontinent, and how the models (ERA-interim and CMIP6) compared to the observations (CRU TS4.04).

3.3.5.6 South Western Cape

In the figure below, it can be seen that models CMIP6 and ERA-interim generally agree with observations, with each having about the same and very high (0.99) pattern (in this case Pearson) correlation coefficients (Figure 3.24). This indicates that the annual cycle of rainfall over the south Western Cape closely resembles that of observations. The ERA-interim data exhibits a smaller root-mean-square-error than the CMIP6 ensemble, as well as a scaled standard deviation closer to 1, but still less than one. This implies that for both the ERA-interim and CMIP6 simulations, the annual cycle of rainfall shows less variation than the corresponding observed cycle.

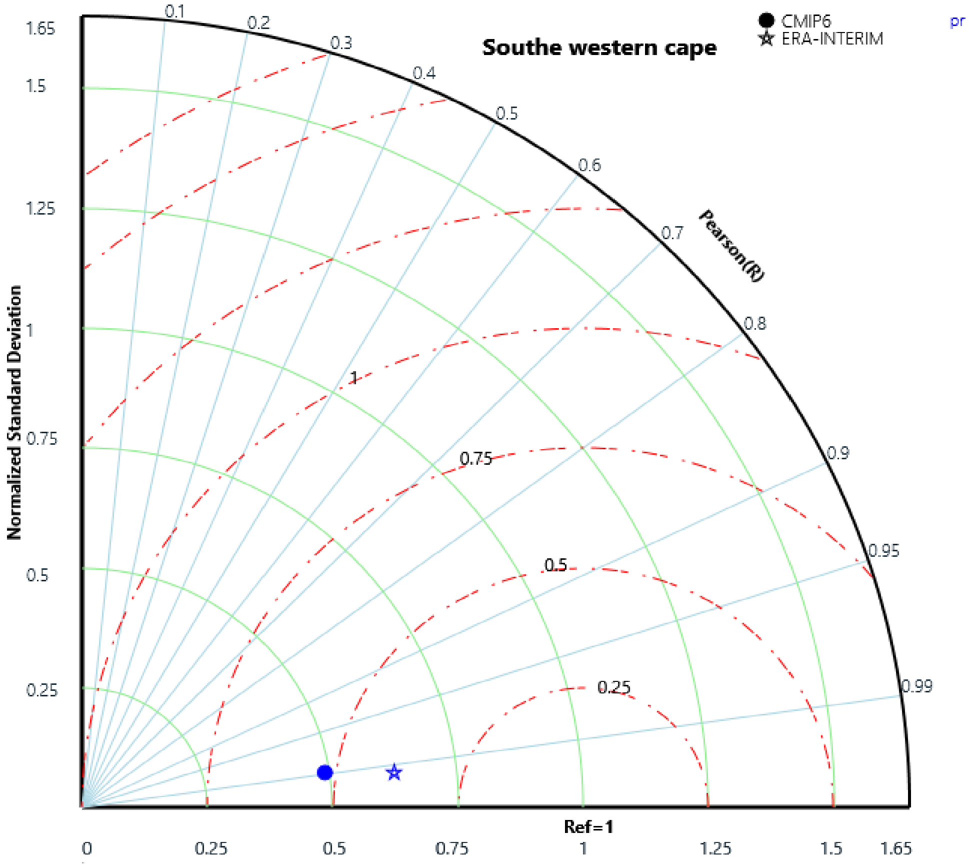

Figure 3.24: Taylor diagram of rainfall in the South Western Cape, and how the models (ERA-interim and CMIP6) compared to the observations (CRU TS4.04).

3.3.5.7 N Mozambique and Tanzania

Figure 3.25 shows that for the northern Mozambique and Tanzanian region, both the CMIP6 ensemble average and ERA-interim monthly time-series data are strongly correlated to the observed time-series. The root-mean-square-error is smaller for ERA-interim, which has a scaled standard deviation greater than 1. This means that the annual cycle in ERA-interim shows more variation across months than the CRU TS4.04 cycle. For the CMIP6 ensemble average, the monthly variations are less variable than is observed (scaled standard deviation less than one).

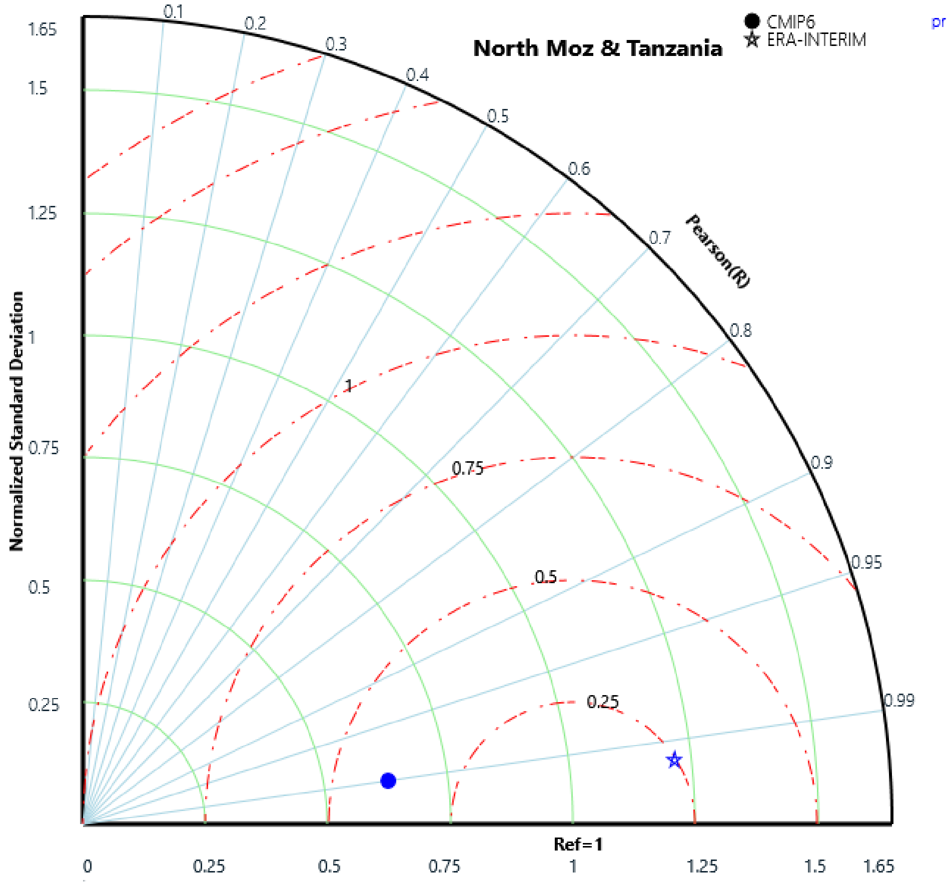

Figure 3.25: Taylor diagram of rainfall in the Northern Mozambique and Tanzania, and how the models (ERA-interim and CMIP6) compared to the observations (CRU TS4.04).

3.3.5.8 Central subcontinent

For the northern subcontinent (Figure 3.26), the Pearson correlations are high for both simulation data sets, but with ERA-interim a higher Pearson correlation, smaller root-mean-square error and a scaled standard deviation close to one compared to that of the CMIP6 ensemble. For both simulation data sets, the scaled standard deviation is less than one, indicating an annual cycle showing less variability across months compared to reality.

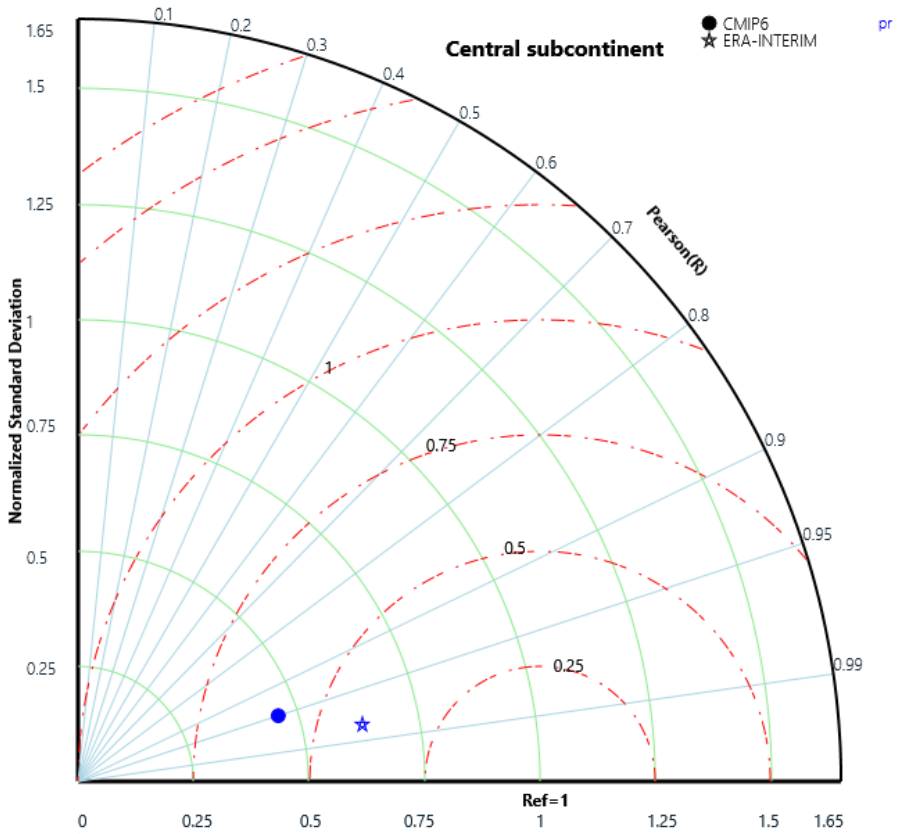

Figure 3.26: Taylor diagram of rainfall in the Central subcontinent, and how the models (ERA-interim and CMIP6) compared to the observations (CRU TS4.04).

3.4 Model verification: Temperature verification

In this section, the ERA-interim and CMIP6 ensemble simulations of temperature patterns over southern Africa are verified, as before, with a focus on seasonality. Average temperature from the CRU TS4.04 data set is used as a representation of reality. The verification period, as before, is 1979-2014.

3.4.1 Mean annual temperature

Figures 3.27 to 3.29 show the mean annual temperature from our three data sets used (CRU TS4.04, ERA-interim, and CMIP6, respectively). Results are shown for the period 1979-2014, as before. This comparison is done to see how well the models simulate present-day annual temperature, compared to the observed/reference dataset (CRU).

The CRU dataset (observed/reference), indicates low temperatures over the central interior of southern Africa, which decline particularly over the eastern escarpment of South. A local temperature maximum occurs in the Zambezi river valley (Figure 3.27). The ERA-interim mean annual temperatures also indicate the same temperature pattern as the reference dataset, with lowest temperatures over the eastern escarpment of South Africa. The ERA-interim data has sufficiently high spatial resolution to realistically portray the Zambezi river temperature maximum (Figure 3.28). The CMIP6 ensemble average also portrays this general pattern of lowest temperatures over the eastern escarpment of South Africa. The CMIP6 simulations are not of sufficiently high resolution to represent the temperature maximum in the Zambezi river valley (Figure 3.29).

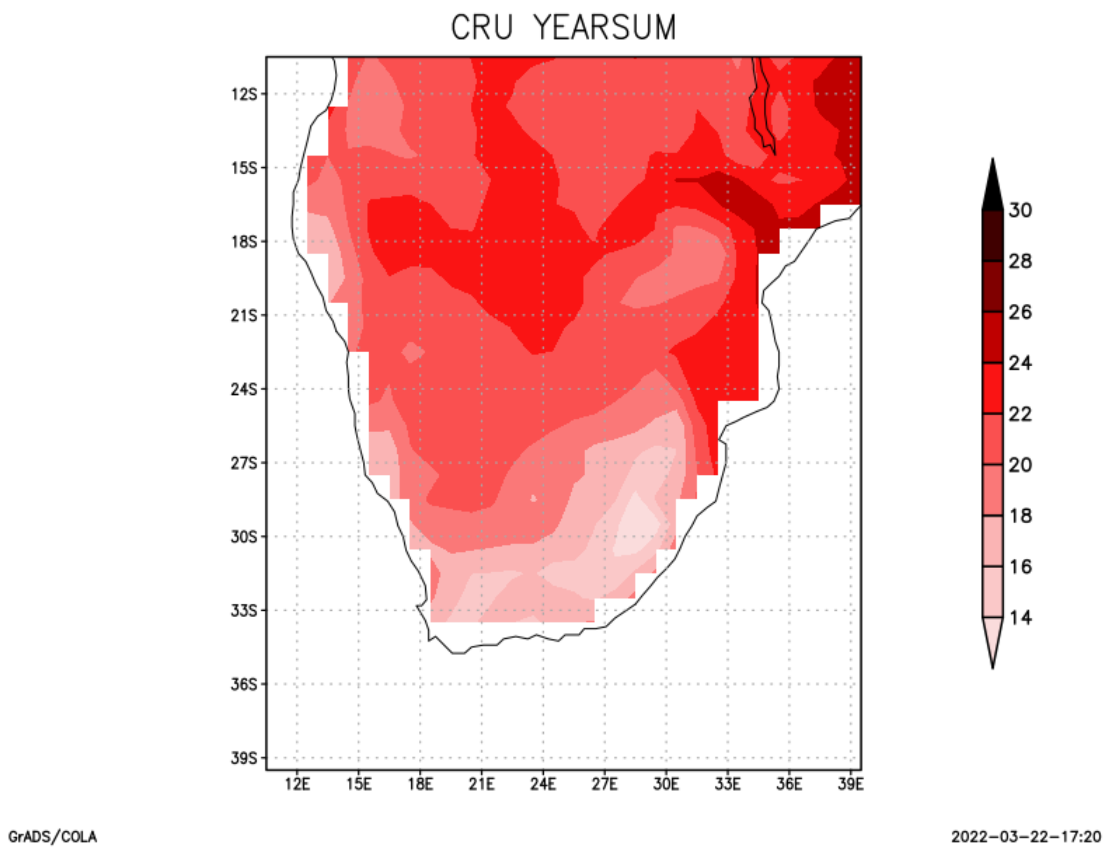

Figure 3.27: CRU TS4.04 annual average temperature (°C) over southern Africa for the period 1979-2014.

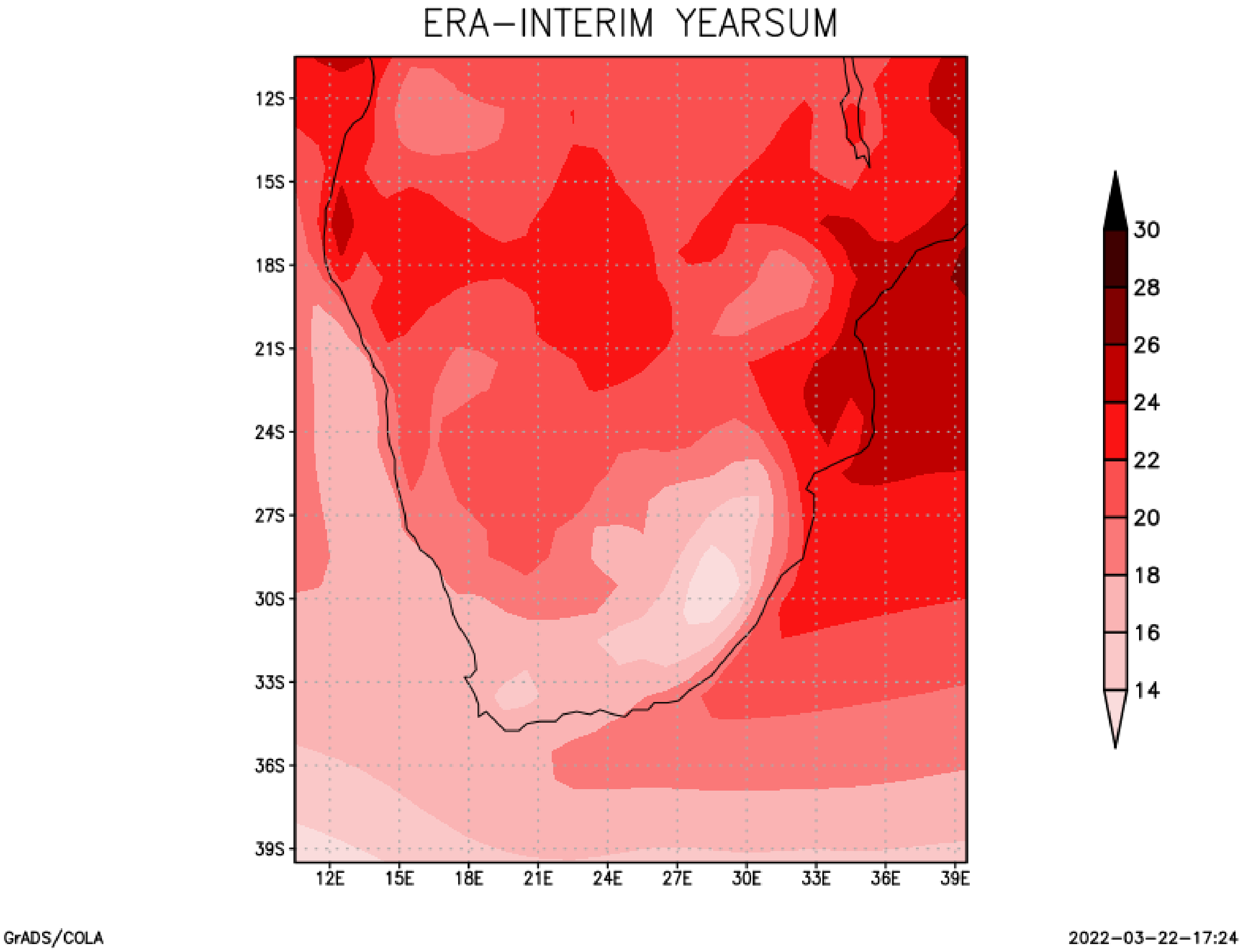

Figure 3.28: ERA-interim annual average temperature (°C) over southern Africa for the period 1979-2014.

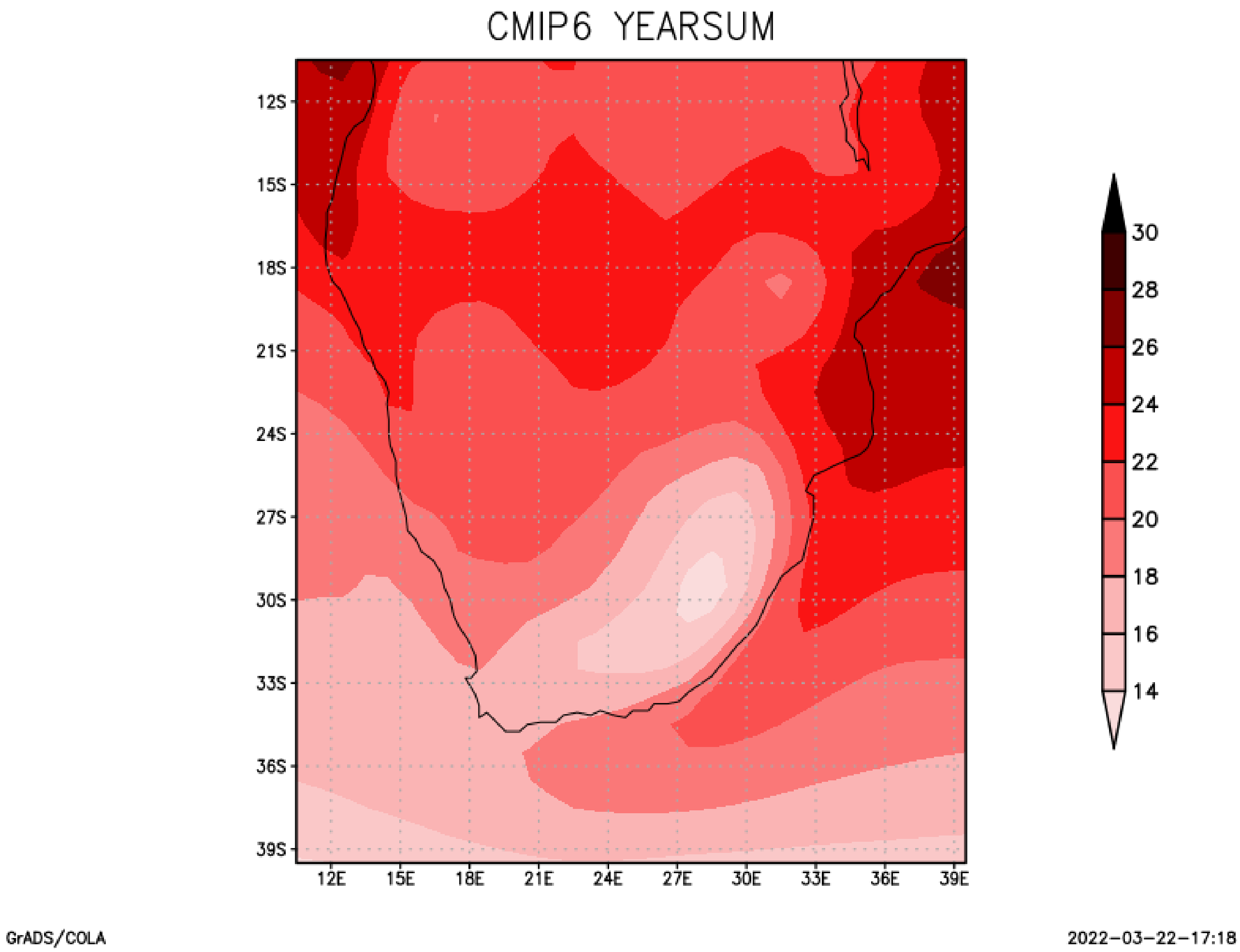

Figure 3.29: CMIP6 annual average temperature (°C) over southern Africa for the period 1979-2014.

3.4.2 Mean annual temperature bias

The annual bias for the ERA-INTERIM versus the CRU dataset indicates a general trend of temperature underestimates over the entire spatial extent. However, there is a positive bias from the coast of Namibia towards the coast of Congo. Additionally, some regional patches with a positive bias over Namibia and the North West province of South Africa (figure 3.30).

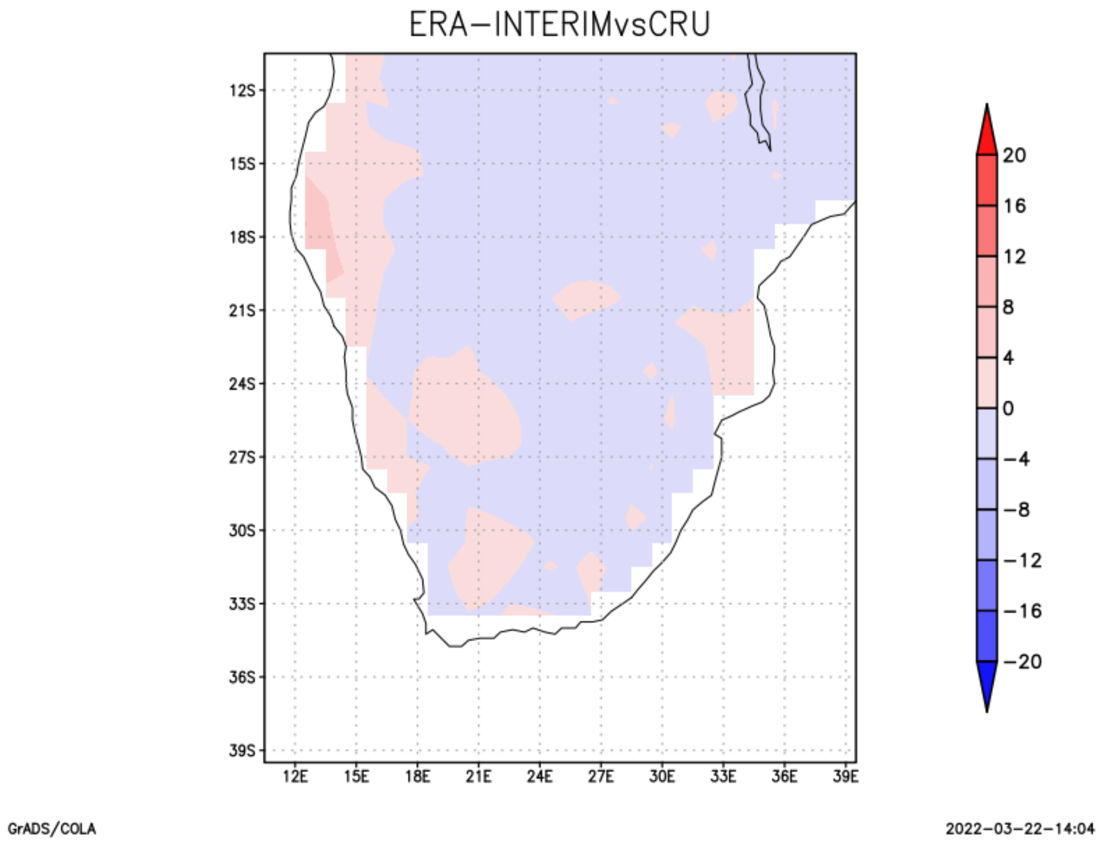

Figure 3.30: ERA-interim bias (°C) in representing average annual temperature over southern Africa.

The bias relation between the CMIP6 model and the CRU datasets is spatially dispersed. The CMIP6 model indicates a slight annual temperature underestimate (negative bias) over the eastern portion of southern Africa, from South Africa, and extending northwards towards the equator. However, the overestimation (positive bias) seen on the ERA-INTERIM data over the western border is also observed in the CMIP6 data. Although, not to the same extent as in the ERA-INTERIM dataset. In the case of CMIP6, the positive bias extends from the western border of Namibia and Congo towards the central subcontinent and inhibits a majority of the central subcontinent.

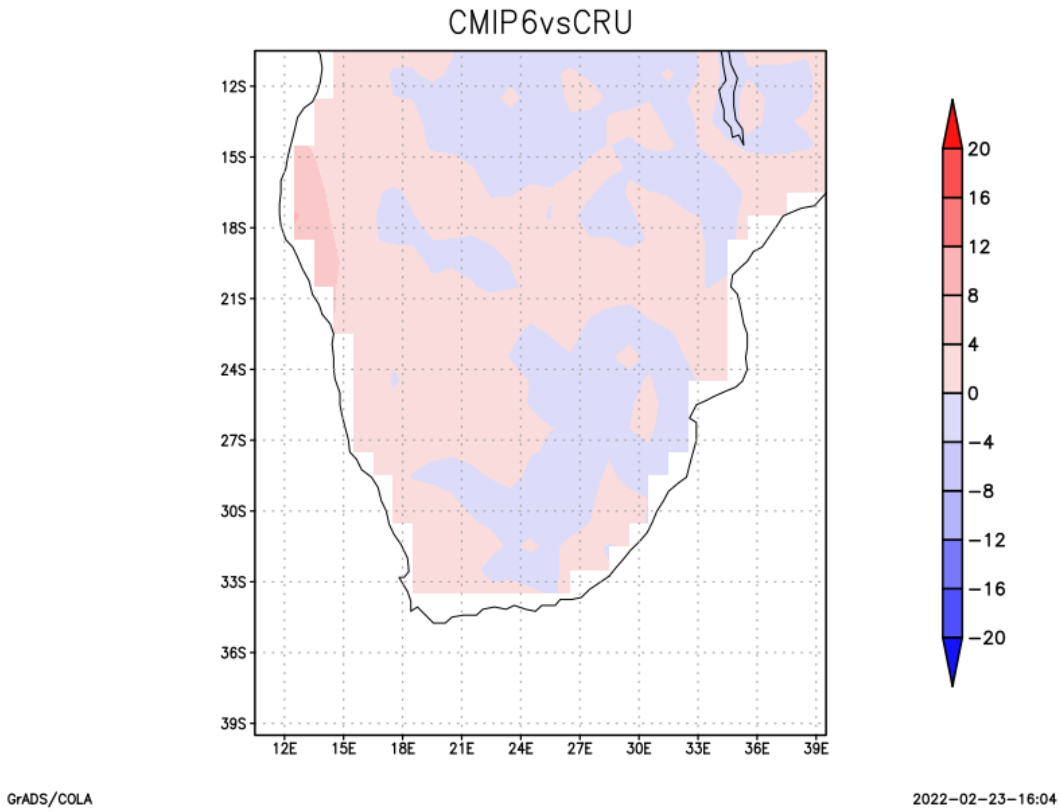

Figure 3.31: CMIP6 bias (°C) in representing average annual temperature over southern Africa.

3.4.3 Mean seasonal temperature

Figure 3.32 below, indicates CRU TS 4.04 seasonal temperature patterns indicate that southern Africa (10 degrees south of the African continent) experiences summer highs up to 28°C, with averages at 25°C seasonally. According to the CRU data, the JJA season is a cold season, with persisting low temperature over the eastern escarpment and extending towards the cape Fold Mountains, with a temperature of 4°C. The cold temperatures persist for this season northwards, but gradually start increasing towards the equator (Northern subcontinent). Furthermore, during the spring month SON, temperatures begin to get slightly hoter. However, the cold trend over the eastern portion of South Africa is slightly persisting, with observed temperatures of 8-10°C. These cold temperatures are also slightly apparent on the coast of Namibia and Angola, with temperatures 10-12°C. During the DJF season, which is the summer month temperatures are generally high over the subcontinent, except for a small portion bordered in Lesotho. Generally, average temperatures for the DJF season are above 20°C for the entire southern Africa region. Furthermore, for the autumn month (MAM) there is a general trend of lower temperatures over the interior of South Africa, with intensified cold peaks over Lesotho. Moreover, from the border of South Africa moving northward temperatures begin to increase towards the equator (figure 3.31).

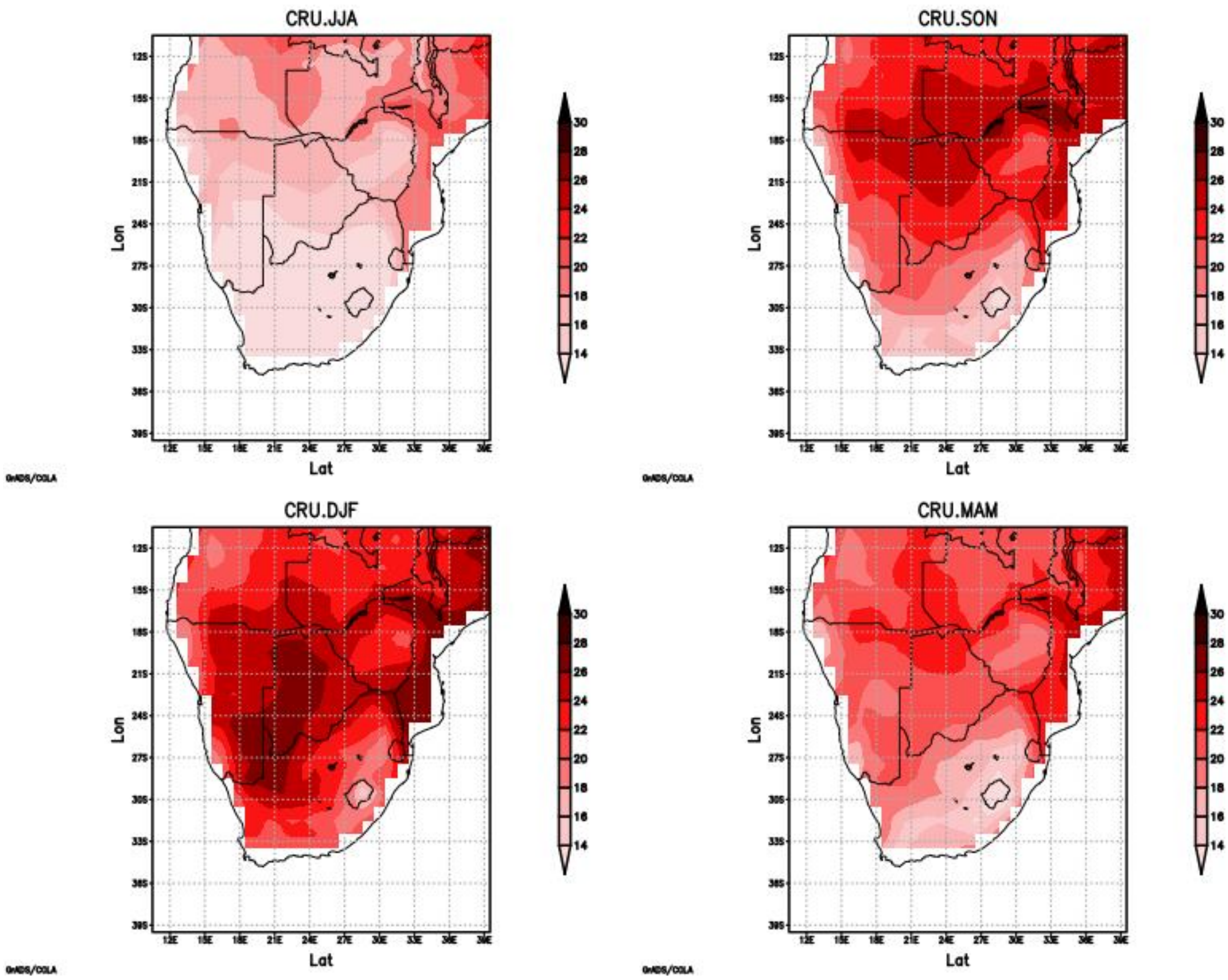

Figure 3.32: CRU TS4.04 representation of seasonal average temperatures (°C) over southern Africa, for the period 1979-2014.

The figure 3.32 below, indicates ERA-interim seasonal temperature trends. For the JJA season, the cold temperatures persist over the interior of South Africa. Temperatures over the interior of South Africa for JJA are between 10-14°C. In the ERA-interim dataset for winter, we see these cold temperatures persisting northward. The ERA-interim dataset for the JJA season indicates that from the northern border of South Africa extending northwards temperatures increase. Therefore, the northern and central subcontinent experience average temperatures of 20-25°C approaching the equator for the ERA-interim dataset. Furthermore, for the spring month (SON), according to the ERA data the entire sub-continent experience predominantly high temperatures reaching over 30°C in the central subcontinent, with the eastern escarpment remaining generally cold for SON. The cold southern Africa temperatures and the Lesotho cold temperatures are apparent over the ERA-interim dataset. Moving over to the summer season, which is the (DJF) season, this season is generally hotter. However, the ERA dataset shows these temperature increases to be slightly lower than the reference dataset CRU. The cold temperatures over Lesotho are still apparent in this dataset for the DJF season. Furthermore, the autumn season (MAM), indicates the cold trend over Lesotho. Moreover, the hot temperature trends persist for this season as well with high temperatures on the coast of Namibia, Angola, and Mozambique.

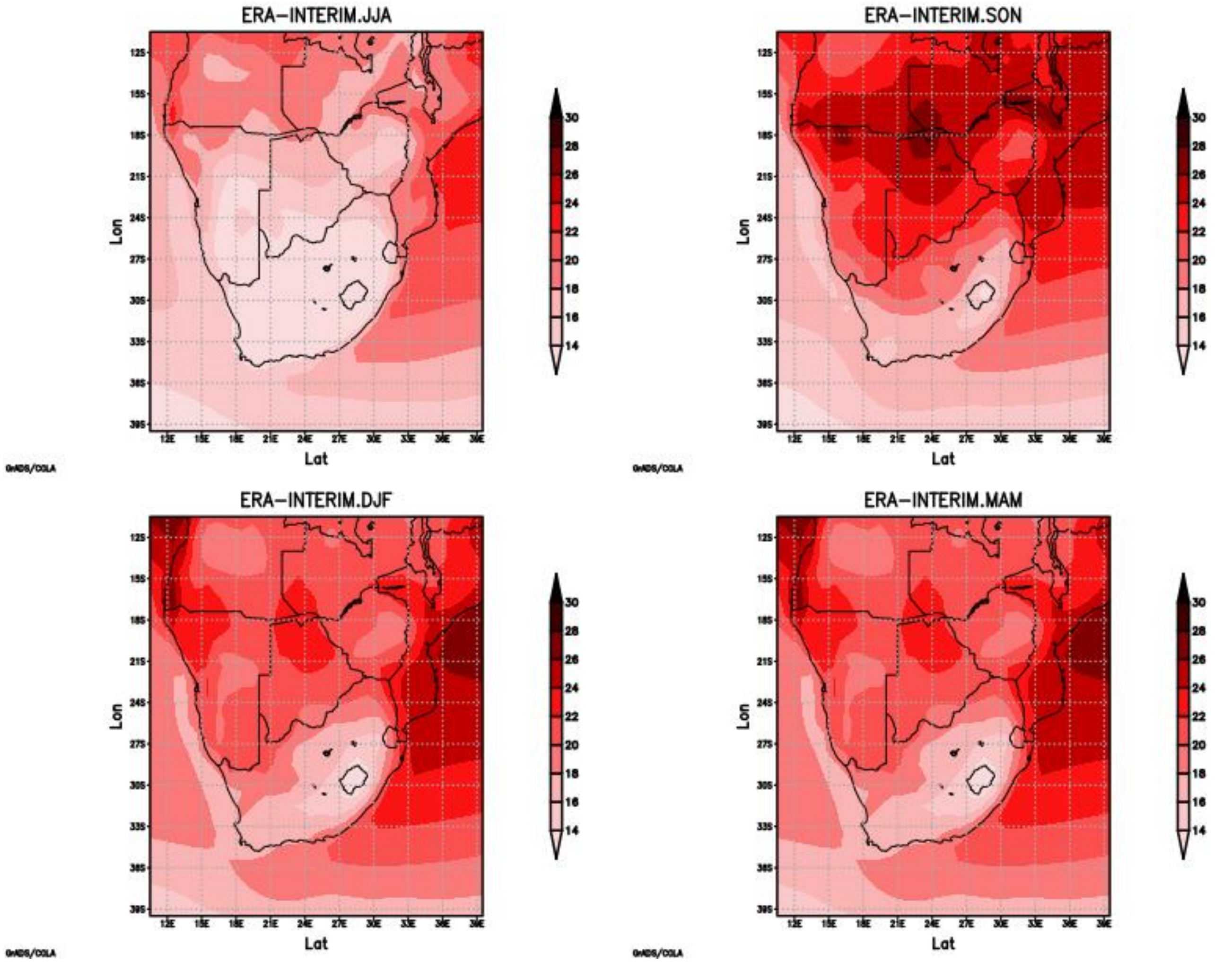

Figure 3.33: ERA-interim representation of seasonal average temperatures (°C) over southern Africa, for the period 1979-2014.

The figure 3.33 below, represents results for mean seasonal temperatures for the CMIP6 model dataset. For the JJA season, the CMIP6 dataset indicates general cold temperatures, since this is the winter season. The cold temperatures persist for the JJA northward towards the equator, with only Mozambique remaining generally hot with above 20°C temperatures. Moreover, for the spring season (SON), temperatures are generally cold over the entire interior of South Africa. However, for SON hot temperatures over the central subcontinent and the northern subcontinent (>20°C). Moreover, the summer season (DJF), indicates generally hot trends over this season, average temperatures for this season are above 25°C. Furthermore, for the autumn season (MAM), there are general hot temperatures, however, only the eastern escarpment is cold for this season.

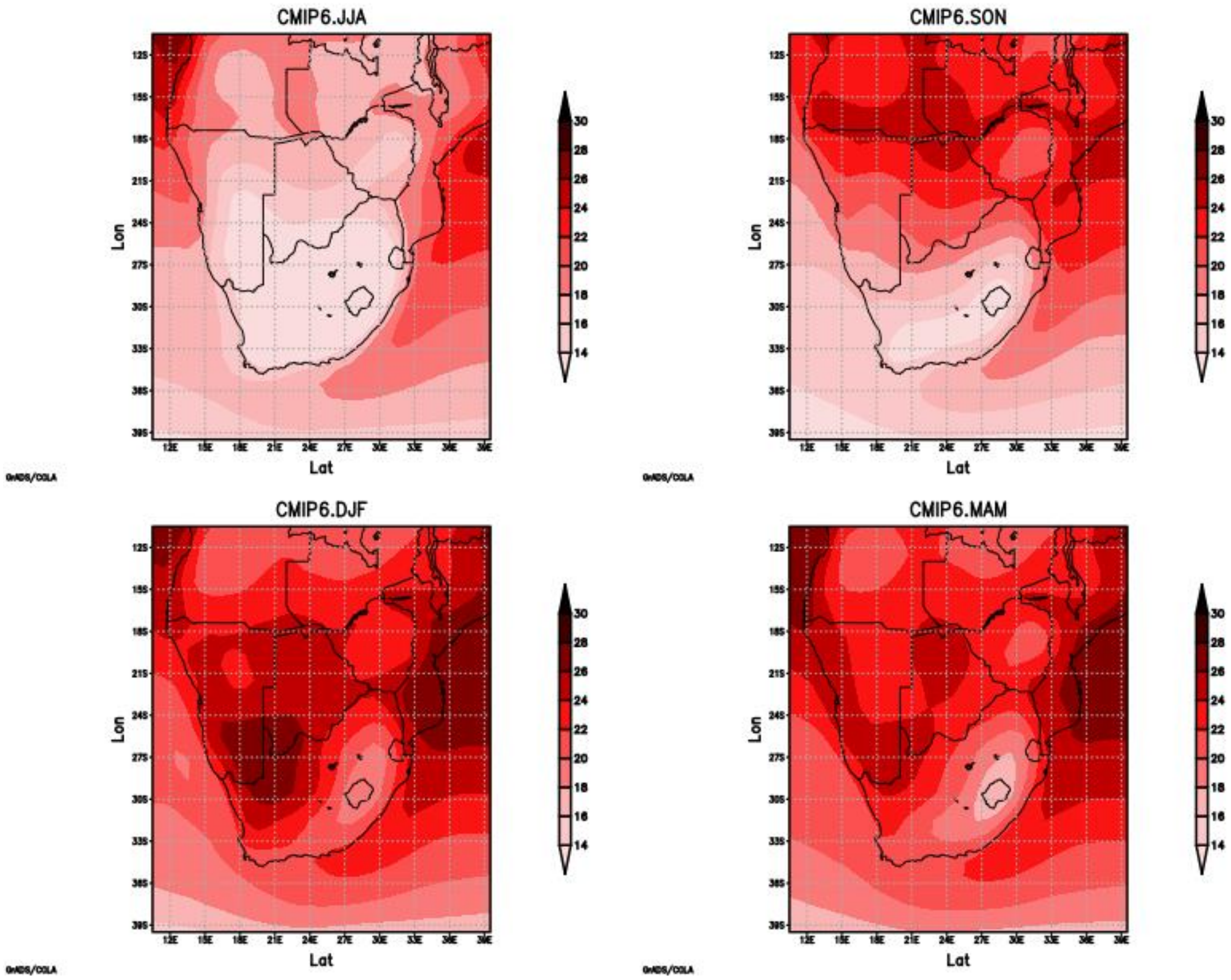

Figure 3.34: CMIP6 representation of seasonal average temperatures (°C) over southern Africa, for the period 1979-2014.

3.4.4 Mean seasonal temperature bias

The illustration below (figure 3.34) indicates the seasonal bias of the ERA-interim dataset versus the observations on the CRU dataset. The winter season (JJA), indicates that there is a negative (shows a declining pattern), with temperature underestimates of -4°C particularly over the eastern portion of southern Africa, from the west coast of South Africa reaching the coastlines of the interior of Namibia. Therefore, the general bias for this season a predominantly negative/low over most of the subcontinent. However, there is a persistent positive/high bias on the coast of Angola during the JJA season. Furthermore, the spring season (SON), has an increased/positive bias to the observed reference data, spreading even to the eastern portion of the region and extending northward towards the equator. Although, with slight patches of negative bias in the Interior of Mozambique, Botswana, and central Congo. However, it is also worth noting the persisting high bias over the Congo coast, which translated from the JJA season. Furthermore, for the summer (DJF) season, this season experiences negative/low bias over the northern subcontinent. Moreover, for the DJF season, South Africa mostly has a positive bias and the sharp positive bias on the coast of Congo. Finally, this MAM season has a general negative bias over this region.

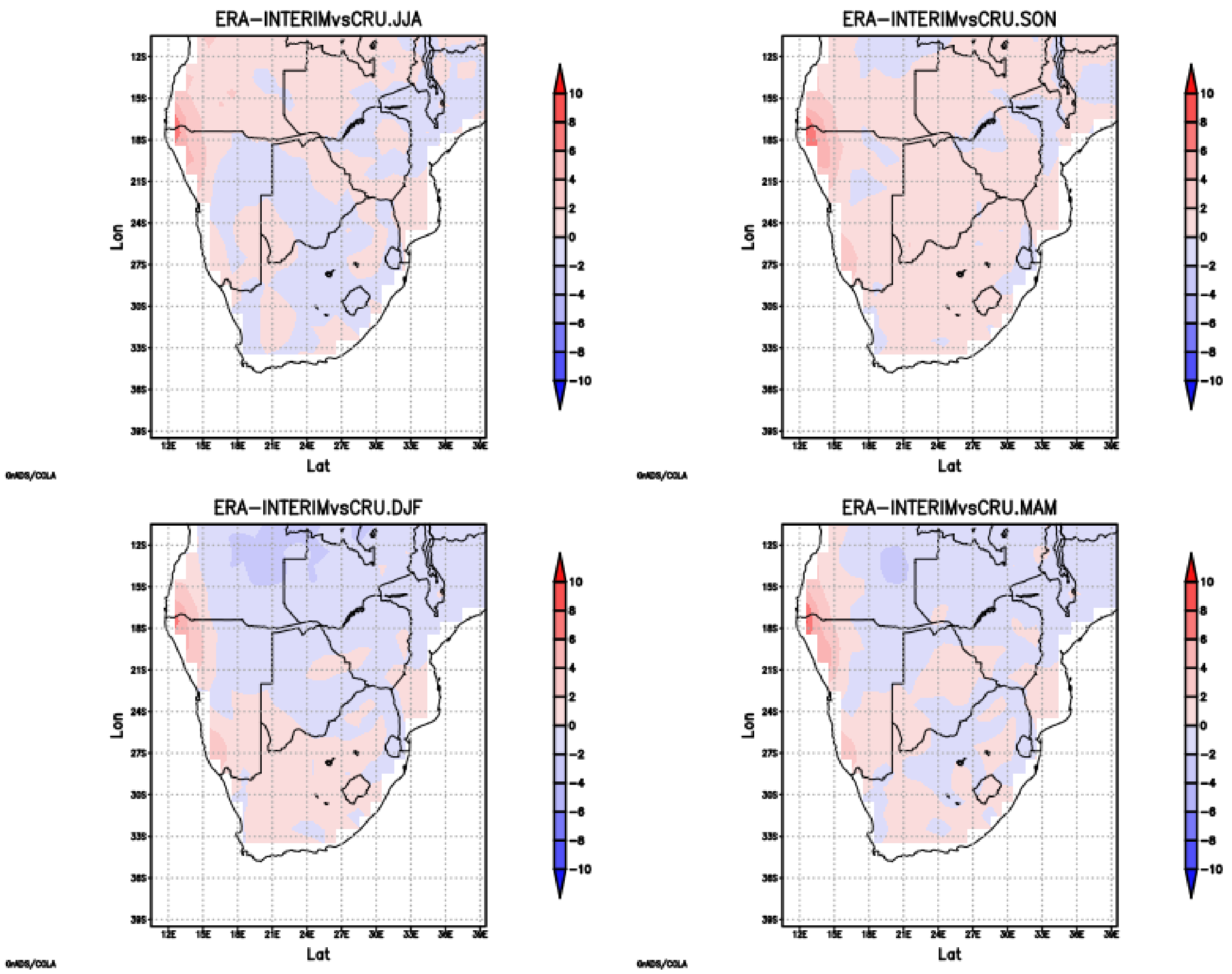

Figure 3.35: ERA-interim biases in representing seasonal average temperatures (°C) over southern Africa, over the period 1979-2014.

The figure 3.35 below is an illustration of the bias between the CMIP6 data versus the CRU dataset. The first spatial map is an illustration of the winter temperature trend. The general trend for this season is generally low, with only a small portion on the border of Angola and Namibia being over 2°C. However, the general bias for JJA is largely negative over the subcontinent. Moreover, during the spring season, the general bias, for this reason, is negative, meaning there are slight underestimates over the region. Therefore, for the summer season, the general negative bias is persistent over the region during this season. However, for the same season DJF, there are also slight overestimates on the south western coast of above 2°C. Furthermore, the general bias for autumn (MAM) is generally high over the entire subcontinent, and the overestimates increase towards the western subcontinent with a bias at over 4°C.

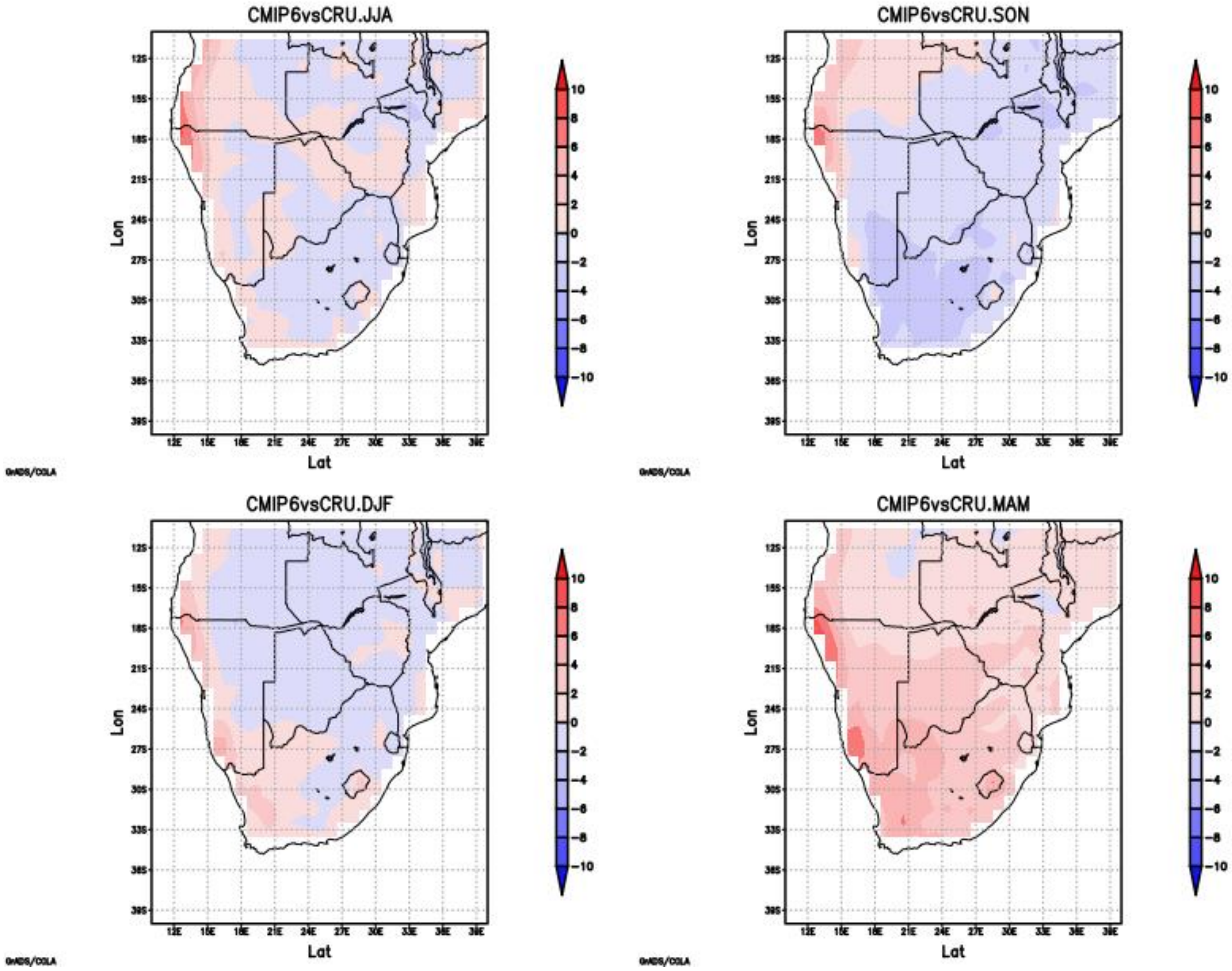

Figure 3.36: CMIP6 biases in representing seasonal average temperatures (°C) over southern Africa, over the period 1979-2014.

3.4.5 Regional temperature

Graphs below demonstrate regional temperature patterns between the observed dataset from (CRU) and the model ensembles (ERA-interim and CMIP6).

3.4.5.1 Cape south coast

Figure 3.37 indicates observational results from the CRU dataset for temperature during the period 1979-2014. This region is a generally cold region, with average monthly temperature reaching about 23°C in February, and the lowest monthly average temperature recorded in the winter months (~ 12°C). The ERA-interim dataset follows the same pattern as the CRU dataset, however, it overestimates the temperature over the region by about 3°C during the winter months. The CMIP6 also correctly portrays the pattern of cold-hot seasonality, and similarly overestimates the winter temperature by 3°C.

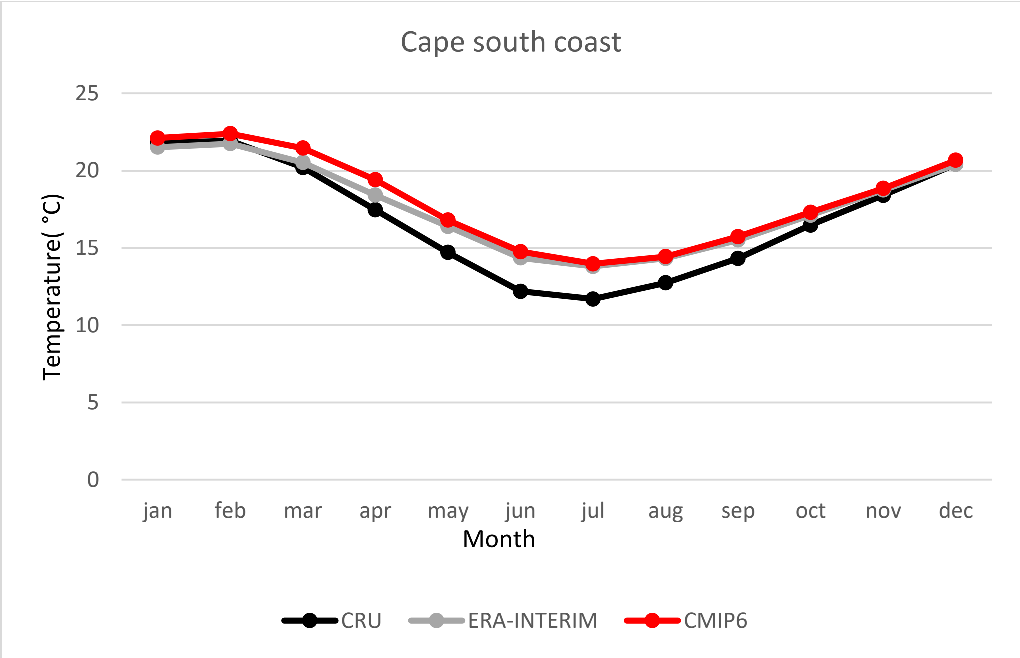

Figure 3.37: Annual cycle in temperature (°C) over the Cape south coast region of southern Africa.

3.4.5.2 Eastern southern Africa

In the graph below, the reference dataset (CRU) shows temperature maximums to be occurring in the summer month at 21°C and temperature lows occur during the winter months to 10°C (figure 3.38). The ERA-interim dataset follows the same trend and trajectory as the reference dataset (CRU), however, very high temperatures are observed throughout the entire region, with an overestimated difference for the winter month at above 5°C. Furthermore, the CMIP6 dataset also follows the same trend as the CRU dataset. Moreover, the CMIP6 dataset correctly simulates the summer temperature, with an overestimation of 10°C over the winter season (figure 3.38).

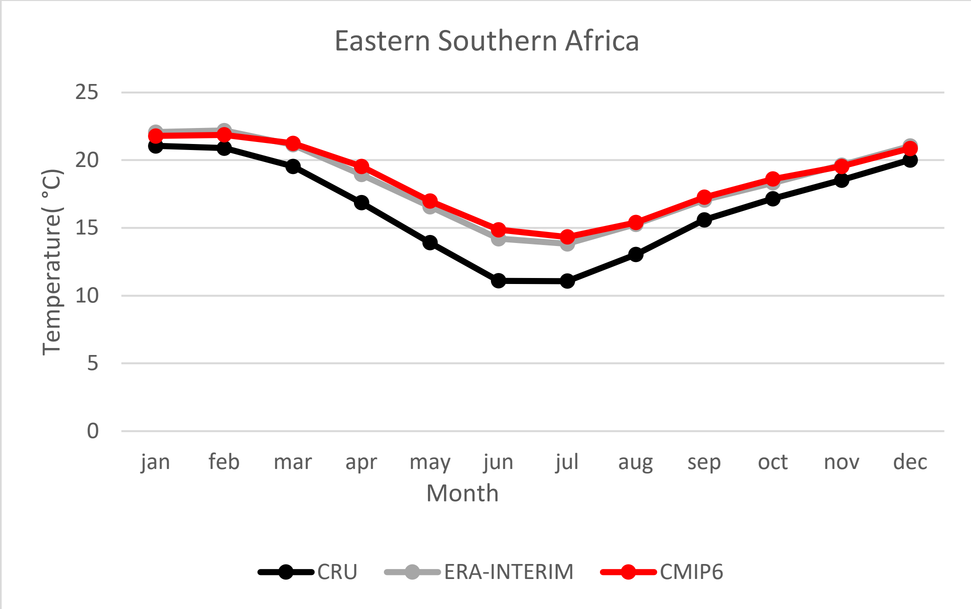

Figure 3.38: Annual cycle in temperature (°C) over the Eastern southern Africa region of southern Africa.

3.4.5.3 Northern subcontinent

For the northern subcontinent, the figure 3.39 below indicates a hot trend in temperature for the northern subcontinent. The Era-interim model and the CMIP6 model agree well with the pattern of the observations. Whereby, the CMIP6 model overestimates temperature in this region and the ERA-interim data depicts substantial underestimates.

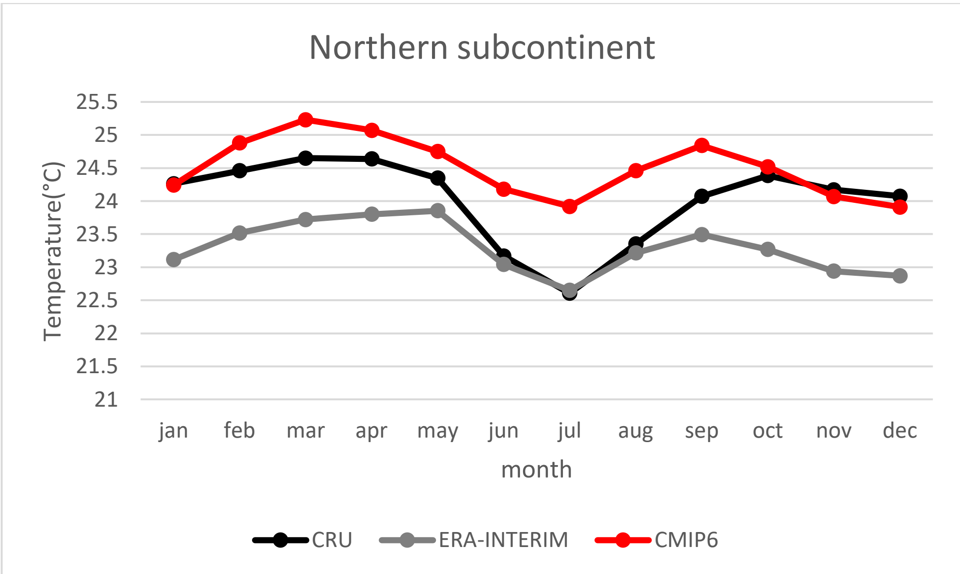

Figure 3.39: Annual cycle in temperature (°C) over the Northern subcontinent of southern Africa.

3.4.5.4 North-eastern South Africa, S Zimbabwe, and S Mozambique

The figure (3.40) below, indicates temperature results for the NESA region. This region outlines itself as a high-temperature region. According to the reference dataset CRU, temperature maximums for NESA reach above 25°C, whereas the low temperature reaches 16°C during the winter months. Moreover, temperature results from the ERA-interim dataset follow the same pattern as the reference (CRU) for the NESA region. The CMIP6 model correctly simulates the temperature compared to the reference dataset for all the seasons.

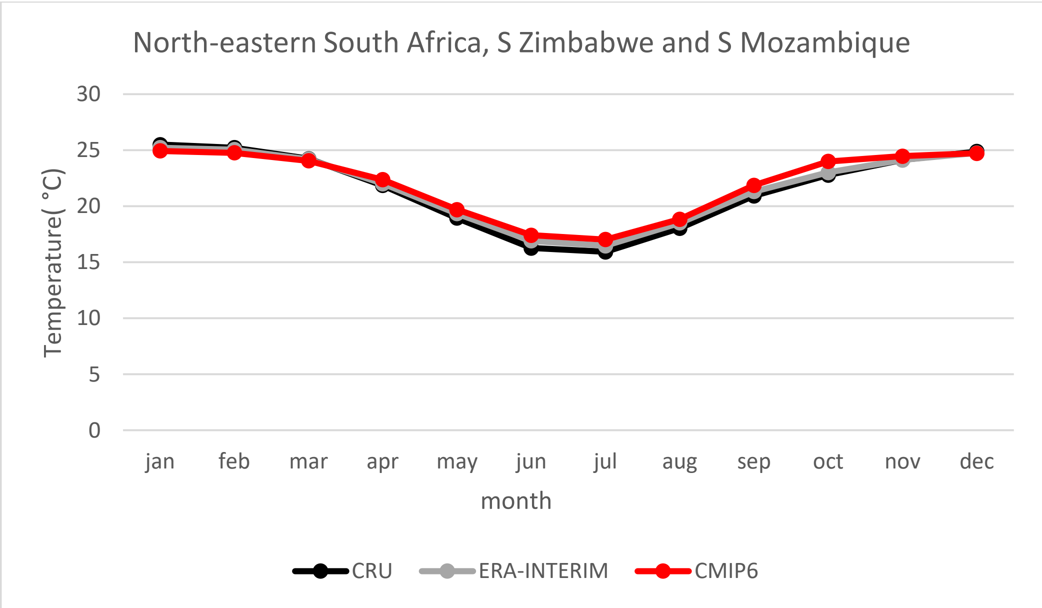

Figure 3.40: Annual cycle in temperature (°C) over the North-eastern South Africa, S Zimbabwe, and S Mozambique region of southern Africa.

3.4.5.5 Western subcontinent

In figure 3.41 below, the western subcontinent indicates generally high temperatures for this region. Temperature maximums for this region reach 25°C for the summer season. Temperature lows are experienced during the winter months with 14°C, according to the CRU dataset. The ERA-interim dataset follows the same pattern as the observed reference data. However, the observed temperatures depict an overestimation from the reference dataset from JFM. Mainly during the summer/spring season. For the CMIP6 model data, the simulations for the season, follow the same pattern as the observed reference data and depicts temperature correctly during the summer season. However, there is a slight overestimation of temperature during the winter months over this region, according to the CMIP6 dataset.

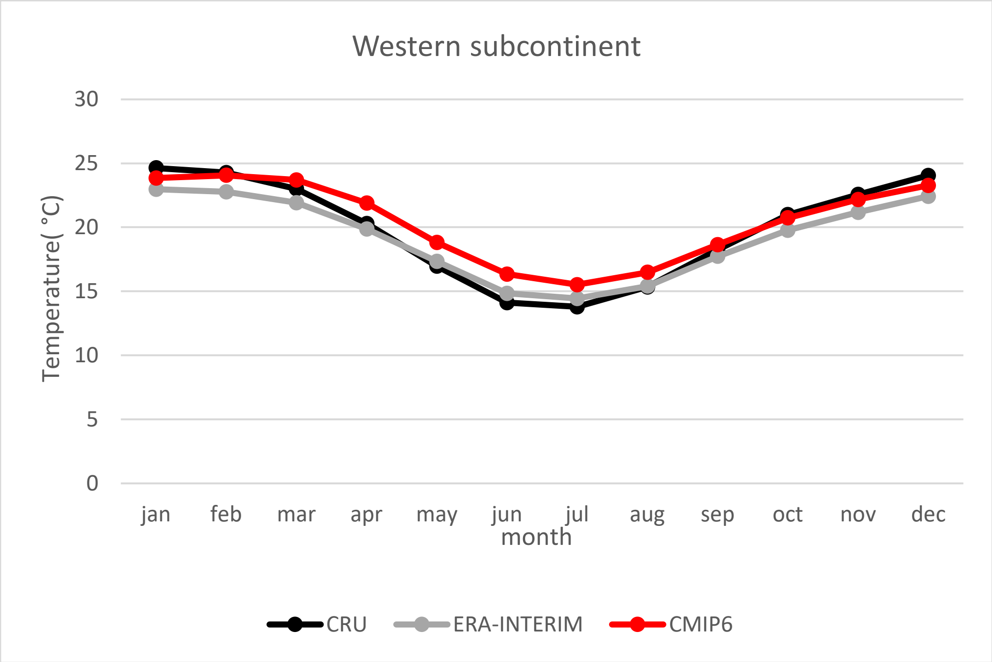

Figure 3.41: Annual cycle in temperature (°C) over the Western subcontinent region of southern Africa.

3.4.5.6 South Western Cape

For the South Western Cape (figure 3.42), the CRU dataset depicts observed maximum temperatures to be occurring during the summer and spring season at above 20°C. Minimum Cru temperatures for this region occur during winter with 12°C. The ERA-interim dataset follows the same spatial pattern as the reference data, however, there is an apparent trend of rainfall underestimation during the summer and spring months. The CMIP6 data correctly simulates the summer and spring season, however, slightly overestimates the summer temperature.

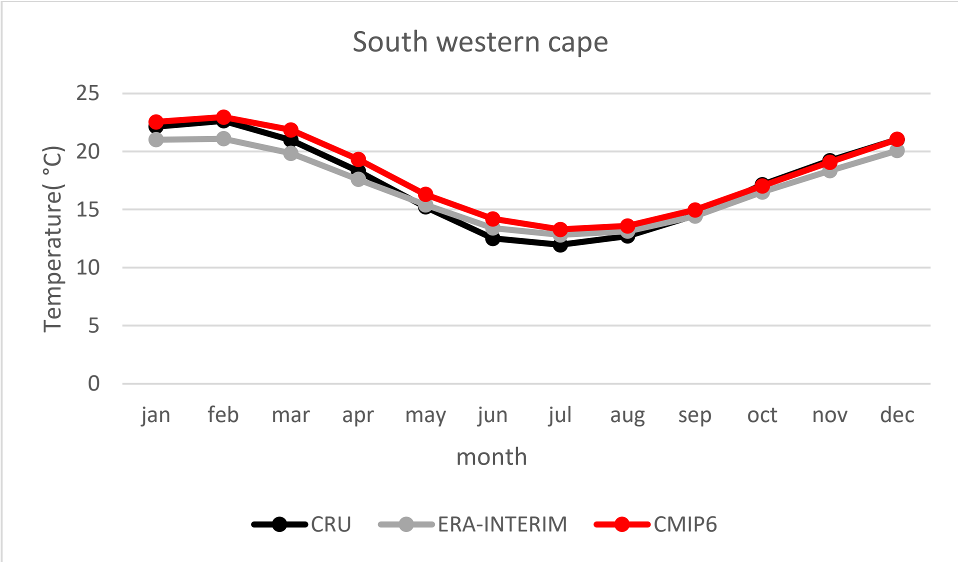

Figure 3.42: Annual cycle in temperature (°C) over the South Western Cape region of southern Africa.

3.4.5.7 Northern Mozambique & Tanzania

For northern Mozambique and Tanzania, the CRU dataset notes very high temperatures throughout all the seasons (figure 3.43). The temperature maximum for this region is 25°C experienced in the temperature minimum for this region is 19°C which is experienced during the winter cold months. The CMIP6 for this region follows precisely the same trajectory as the observed reference dataset CRU, from the first month up until the last month, the CMIP model simulations, simulate temperatures precisely for this region. The ERA-interim dataset follows the same pattern as the reference data, from the beginning up until the end, with very slight overestimates in JJA (figure 3.43).

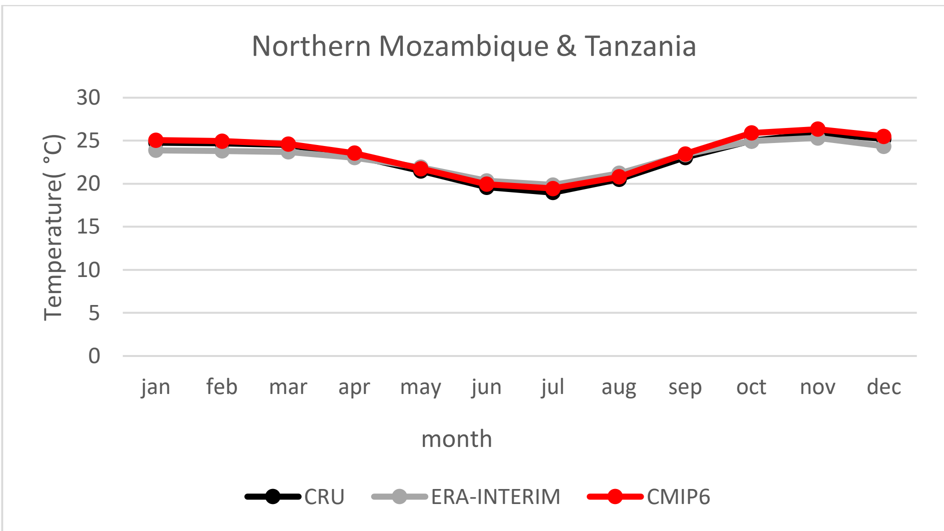

Figure 3.43: Annual cycle in temperature (°C) over the Northern Mozambique and Tanzania region of southern Africa.

3.4.5.8 Central subcontinent

Furthermore, the figure (3.44) below is representative of temperatures over the central subcontinent. According to the CRU dataset, temperature maximums are experienced over the summer seasons with a maximum of 25°C. Temperature lows for this region according to the CRU datasets are observed in the winter season with temperatures at <10°C for the winter season. According to the ERA-interim dataset, temperature trends follow the same seasonal pattern as the observed reference dataset (CRU). However, the ERA-interim data underestimate temperatures slightly in February. Furthermore, according to the CMIP6 model, simulation follows the same seasonal trends and the same spatial trend as the observed referenced dataset (CRU) from the beginning till the end of the season. Moreover, this means that the CMIP6 simulations correctly simulate temperature for this region.

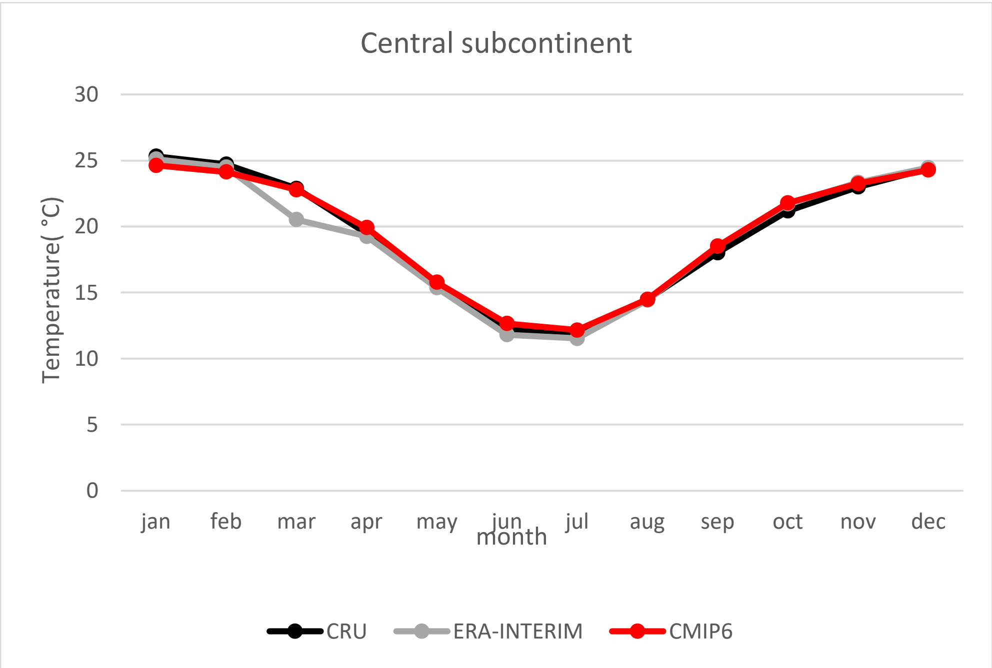

Figure 3.44: Annual cycle in temperature (°C) over the central subcontinent region of southern Africa.

3.4.6 Statistical verification

In this section Taylor diagrams are applied to statistically formalize how close the annual cycle of monthly means as represented in ERA-interim and the CMIP6 ensemble average corresponds to observations. Simulated patterns that agree well with observations will lie nearest to the 'observational' point on the x-axis. These models will have relatively high correlations, low root-mean-square errors and a scaled standard deviation close to 1.

3.4.6.1 Cape south coast

Figure 3.45 reveals a close match between both the ERA-interim and CMIP6 ensemble's annual cycle of monthly mean temperature, and that observed by CRU TS4.04. The scaled standard deviations are close 2 but less than 1, revealing that intra-annual variability is less in the simulations than in reality. The root-mean-square errors are small, for both ERA-interim and the CMIP6 ensemble average.

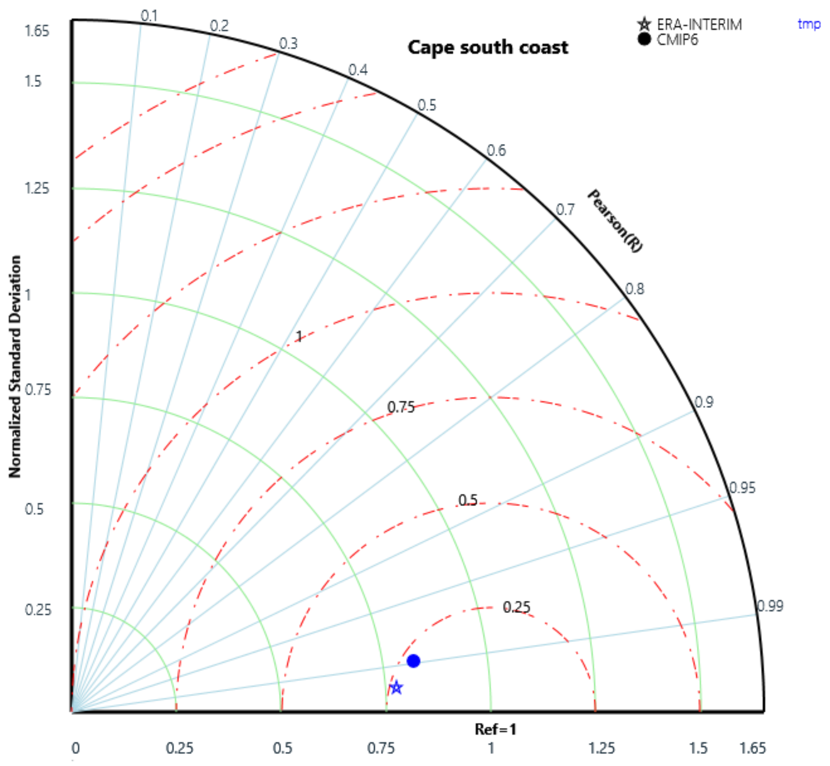

Figure 3.45: Taylor diagram showing the pattern correlation, scaled root mean-square error and scaled standard deviation for ERA interim data (star) and the CMIP6 ensemble average (dot) vs observations (CRU), for the case of the annual cycle of monthly mean temperature over the Cape south coast.

3.4.6.2 Eastern southern Africa

For eastern southern Africa (Figure 3.46) both simulations sets behave in a similar way compared to other regions. Pearson correlation coefficients are high, root-mean-square errors are low and the scaled standard deviations are close to 1. There is a strong positive correlation with the ERA-interim model of (0.986), which is slightly higher than the CMIP6 model at (0.986). Therefore, the ERA-interim data for eastern South Africa has a close pattern correlation with the ERA-interim model. Moreover, the standard deviation of the CMIP6 dataset is (0.751 mm/day) and the ERA-interim dataset's standard deviation is (0.822 mm/day). The model that better simulates the standard deviation of the observed referenced dataset is (0.75 mm/day).

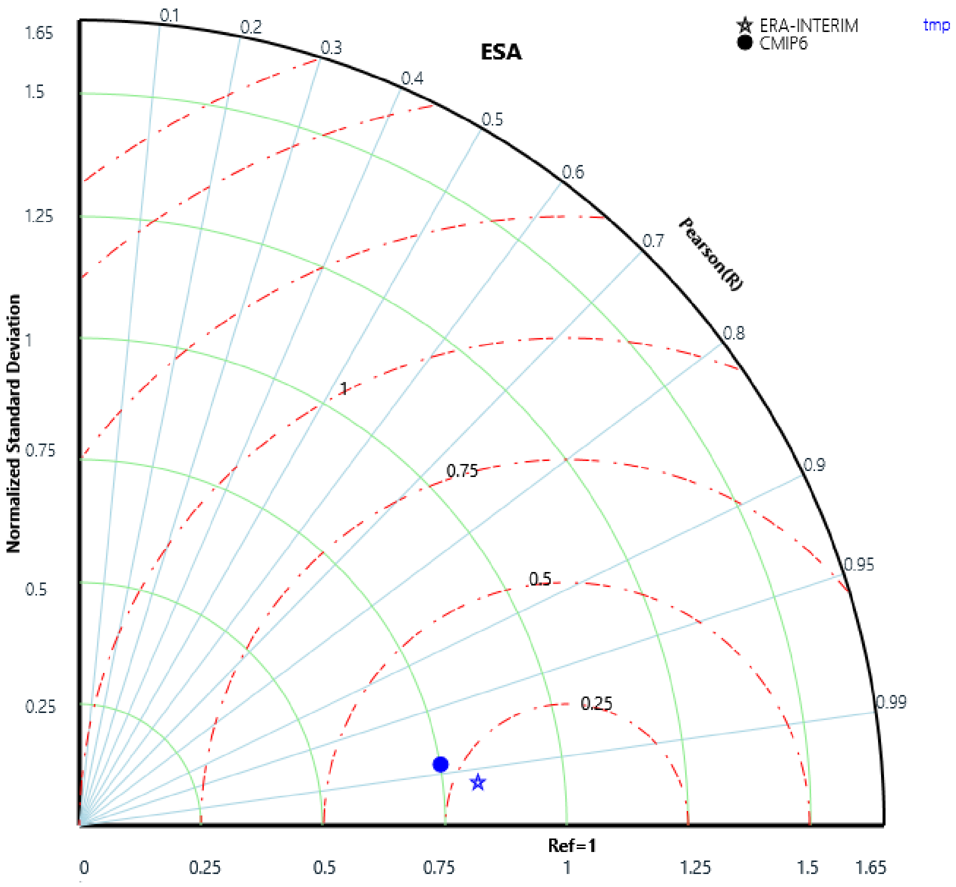

Figure 3.46: Taylor diagram showing the pattern correlation, scaled root mean-square error and scaled standard deviation for ERA interim data (star) and the CMIP6 ensemble average

(dot) vs observations (CRU), for the case of the annual cycle of monthly mean temperature over the Eastern southern Africa.

3.4.6.3 Northern subcontinent

In the illustration below (figure 3.47), temperature simulations indicate that both the models simulate temperature well over the northern subcontinent, however, with the CMIP6 being the better performing model based on it relatively low standard deviation and high correlation. See figure below.

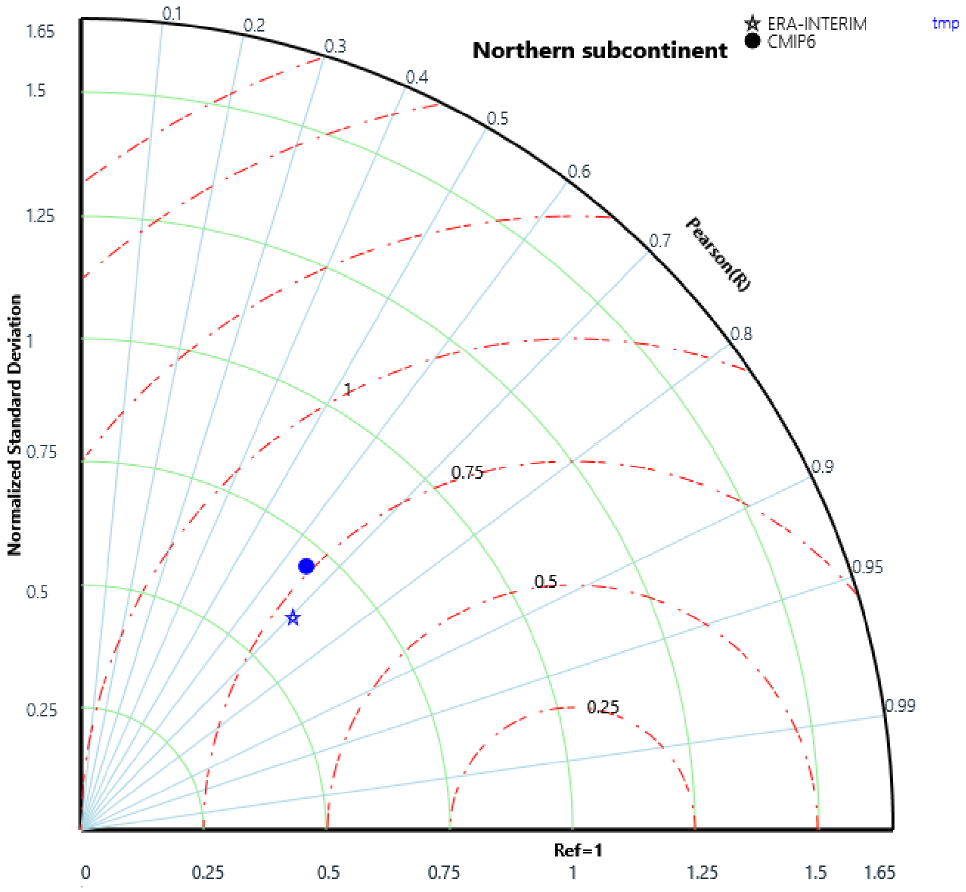

Figure 3.47: Taylor diagram showing the pattern correlation, scaled root mean-square error and scaled standard deviation for ERA-interim data (star) and the CMIP6 ensemble average (dot) vs observations (CRU), for the case of the annual cycle of monthly mean temperature over the Northern subcontinent.

3.4.6.4 North-eastern South Africa, S Zimbabwe, and S Mozambique

For the north-eastern South Africa and Mozambique region, ERA-interim provides an almost perfect (figure 3.48). Pearson correlation, suggesting that the simulations very closely follows the observed intra-annual cycle monthly temperature. Root-mean-square errors are low, and person correlations are high.

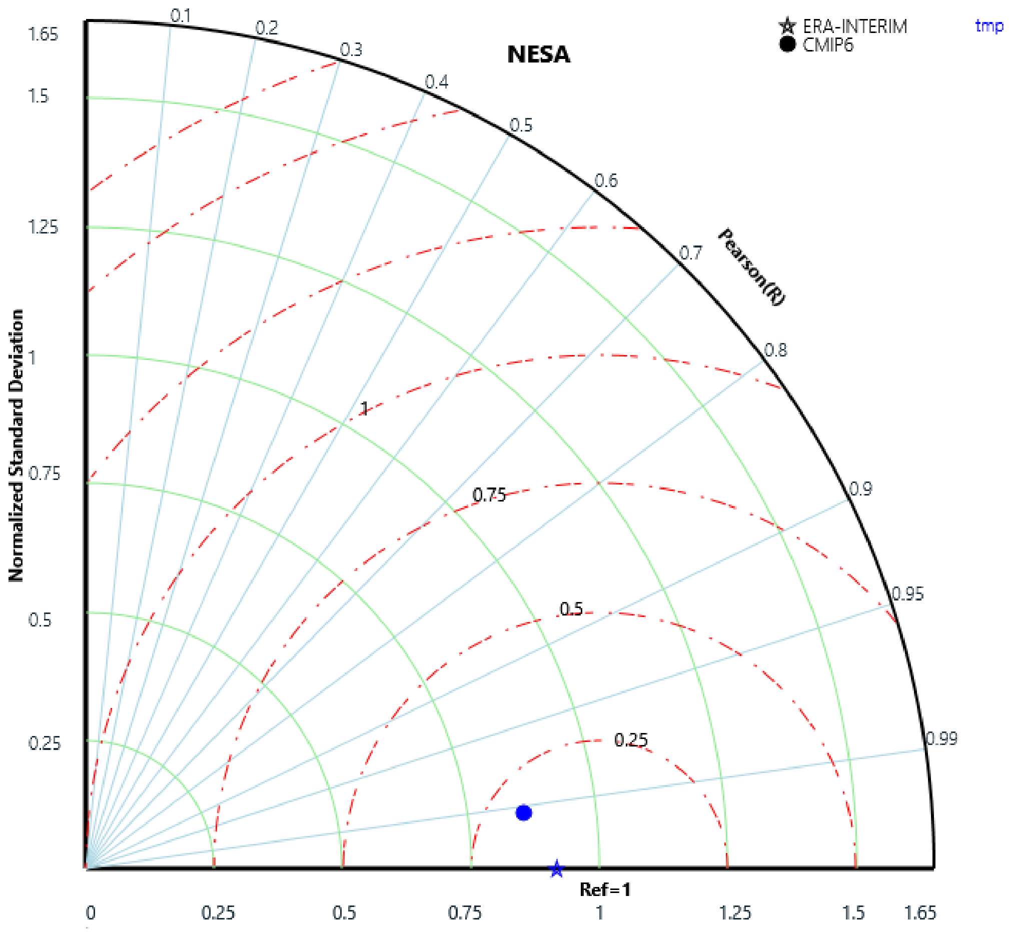

Figure 3.48: Taylor diagram showing the pattern correlation, scaled root mean-square error and scaled standard deviation for ERA interim data (star) and the CMIP6 ensemble average (dot) vs observations (CRU), for the case of the annual cycle of monthly mean temperature over the North-eastern South Africa, S Zimbabwe, and S Mozambique.

3.4.6.5 Western subcontinent

For the Western subcontinent (figure 4.49). Model performance is very similar than for the Cape South coast. Both the ERA-interim data and CMIP6 ensemble average show small root-mean-square errors and high Pearson correlations. The standard deviations are close to but less than 1, suggesting underestimations of the observed intra-annual variability.

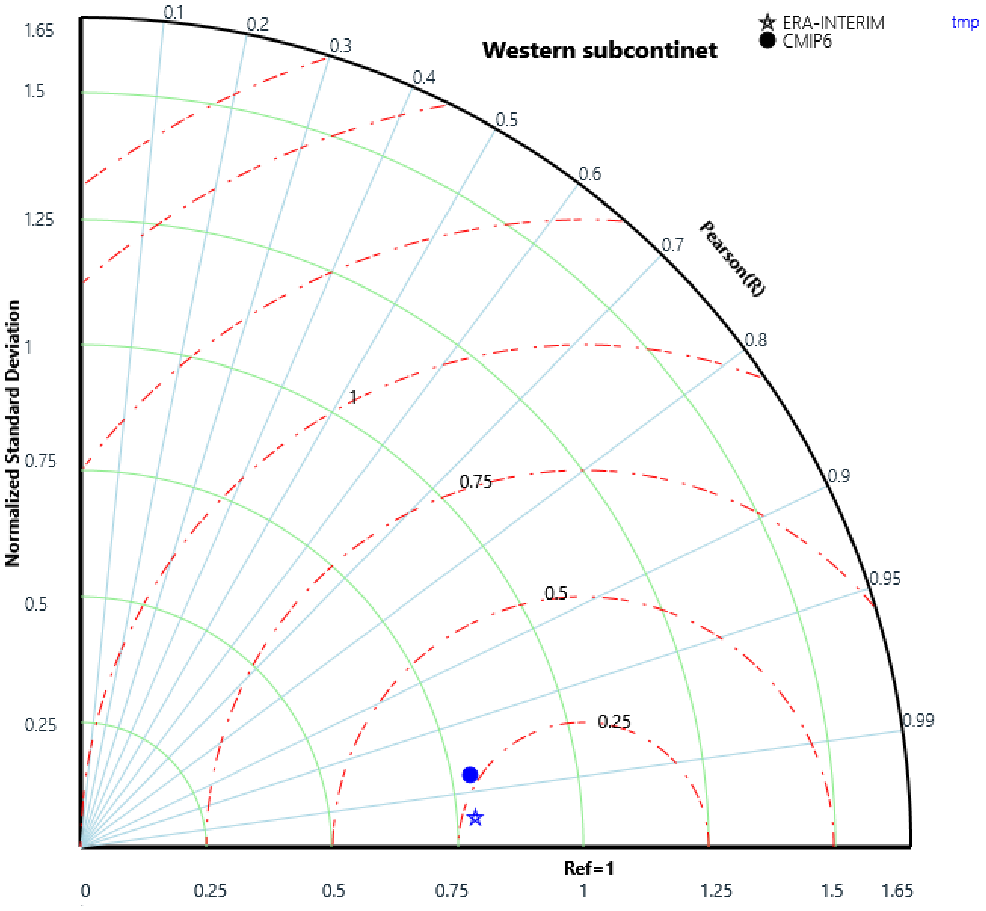

Figure 3.49: Taylor diagram showing the pattern correlation, scaled root mean-square error and scaled standard deviation for ERA interim data (star) and the CMIP6 ensemble average (dot) vs observations (CRU), for the case of the annual cycle of monthly mean temperature over the Western subcontinent.

3.4.6.6 South Western Cape

In the south Western Cape (Figure 3.50), the winter rainfall region of South Africa, model performance similar but even more accurate than for the Cape South Coast (Figure 3.44). Pearson correlation coefficients are high and root-mean-square errors are low. The scaled standard deviations are close but less than one, suggesting that both ERA-interim and the CMIP6 ensemble underestimate intra-annual variability.

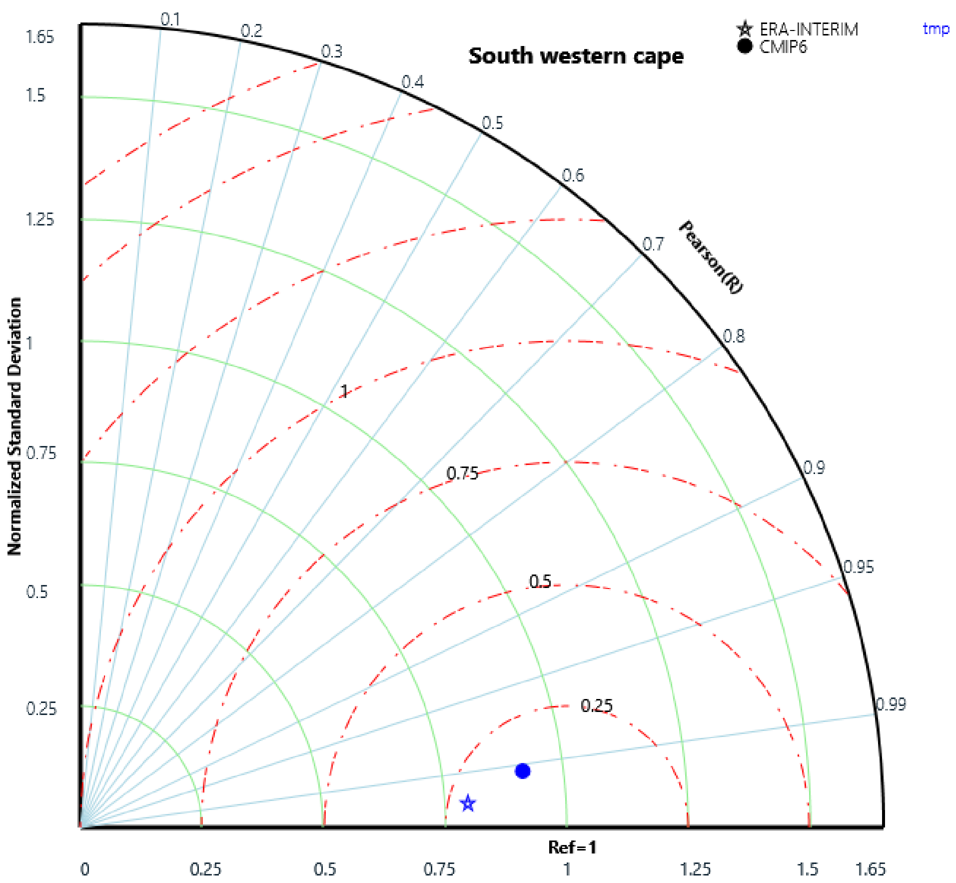

Figure 3.50: Taylor diagram showing the pattern correlation, scaled root mean-square error and scaled standard deviation for ERA interim data (star) and the CMIP6 ensemble average (dot) vs observations (CRU), for the case of the annual cycle of monthly mean temperature over the South Western Cape.

3.4.6.7 Northern Mozambique and Tanzania

Figure 3.51 reveals that the intra-annual variability in monthly temperature means are well represented in northern Mozambique and Tanzania, for both the cases of ERA-interim and the CMIP6 ensemble. The scaled standard deviation is almost exactly 1 for the CMIP6 ensemble, which suggests a highly realistic depiction of intra-annual variability in the CMIP6 ensemble. Pearson correlations are high, and root-mean-square errors are small, for both ERA-interim and the CMIP6 ensemble.

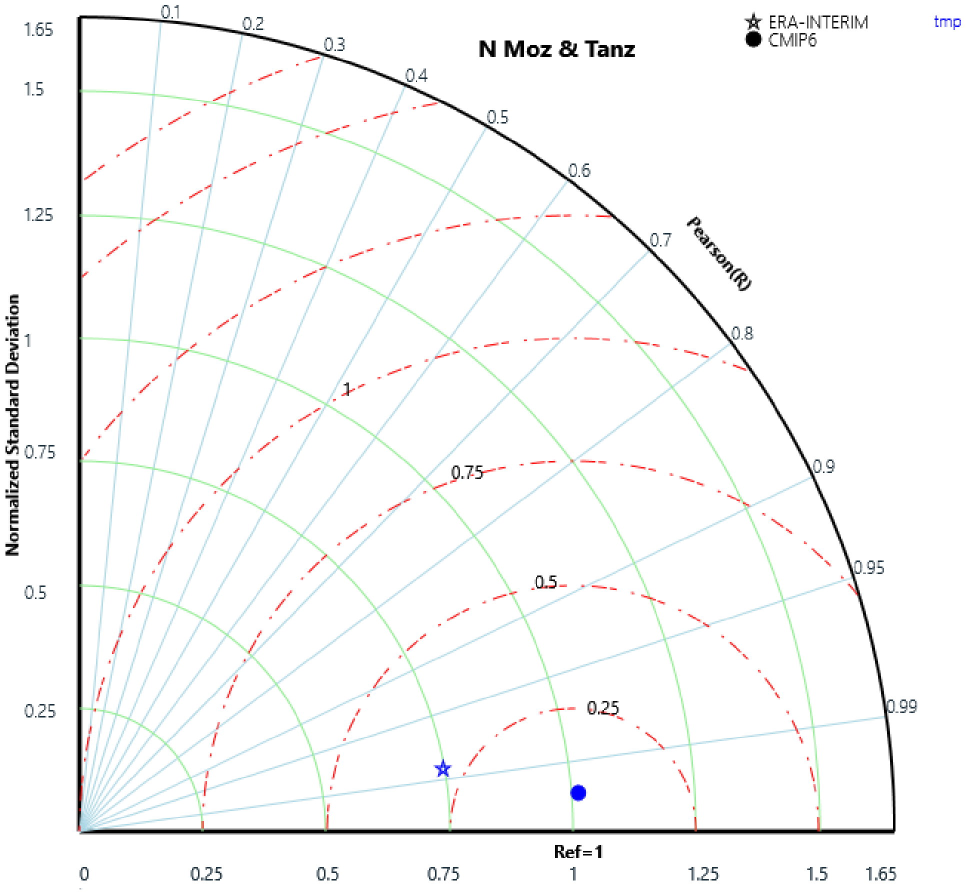

Figure 3.51: Taylor diagram showing the pattern correlation, scaled root mean-square error and scaled standard deviation for ERA interim data (star) and the CMIP6 ensemble average (dot) vs observations (CRU), for the case of the annual cycle of monthly mean temperature over the Northern Mozambique and Tanzania.

3.4.6.8 Central subcontinent

Over the central subcontinent (Figure 3.52), both simulation data sets exhibit standard deviations close to 1. This means that the model simulations closely represent the observed intra-annual variability in monthly temperature means. Root-mean-square errors are small, and Pearson correlations are high.

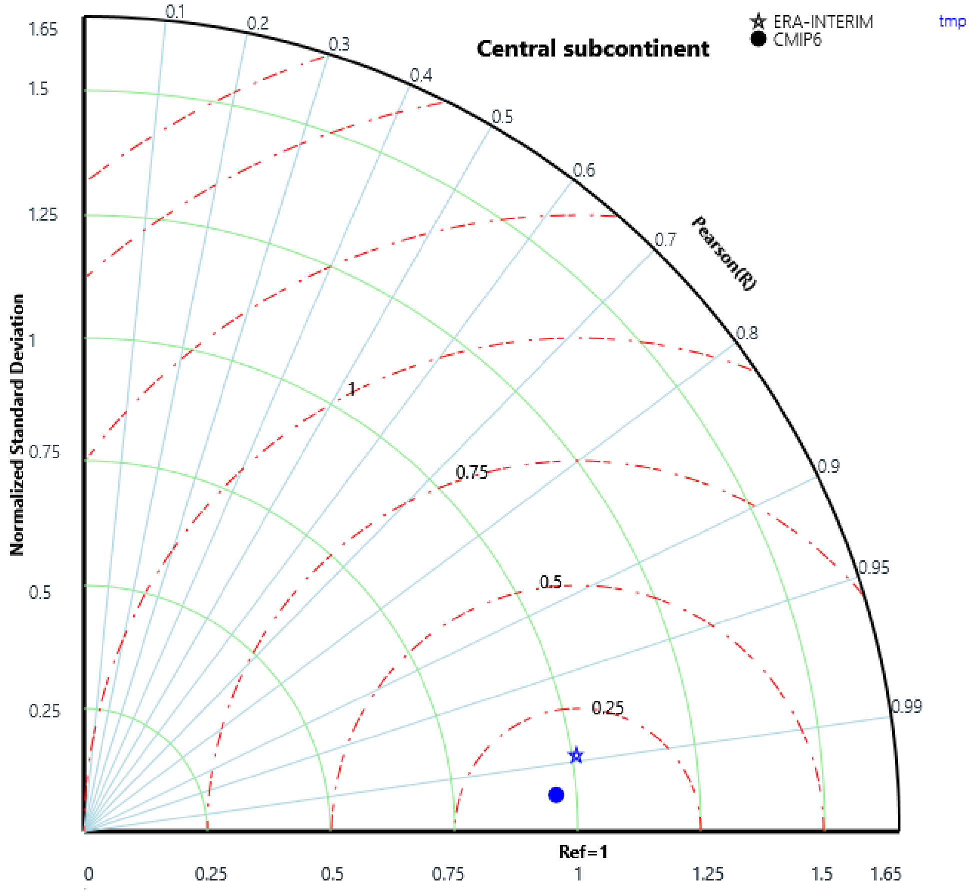

Figure 3.52: Taylor diagram showing the pattern correlation, scaled root mean-square error and scaled standard deviation for ERA interim data (star) and the CMIP6 ensemble average (dot) vs observations (CRU), for the case of the annual cycle of monthly mean temperature over the Central subcontinent.

3.5 Discussion

In terms of the mean annual rainfall patterns, the CMIP6 model ensembles are unable to depict the elevation over the eastern escarpment of southern Africa, and therefore notes a rainfall intensity over Kwa-Zulu Natal and parts of Mpumalanga, extending towards the interior of South Africa towards Lesotho. The ERA-interim data underestimate rainfall over the eastern escarpment, and also towards north Namibia and some parts of southern Angola. The ERA-interim data also denotes rainfall underestimates over the northern interior of Zimbabwe, and in Malawi bordering Mozambique. Moreover, there are some underestimates observed towards the coast of Mozambique, and also on the south Western Cape (winter rainfall region), and does not correctly simulate these frontal induced rainfall patterns.

For the mean seasonal rainfall, results indicate that southern Africa (Africa south of 10° S) is largely a summer and spring rainfall region. Another noticeable occurrence is that the CMIP6 dataset does not take note of the winter rainfall peak in the south Western Cape during the winter (JJA) season. During the summer season (DJF) and spring season (SON), CMIP6 notes these seasons as seasons of intense rainfall (which is true with the observations).

Regional rainfall for the Cape South coast depicts that the ERA-interim data do capture the bimodal nature of the rainfall, including the April and October peaks, although the amplitude of the second rainfall peak (October) is underestimated by about 10 mm. The CMIP6 does not in any way capture these, however it is in consensus with the general agreement that this region is an all year round region, however does not capture the modulations. For eastern southern Africa, the CMIP6 dataset overestimates rainfall for the winter months by 20mm, beginning April ending September, however, the overall trend follows that of the observations. For the summer months, CMIP6 correctly simulates the rainfall getting the summer rainfall values correct for four of the months. Moreover, for the northern subcontinent, what is important to note is that the ERA interim data overestimate rainfall for the northern subcontinent by a very large margin of over 250 mm in the summer months and 100 mm for the winter and is nowhere close to feasible with the results outlined by CRU.

Regarding temperature, the CMIP6 ensemble average portrays the general pattern of lowest temperatures over the eastern escarpment of South Africa. The CMIP6 simulations are not of sufficiently high resolution to represent the temperature maximum in the Zambezi river valley. The bias relation between the CMIP6 model and the CRU datasets is spatially dispersed. The CMIP6 model indicates a slight annual temperature underestimate (negative bias) over the eastern portion of southern Africa, from South Africa, and extending northwards towards the equator. For most of these sections, it can be pointed out that the modelled data underestimates the observed seasonal temperature profile amplitude.

3.6 Conclusion

Generally, the CMIP6-ensemble average correctly simulates the spatial patterns of rainfall and temperature in most of the southern African region, both annually and on a seasonal basis. The model ensemble also correctly portrays the intra-annual cycle in monthly rainfall totals across several African regions. The region least well represented in terms of intra-annual variability is the Cape south coast of South Africa, where bimodal rainfall peaks occur in an all-year rainfall region. Overall, and for most regions, ERA-interim provides a more accurate depiction of observed intra-annual variability than the CMIP6 ensemble does. Nevertheless, the CMIP6 ensemble’s realistic representation of present-day intra-annual variability creates confidence in the ensemble’s ability to project future climate change in Africa.

CHAPTER 4: PROJECTIONS OF FUTURE CLIMATE CHANGE OVER SOUTHERN AFRICA USING THE CMIP6 ENSEMBLE CLIMATE

4.1 Introduction

Generating projections of future climate change rely on the use of sophisticated climate models (see Chapters 1 and 2) that make use of the laws of physics to determine how future changes in radiative forcing may translate to changes in the climate system. In the context of the research presented here, ‘future radiative forcing’ means future anthropogenic forcing of the climate system (i.e., changes in greenhouse gas concentrations, changes in aerosols emissions, and changes in land use). Such scenarios of changing anthropogenic forcing are underpinned by socio-economic pathways into the future (O’Neil et al., 2016). Future socio-economic pathways translate effectively into scenarios of future greenhouse gas concentrations in the atmosphere, with increasing greenhouse gas concentrations being the main driver of future global warming and climate change (see chapters 1 and 2). There are two main types of scenarios: low mitigation, and high mitigation. The former refers to a fossil-fuel future, where little action is taken to divert from the current situation of high annual emissions of CO_2 through the burning of fossil fuels. The latter refers to a Paris Agreement type future, where rapid reductions in emissions are achieved in the 2020s, with carbon neutrality reached around 2050.

Future climate change projections are critical for bettering our understanding of the societal risks and environmental risk in a changing world, towards formulating response options (O’Neil et al., 2016). The Scenario Model Inter-comparison Project (ScenarioMIP) is the main activity of Phase 6 of the Coupled Model Inter-Comparison Projection (CMIP6). This international endeavour provides multi-model climate projections based on alternative scenarios of future emissions and land-use changes generated by integrated assessment models (O’Neil et al., 2016; Riahi et al., 2016). The ScenarioMIP model projections of CMIP6 were undertaken for different Shared Socio-economic Pathways (SSPs), ranging from low to high mitigation.

In this section, of the projections of future climate change generated by GCMs that participated in the ScenarioMIP experiment of CMIP6 will be analysed. The projections of future climate change are considered for specifically SSP5-8.5). This is a low mitigation pathway into the future, where humanity remains critically dependent on fossil fuels to generate energy. Low mitigation futures pose the highest risks in terms of future climate change, and it is a common approach to focus adaptation strategies on low mitigation futures. The philosophy is that if sectors/communities/governments take adaptation action to prepare for low mitigation futures, these will also suffice should the future development pathway is less extreme in terms of emissions and associated climate change.

The remainder of the chapter consists of a data and methods section, and results sections. The methods section describes the intensive conversion of raw CMIP6 data to machine-readable form, towards eventually generating results. The core aim of this chapter is to present the CMIP6 GCMs' projected changes of changes in rainfall and temperature seasonality in southern Africa, under the low mitigation scenario SSP5-8.5. This section also contains a brief discussion/summary of the key results obtained.

4.2 Data and methods

The section below details how the model projections of future climate change were obtained, including a discussion of the extensive underlying data processing that was undertaken.

4.2.1 Greenhouse gas emission scenarios

The SSPs were created as a collaborative community effort over the last several years, and depict vastly diverse global development pathways that underpin various greenhouse gas emission scenarios and levels of global warming reached by the end of the century. (Van Vuuren et al.,2012) presented an initial conceptual framework for SSPs and how they may be utilized with climate simulations to conduct integrated research (O'Neill et al., 2014b; Kriegler et al., 2012, 2014a).

The study follows SSP5-8.5, which is allow mitigation baseline scenario. This high-emissions scenario is sometimes referred to as "business as usual," implying that it will occur until society makes substantial steps to reduce greenhouse gas emissions. Adaptation strategies designed to alleviate us avoid climate change impacts under SSP5-8.5 is highly likely to also suffice for higher mitigation futures. It is thus a standard approach for climate change impact and adaptation studies to largely focus on low mitigation futures, since these do represent humanity's current pathway, and cannot be ruled out as future pathways. This scenario is used to inform modelling at three different future periods: The near-term future (2021-2040), medium-term future (2041-2060) and the long term future (2081-2099). These selection follows the IPCC AR6 (Lee et al., 2021).

4.2.3 Model selection and data processing

The Scenario-MIP experiment of CMIP6 grew substantially during 2020 and 2021, and eventually 30 GCM projections under SSP5-8.5 were available for analysis. The list of models analysed is provided in Chapter 3, and as in that chapter we will refer to this group of models as the 'CMIP6 ensemble'. The analysis shown in the chapter is for the ensemble average of 30 models, following the recent analysis of the IPCC AR6 WGI 1 report, which also uses the ensemble average to communicate the projected changes (Lee et al., 2021). It should be noted that there is overwhelming agreement across climate models (100% agreement, in fact), that future climates will be hotter under low mitigation. The IPCC uses the term 'virtually certain' to denote that there is no uncertainty in terms of this aspect of future climate change. Rainfall futures are less certain, but across the IPCC Fourth Assessment Report of 2007, the Fifth Assessment Report of 2013, the IPCC Special Report on Global Warming of 1.5 °C published in 2018 and Assessment Report Six of 2021, the assessment has been made that southern African will 'likely' become drier under low mitigation futures. This assessment is partially the result of strong model agreement – most climate models are in agreement in terms of the sign of future rainfall changes over southern Africa. This 'majority view' of climate models is reflected in the CMIP6 ensemble average, and that is why this chapter is largely based on projected changes in temperature and rainfall over southern Africa using the CMIP6 ensemble average.

The analysis to follow explores projected changes in rainfall and temperature for the mentioned future periods, using the 1979-2014 present-day baseline for which model verification was undertaken in Chapter 3. Changes are shown spatially, in terms of annual and seasonal changes across southern Africa, and also for the different sub-regions of (Engelbrecht et al., 2009) and Chapter 3.

Substantial data processing had to be undertaken. First, the CMIP6 model simulations across 30 individual models had to be interpolated from their native grids to a standard 1° latitude-longitude grid, and for this step bilinear interpolation was used. Monthly and seasonal climatology's were subsequently calculated across southern Africa, for the baseline period and each of the three future periods, and from these spatial fields the various regional averages were calculated.

4.3 Model projections: future changes in rainfall

The ensemble-mean evaluation performed for the historical period (1979–2014) using the CRU, ERA-Interim and CMIP6 dataset revealed that the CMIP6 ensemble simulates rainfall patterns over southern Africa realistically (compared to the observed reference dataset CRU). A general positive bias is present across southern Africa in terms of the representation of annual rainfall totals. In this section, the change in rainfall patterns between the near-term period, the medium-term period, and the future-term period under SSP5-8.5 is analyzed, in terms of both annual and seasonal rainfall. Furthermore, a detailed analysis of change in the annual cycle of rainfall (seasonality) is undertaken for the different southern Africans sub regions.

4.3.1 Change in annual rainfall totals

Figure 4.1 to 4.3 show the change in annual rainfall totals(mm) for the three different future periods under a high emission (low mitigation) scenario (SSP5-8.5), using the period (1979-2014) as the baseline period.

4.3.1.1 Near-term (2021-2040) annual rainfall change

Changes for the near-term (2021-2040) assessment period are shown in figure 4.1. This period is associated with general drying over most of the southern African region. The strongest rainfall reductions are projected for the western subcontinent and Mozambique. Rainfall increases are projected over the norther subcontinent, in association with the southern expansion of the tropical belt in a hotter world (Seidel et al., 2009). Over the eastern escarpment areas of South Africa, and eastwards across KZN, general rainfall increases are projected. Model uncertainty over this area is relatively high, however (Lee et al., 2021).

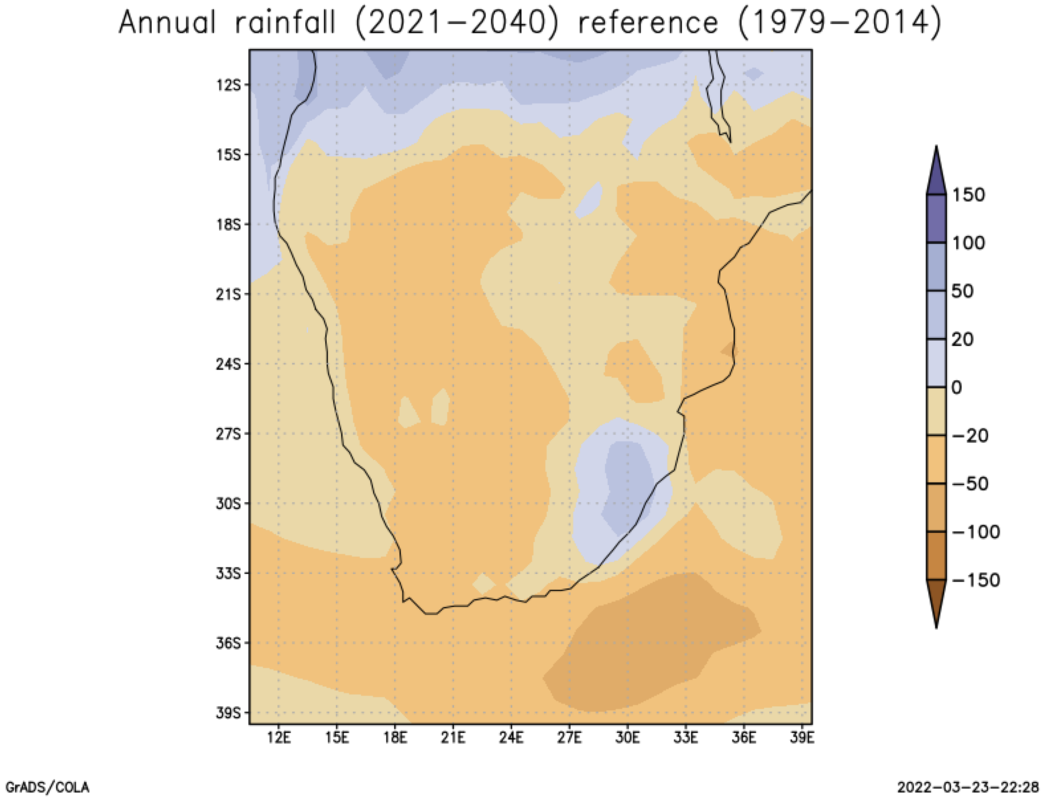

Figure 4.1: Projected change in rainfall (mm) in the near term (2021-2040) relative to 1979-2014 across southern Africa.

4.3.1.2 Medium-term (2041-2060) annual rainfall change

The regional pattern of rainfall change projected for the near-term is projected to strengthen in amplitude for the mid-term, but stay similar in terms of its spatial pattern (figure 4.2). This so called ‘pattern-scaling’ of regional precipitation change as a function of the level of global warming is a well-known feature of global climate change (Lee et al., 2021). Continued general drying is projected, mostly so for the western subcontinent and Mozambique. The precipitation decreases projected over the ocean the south of South Africa is the tell-tale signature of an intensification of blocking highs over this region, which displaces rain-bringing frontal systems poleward. Rainfall increases are projected to amplify over eastern South Africa and over the far northern subcontinent, in the tropical savannah region.

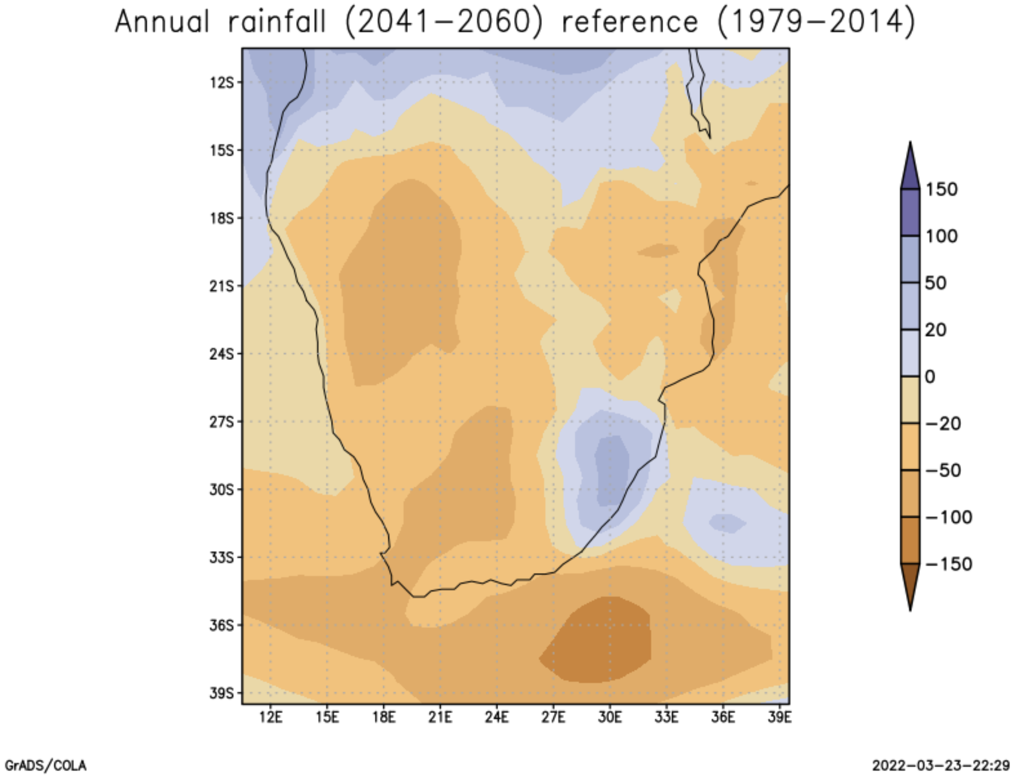

Figure 4.2: Projected change in rainfall (mm) in the medium term (2041-2060) relative to 1979-2014 across southern Africa.

4.3.1.3 Long-term (2081-2099) annual rainfall change

The long-term change in annual rainfall (mm) is shown in Figure 4.3. The regional drying is projected to strengthen further, peaking over the south Western Cape (loss in frontal rainfall), over parts of the western interior, and northern Mozambique. Further amplification of the pattern of rainfall increases over South Africa's eastern escarpment and over the northern subcontinent is projected.

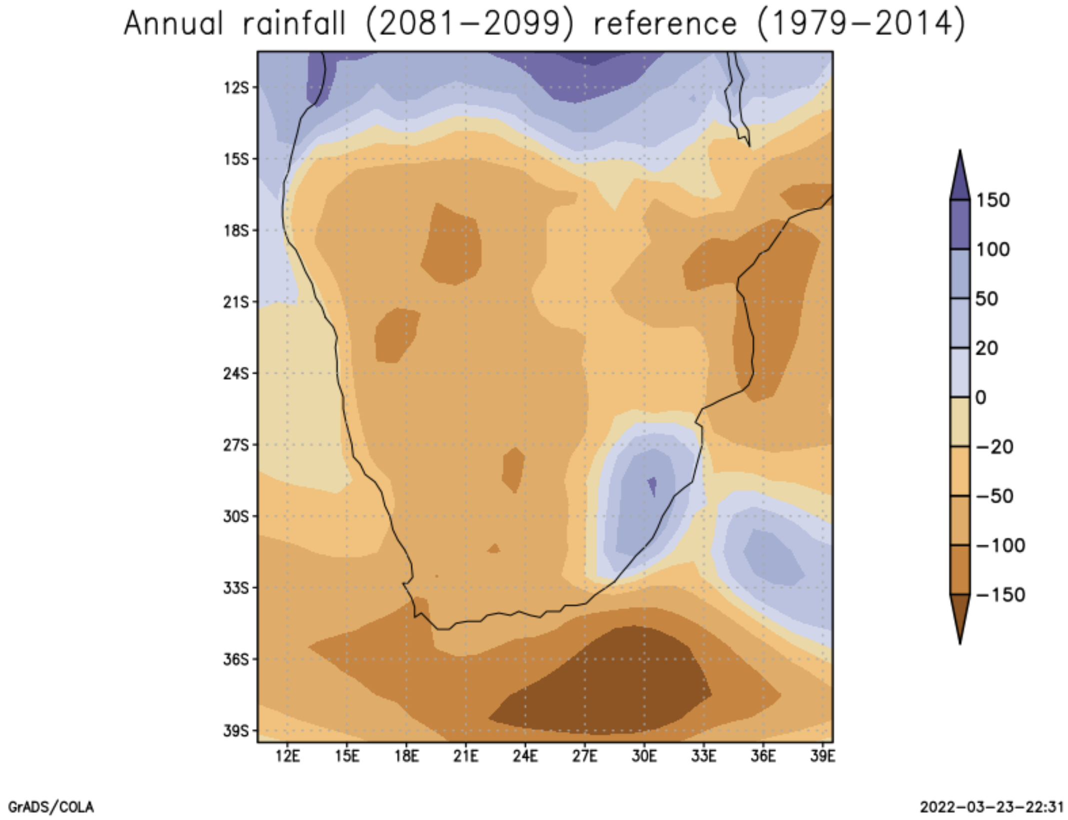

Figure 4.3: Projected change in rainfall (mm) in the long term (2081-2099) relative to 1979-2014 across southern Africa.

4.3.2 Seasonal rainfall change

This section evaluates future seasonal rainfall changes over southern Africa, for the near term (2021-2040), medium-term (2041-2060), and the long-term (2081-2099) periods, against the reference observed period (1979-2014), under the low climate change mitigation scenario SSP5-8.5.

4.3.2.1 Seasonal rainfall change for the near-term period (2021-2040)

Changes in seasonal rainfall totals (mm) for the near-term period are shown in Figure 4.4. For the winter season (JJA), almost the entire subcontinent is projected to dry, most importantly so, over the south Western Cape region of South Africa. However, also during the JJA season, there is a slight projected increase in rainfall over northern Mozambique and the southern Democratic Republic of Congo. During the spring season (SON), the entire subcontinent is projected to be generally drier, except for some rainfall increases over South Africa's eastern escarpment and adjacent coastal areas. Furthermore, during the summer season (DJF) rainfall is projected to increase over most of the eastern half of southern Africa as well as over the northern parts of the subcontinent. Western southern Africa is projected to be generally drier (except for south Angola). The autumn season (MAM) is also projected to be generally drier, exceptions being South Africa's eastern escarpment and the northernmost subcontinent.

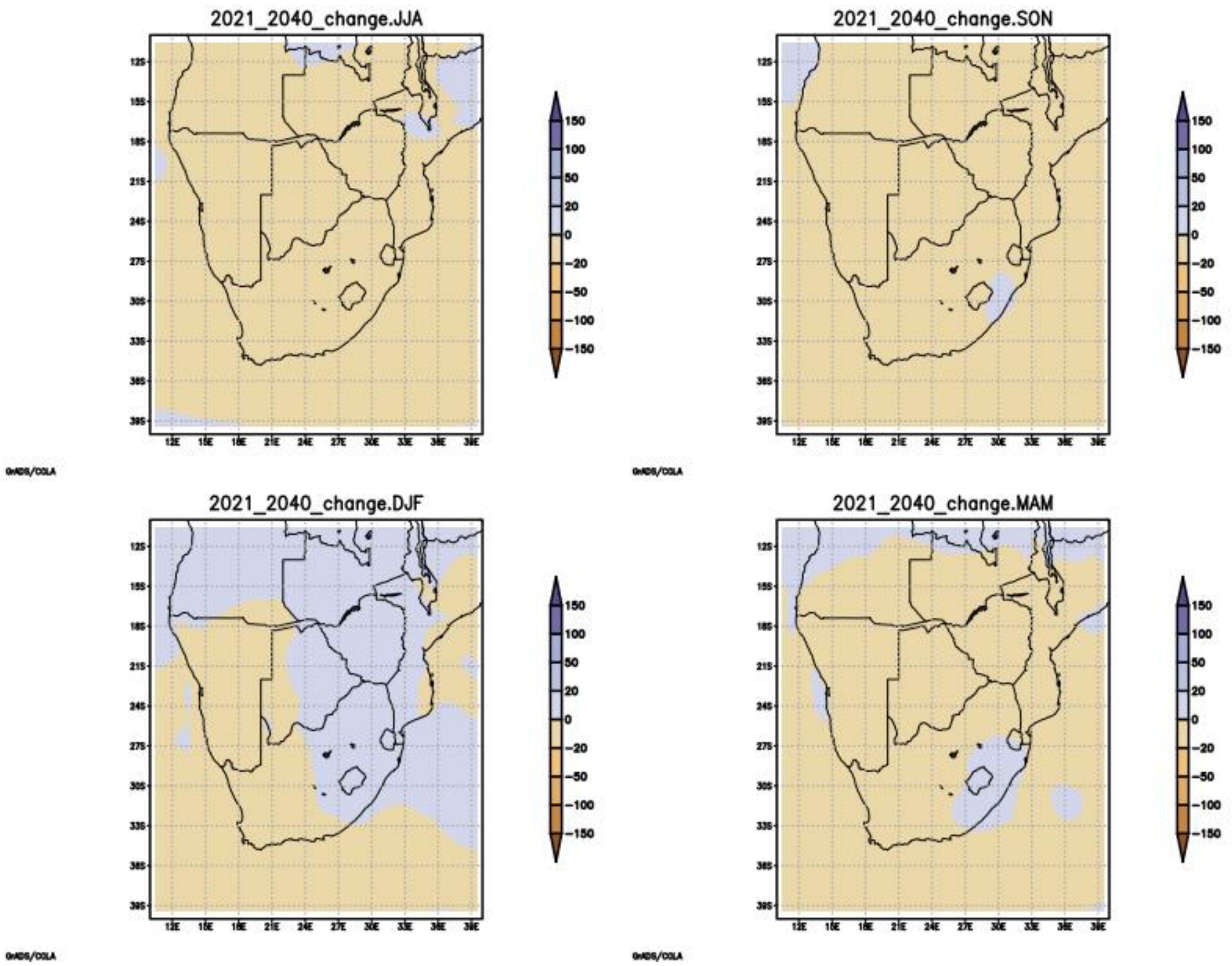

Figure 4.4: Projected change in seasonal rainfall totals (mm) for the near-term (2021-2040) relative to the present-day reference period 1979-2014 over southern Africa.

4.3.2.2 Seasonal rainfall change for the medium-term period (2041-2060)

Projected changes in rainfall totals (mm) during the winter season indicate continued drying over most of the subcontinent, with only the coast of KZN being projected to be wetter (figure 4.5). This pattern of general drying is also projected for SON, also with a very small area on coastal KZN with above-average rainfall. For the DJF season, rainfall is projected to increase over eastern southern Africa, but western southern Africa is projected to become drier, as for the near-term changes. General drying is projected for autumn, the exceptions being the northernmost subcontinent and South Africa’s eastern escarpment.

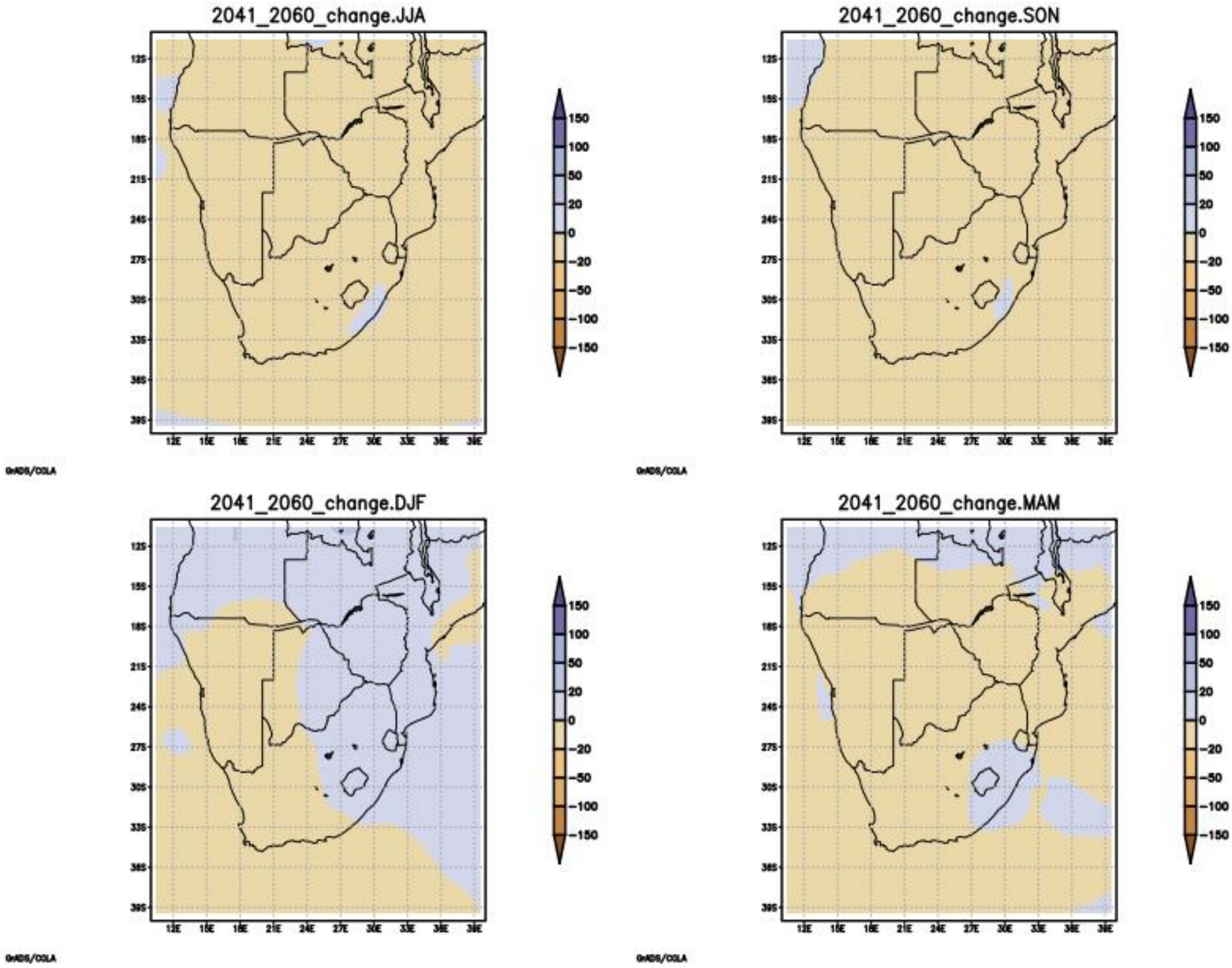

Figure 4.5: Projected change in seasonal rainfall totals (mm) for the medium-term (2041-2060) relative to the present-day reference period 1979-2014 over southern Africa.

4.3.2.3 Seasonal rainfall change for the long-term period (2081-2099)

Seasonal rainfall changes (mm) projected for the long-term under low mitigation scenarios are shown in Figure 4.6. For the JJA season, similar to the near-term and mid-term seasons, general drying is projected. The spring season (SON) is similarly being projected to be generally drier, the only exception being the wetter condition projected for KZN. For the DJF season, rainfall increase is projected over large parts of eastern southern Africa and the northernmost subcontinent, with general drying elsewhere. General drying is also projected for autumn MAM), eastern South Africa and the northernmost continent being the only exception.

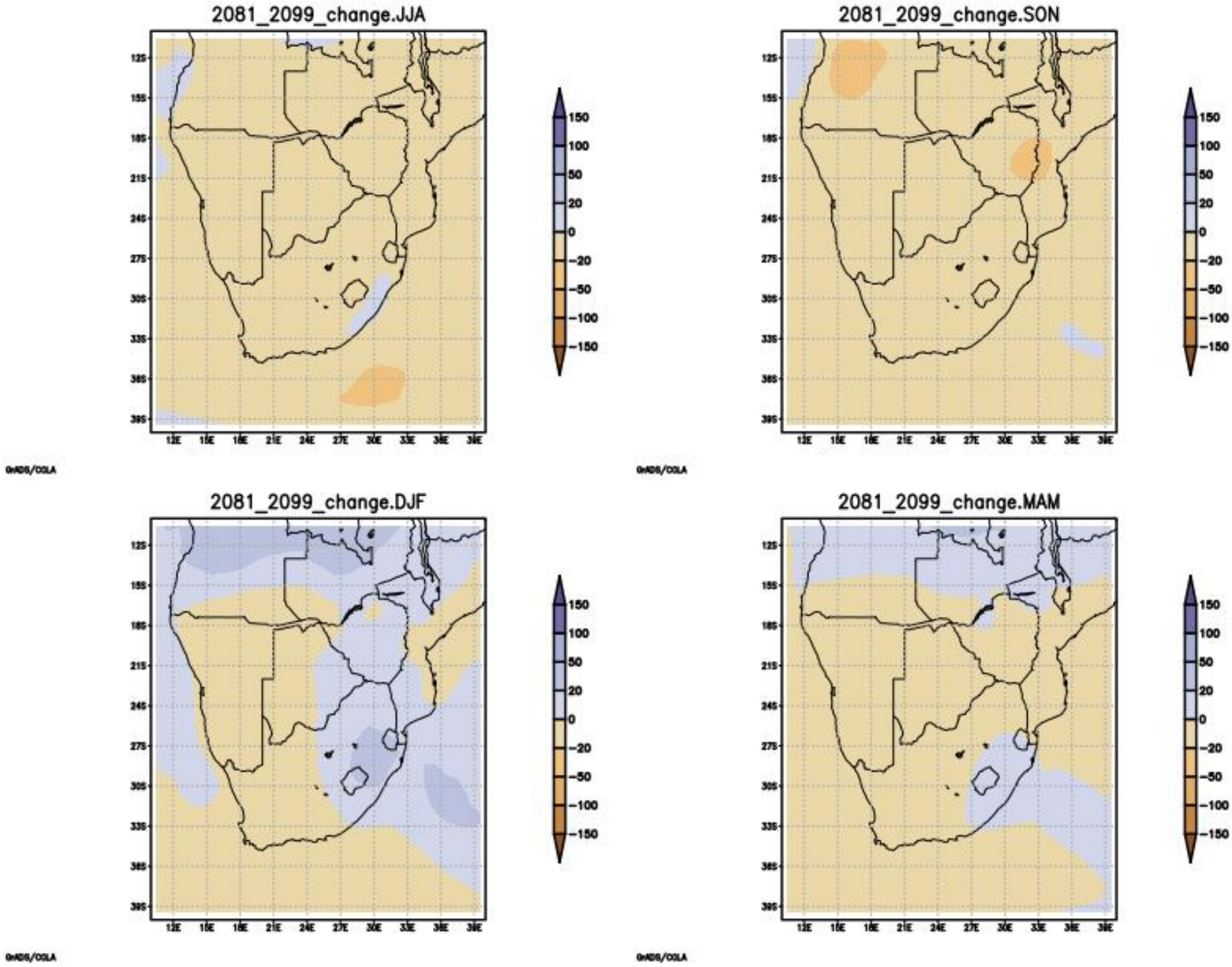

Figure 4.6: Projected change in seasonal rainfall totals (mm) for the long-term (2081-2099) relative to the present-day reference period 1979-2014 over southern Africa.

4.3.3 Regional rainfall

In the following figures projected changes in the annual cycle of monthly rainfall is shown, for the near-term (orange lines), mid-term (grey lines) and long-term (yellow lines) futures under SSP5-8.5, relative to the present-day baseline of 1979-2014 (blue lines), and across the regions of Engelbrecht et al. (2009).

4.3.3.1 Cape south coast

Figure 4.7 indicates the mean monthly rainfall for the Cape south coast, for the reference period under low mitigation measures, and the projected periods. The present-day climatology introduces this area as an annual-rainfall-year-round region. This means that this area experiences rainfall throughout the entire year. The first peak in rainfall for the present-day period is experienced during March and the second rainfall peak is experienced during October, the present-day dataset outlines the monthly rainfall maximum to be during March at slightly above 60 mm/month. Projected rainfall datasets also depict this region as an all-year-round region, however, there are decreases in the rainfall pattern and intensity under low mitigation measures. During the long-term period, sharp rainfall declines will be experienced during September. Moreover, the consensus amongst all the projected periods is a gradual general decline in rainfall.

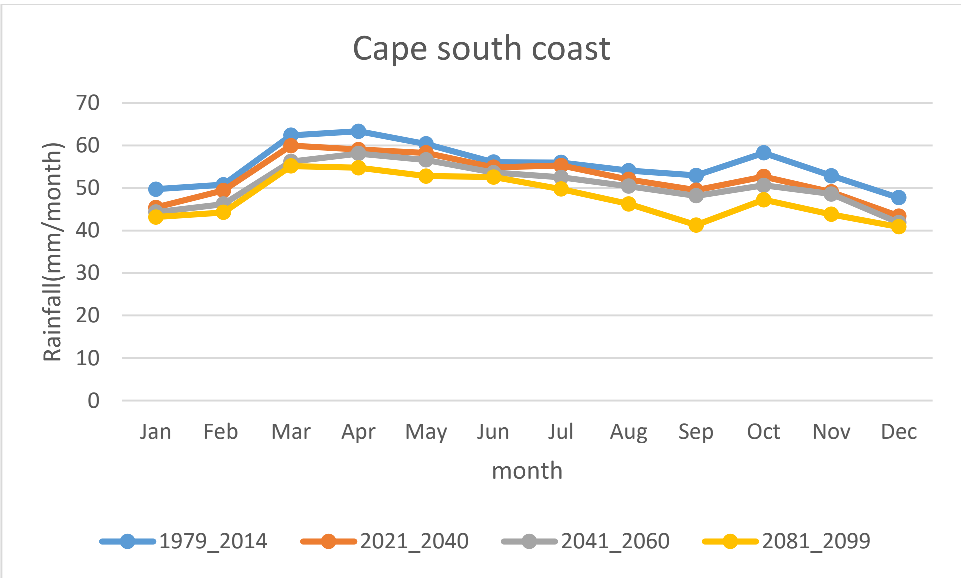

Figure 4.7: Monthly rainfall climatology for the present day climate (blue), near –term (orange), medium term (grey) and long term (yellow) for the Cape south coast in mm.

4.3.3.2 Eastern Southern Africa

Eastern southern Africa is a high rainfall region (figure 4.8). The CMIP6 present-day simulations outlines this region as a high rainfall region with observed rainfall peaks during summer DJF and spring SON. The simulated present-day rainfall minimum over this region is over 60 mm/month. The simulated present-day rainfall peaks over eastern southern Africa can reach up to 160 mm/month. For the projected periods, under low mitigation measures, there is a gradual increase in rainfall intensity over this region. Projected near-term scenarios, simulate rainfall to be just above the observed 160 mm/month, and over long-term periods rainfall increases drastically over this region reaching a peak of 180 mm/month under low mitigation measures.

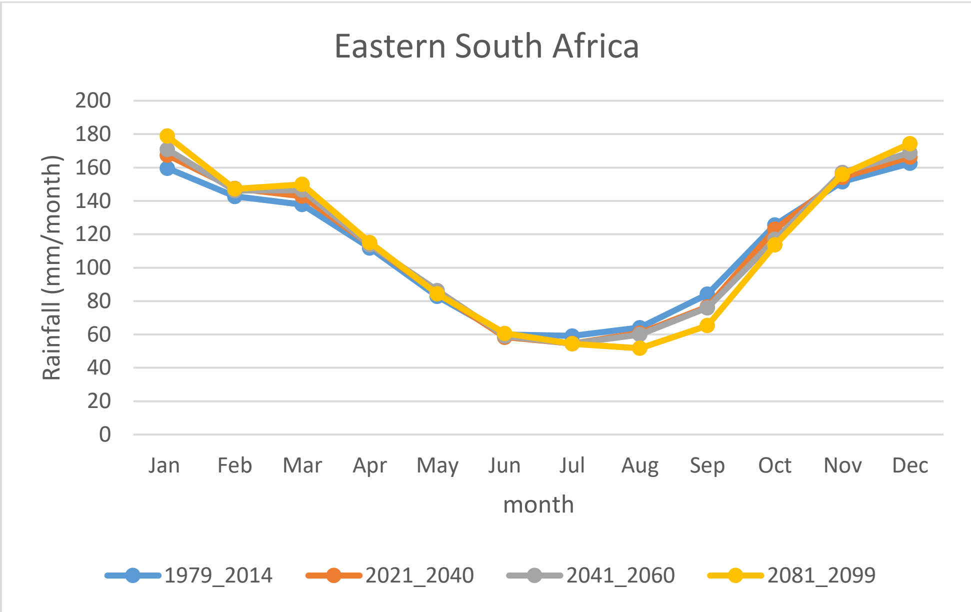

Figure 4.8: Monthly rainfall climatology for the present day climate (blue), near –term (orange), medium term (grey) and long term (yellow) for the eastern South Africa in mm.

4.3.3.3 Northern subcontinent

The northern subcontinent is also a high rainfall region. The rainfall peak from the simulated historical period in October is at above 200 mm/month (Figure 4.9). In the same month (October), during the near-term period under low mitigation, the peak will be right under 250 mm/month, for medium-term observation, the October rainfall peak is also slightly under 250 mm/month, and at long-term periods the October peak goes to above 250 mm/month. Rainfall is clearly projected to increase over the different periods.

.

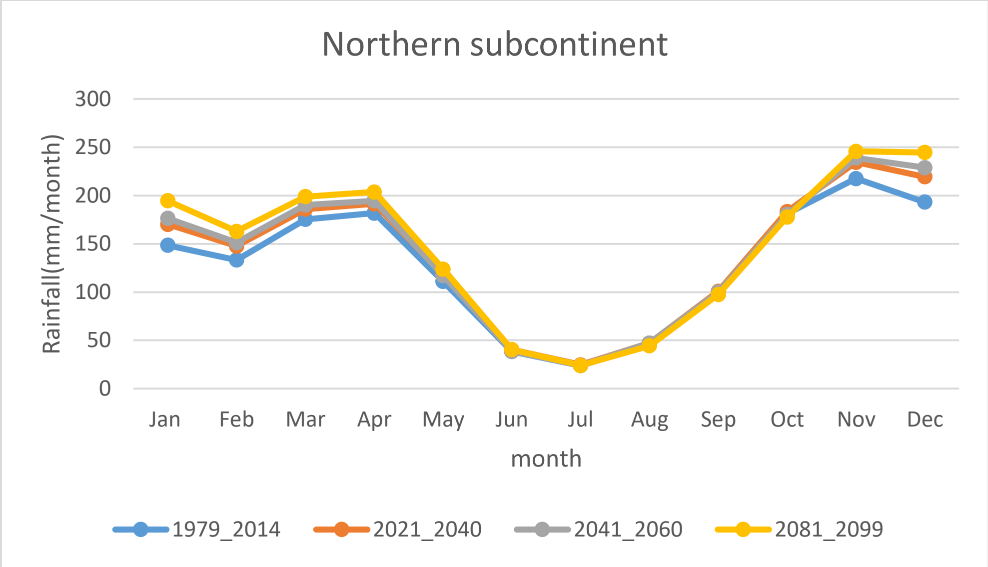

Figure 4.9: Monthly rainfall climatology for the present day climate (blue), near –term (orange), medium term (grey) and long term (yellow) for northern subcontinent in mm.

.

4.3.3.4 North-eastern South Africa, S Zimbabwe, and S Mozambique

The NESA region is a predominantly high rainfall region, according to the CMIP6 simulations for the historical period (Figure 4.10). The simulated rainfall peak for the present-day period over this region is above 180 mm/month. Moreover, the mean monthly minimum rainfall is below 20 mm/month. According to the three projected periods under low mitigation scenarios this region experiences a slight decline in rainfall. With NESA being a high rainfall region, one would anticipate that under a low mitigation future, rainfall patterns would increase, however, this is not the case.

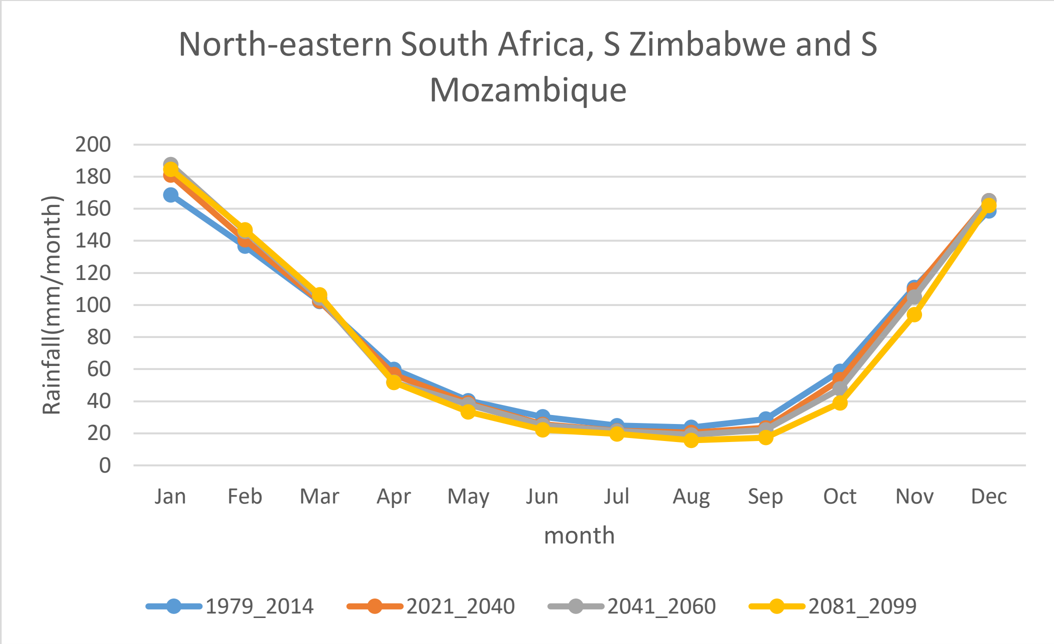

Figure 4.10: Monthly rainfall climatology for the present day climate (blue), near –term (orange), medium term (grey) and long term (yellow) for north eastern South Africa, south Zimbabwe and south Mozambique in mm.

4.3.3.5 Western subcontinent

CMIP6 simulations for the present-day period outline the western subcontinent as a low rainfall region (Figure 4.11). The present-day rainfall pattern experiences rainfall peaks during the summer and autumn seasons. The present-day rainfall peak is observed to be above 50 mm/month. Moreover, present-day rainfall minimums are under 10 mm/month from June to October. The ScenarioMIP future periods indicate that this region will experience declines in rainfall. With the western subcontinent already being a dry region, droughts are set to increase over this region during the different periods and set to increase as we move further into time under low mitigation measures.

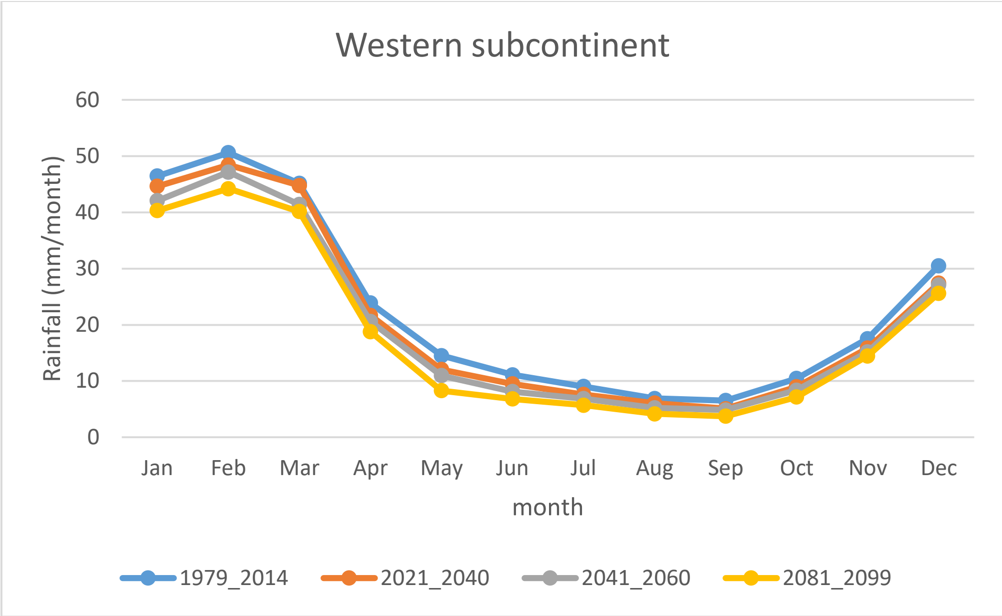

Figure 4.11: Monthly rainfall climatology for the present day climate (blue), near –term (orange), medium term (grey) and long term (yellow) for the western subcontinent in mm.

4.3.3.6 South Western Cape

Present-day regional rainfall for the South Western Cape, identifies this region as a winter rainfall region, with the highest rainfall occurring during June and July with above 50 mm/month in rainfall for these two months (Figure 4.7). A decline in rainfall can already be detected in the near-term projections. During near-term projections, the rainfall peak is projected to be below 50 mm/month. Over longer-term periods, the rainfall peak declines to below 40 mm/month. The Cape Town region from 2015-17 suffered a multi-year drought and associated water crisis, the projections shown here are indicative that such droughts may occur more frequently under low mitigation futures.

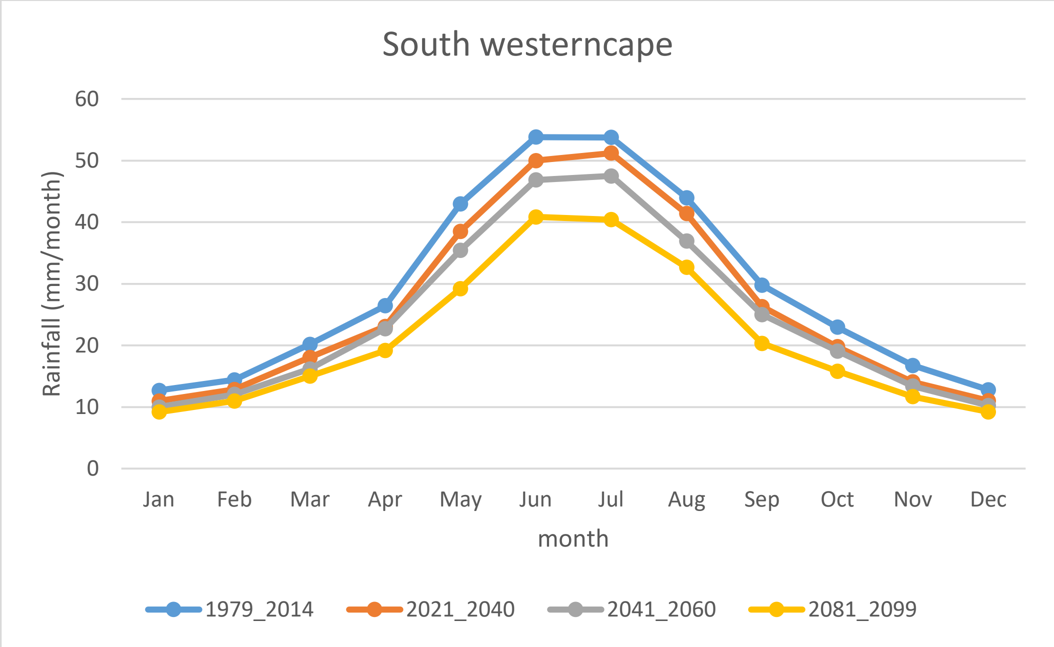

Figure 4.12: Monthly rainfall climatology for the present day climate (blue), near –term (orange), medium term (grey) and long term (yellow) for the South Western Cape in mm.

4.3.3.7 N Mozambique and Tanzania

Over northern Mozambique and Tanzania, CMIP6 simulated rainfall patterns for the historical period define this region as a summer rainfall region, with high rainfall peaks occurring during summer at above 200 mm/month (Figure 4.13). Under future rainfall scenarios, the rainfall peak is set to reach under 250 mm/month for the longer-term period. Amongst all the future periods, there is a persistent slight increase in rainfall, under low mitigation measures.

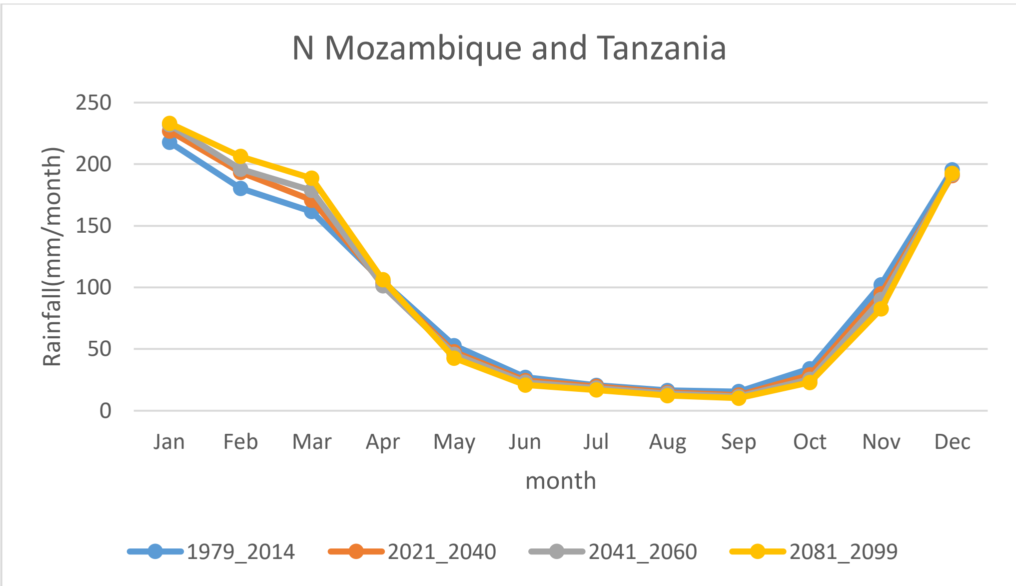

Figure 4.13: Monthly rainfall climatology for the present day climate (blue), near –term (orange), medium term (grey) and long term (yellow) for north Mozambique and Tanzania in mm.

4.3.3.8 Central subcontinent

CMIP6 simulations for the present-day period outlines the central subcontinent as a moderate rainfall region (Figure 4.11). Present-day rainfall peaks over this are above 100 mm/month. The present-day rainfall minimum over this region is below 20 mm/month. The ScenarioMIP future periods indicate a very slight decline in rainfall over this region, even over long periods, the rainfall reduction is slight.

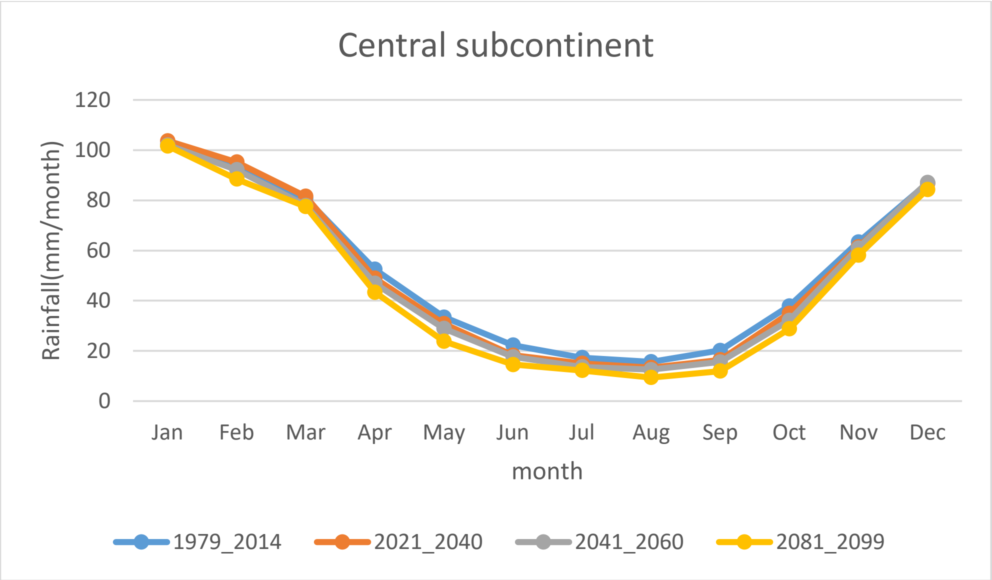

Figure 4.14: Monthly rainfall climatology for the present day climate (blue), near –term (orange), medium term (grey) and long term (yellow) for the central subcontinent in mm.

4.4 Model projections: future changes in temperature

The ensemble-mean evaluation performed for the historical period (1979–2014) using the CRU, ERA-Interim and CMIP6 dataset revealed that the CMIP6 simulates spatial temperature patterns over southern Africa well, and also realistically represents the intra-annual cycle of monthly mean temperature (compared to the observed reference dataset CRU). In this section, of the projected changes in temperature patterns between the near-term period, the medium-term period, and the long-term period under SSP5-8.5 are analysed. This is done spatially across southern Africa for the different seasons, as well as in more detail for each of the regions of (Engelbrecht et al., 2009) and Chapter 3, by considering intra-annual variability at a regional basis.

4.4.1 Change in annual temperature

Figures 4.15 - 4.17 outline annual temperature change results in °C for three different future periods under high emission scenarios (SSP5-8.5), using the period (1979-2014) as the baseline for assessing temperature change.

4.4.1.1 Near-term (2021-2040) annual temperature change

The near-term annual assessment of temperature projections indicates that further heating can be expected across the entire subcontinent (figure 4.15) relative to the 1979-2015 baseline. The coastal border will experience an approximately ~1°C temperature increase, whereas areas inland will experience just under 2°C in temperature increase. The smaller changes along coastal areas can be attributed to the moderating effects of the ocean.

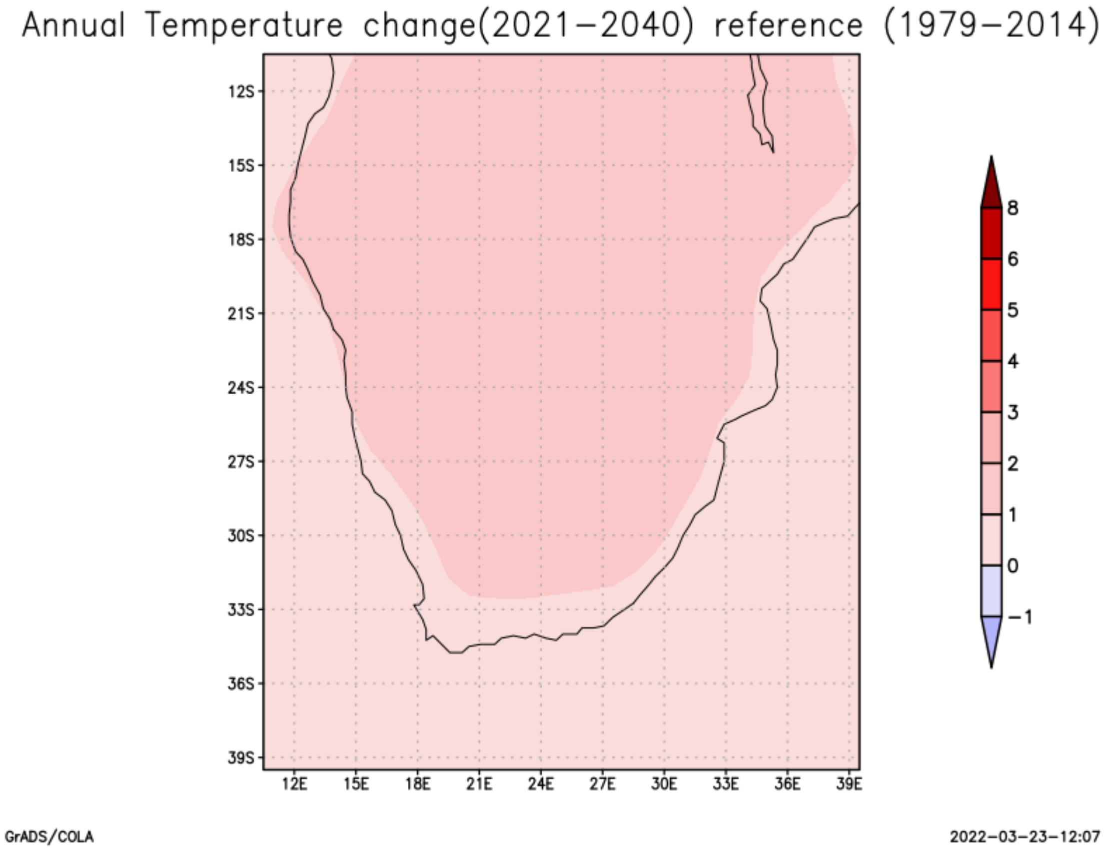

Figure 4.15: Projected change in annual average temperature (°C) in the near-term (2021-2040) relative to 1979-2014 across southern Africa.

4.4.1.2 Medium-term (2041-2060) annual temperature change

Figure 4.16 shows projections of temperature increases for the mid-term future. Coastal areas are projected to experience temperature increases as high as 2 °C, and inland areas temperature increases as high as 3 °C, relative to the 1979-2014 baseline.

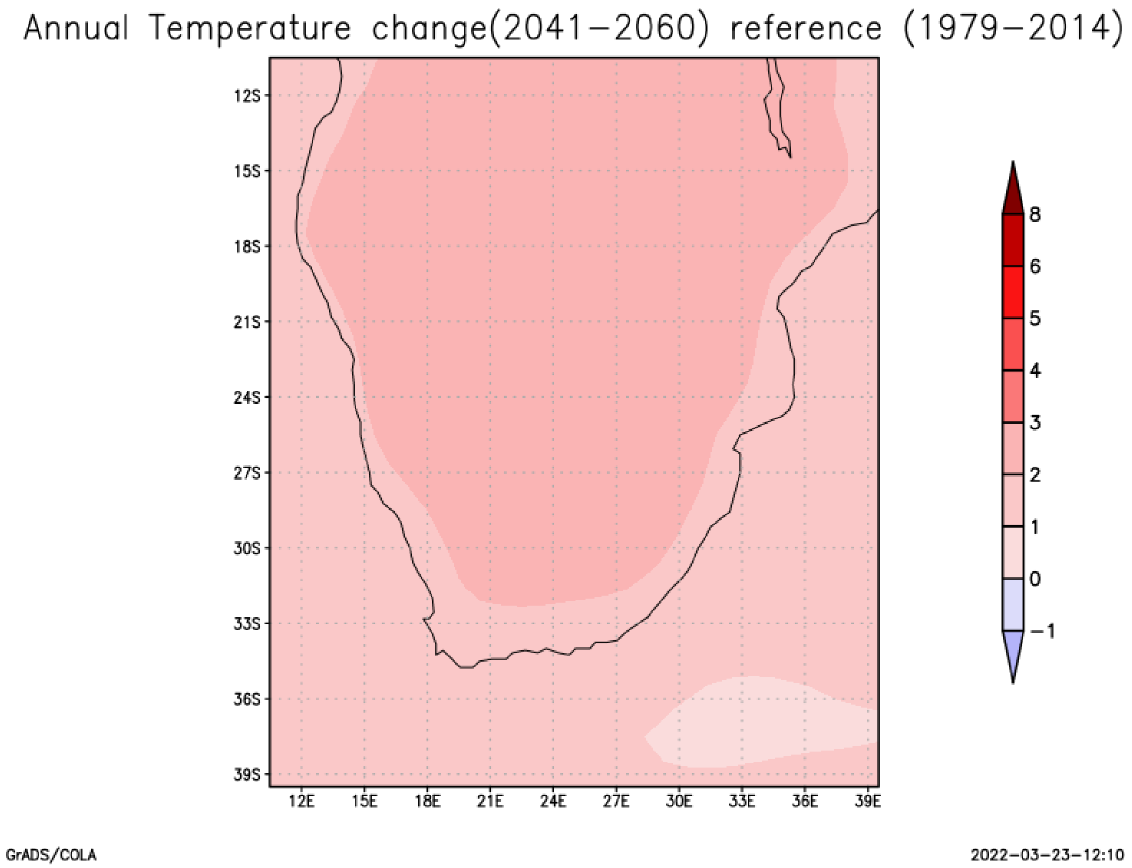

Figure 4.16: Projected change in annual average temperature (°C) in the mid-term (2041-2060) relative to 1979-2014 across southern Africa.

4.4.1.3 Long-term (2081-2099) annual temperature change

For the long-term future under low mitigation measures, temperatures increases are projected to be substantial (figure 4.17). These increases will range between 5 and 6 C° over large parts of the western and central interior regions. Moreover, the coastal border will experience an above 3°C temperature increase with the degree of heating increasing moving from the coast to the interior.

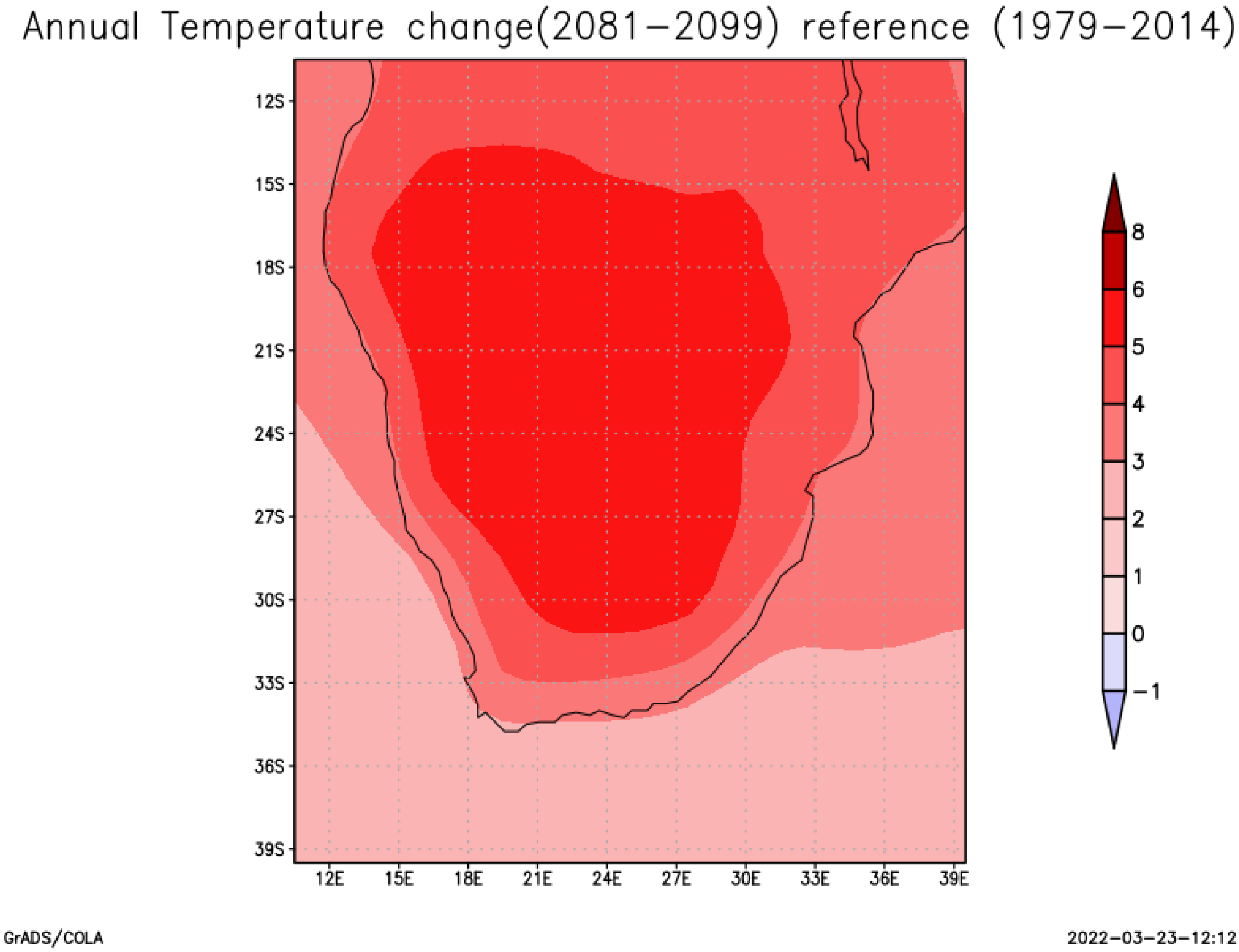

Figure 4.17: Projected change in annual average temperature (°C) in the long-term (2081-2099) relative to 1979-2014 across southern Africa.

4.4.2 Seasonal temperature change

Figures 4.18 – 4.20 examine future seasonal temperature changes (°C) over southern Africa, for the near-term (2021-2040), medium-term (2041-2060), and the long-term (2081-2099) periods, against the reference observed period (1979-2014), under the low mitigation scenario SSP5-8.5.

4.4.2.1 Seasonal temperature change for the near-term period (2021-2040)

Figure 4.18 outlines seasonal temperature changes for the near-term period under low mitigation measures (SSP5-8.5). The JJA season shows a general increase in temperature, over the coastal border, the temperature increase is not as intense as in inland areas. The coastal borders of the subcontinent will experience a 1°C temperature increase, and the inland areas a 2°C temperature increase over Southern Africa during the JJA. Moreover, during the SON season, the continued general temperature increase is predominant over the entire subcontinent. Moreover, the entire subcontinent experiences a 2°C temperature increase, and only the coast of South Africa will experience a 1°C temperature increase. Moving over to the summer season DJF, the persistent temperature increase is also inherited throughout this season. However, during the DJF season, the heating travels slightly northwards. Furthermore, during the MAM season, temperature increases are experienced over the entire subcontinent. Moreover, the eastern coastal region experiences a temperature increase of 1°C, and the western inland and the central subcontinent experience a 2°C temperature increase over the southern Africa region for the near-term period under low climate change mitigation measures.

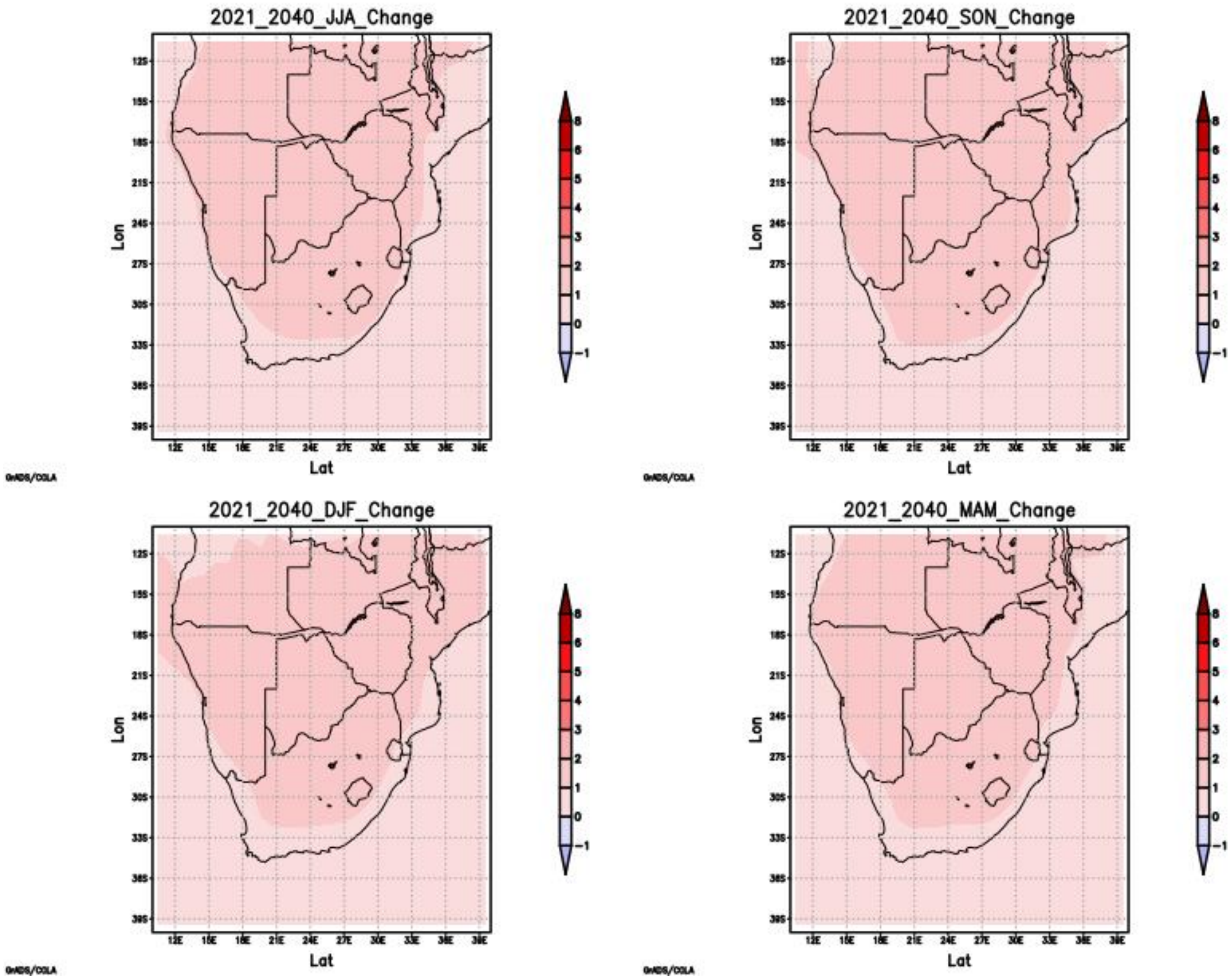

Figure 4.18: Projected change in seasonal average temperatures (°C) in the near-term (2021-2040) relative to 1979-2014 across southern Africa.

4.4.2.2 Seasonal temperature change for the medium-term period (2041-2060)

Seasonal temperatures under the low mitigation measures during the medium-term period are shown in figure 4.19. Temperature will continue to rise in-between seasons, all seasons experience the continued temperature increases, all inland/central areas for all the seasons experience a 2°C temperature increase, and coastal areas between all the seasons experience a 1°C temperature, besides the west coast during JJA. However, Mozambique, in almost all the seasons experiences a lower degree of increase compared to all the countries in the southern Africa region. Furthermore, only during the DJF season do some parts of Angola and western Zambia experience a lesser degree of increase with temperatures at 1°C for the DJF season at medium-term projected periods.

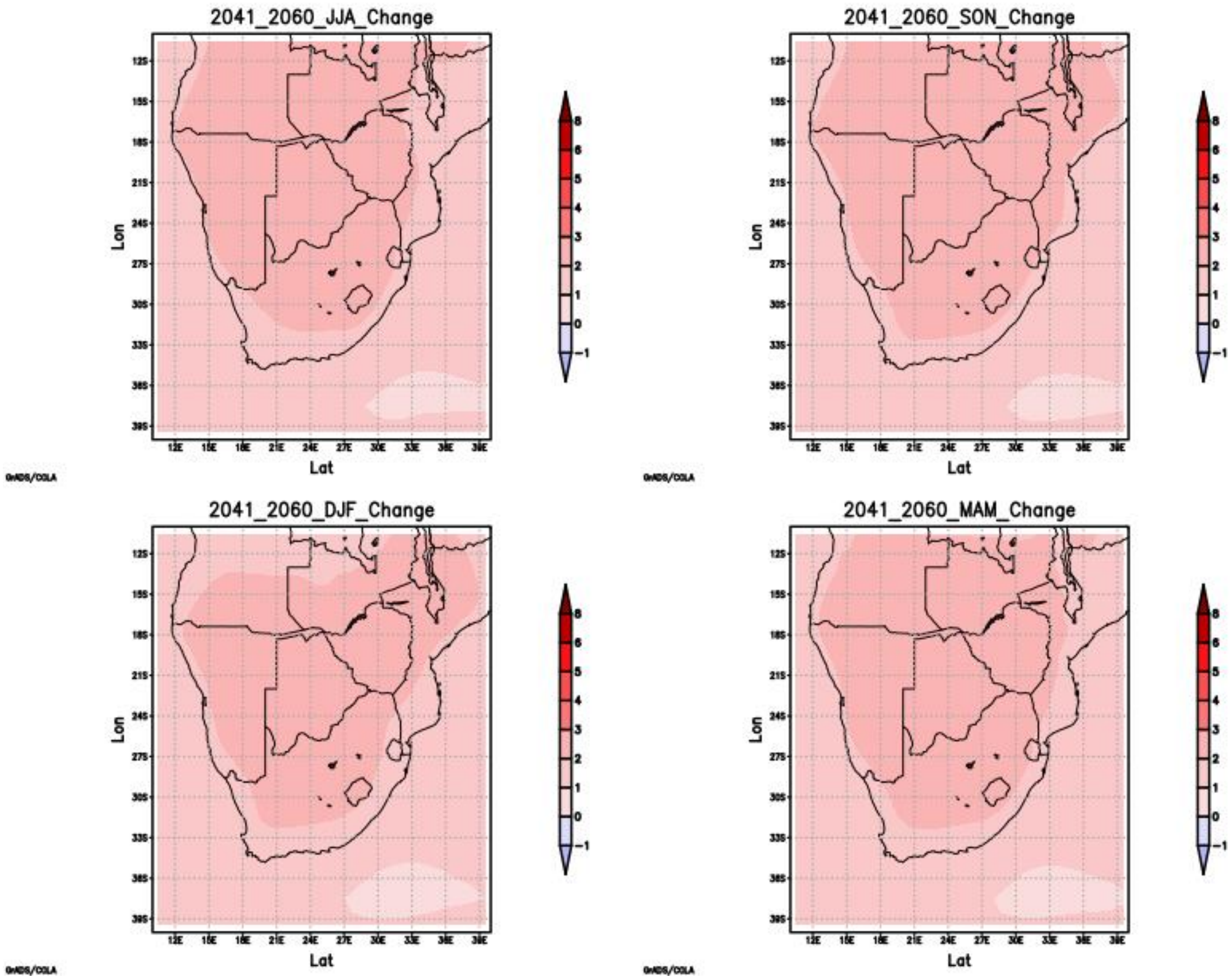

Figure 4.19: Projected change in seasonal average temperatures (°C) in the mid-term (2041-2100) relative to 1979-2014 across southern Africa.

4.4.2.3 Seasonal temperature change for the long-term period (2081-2099)

Figure 4.20 indicate an intensely increased temperature pattern, more intense than in the previous periods during the long-term period, under low mitigation measures. The general rate of temperature increase throughout all the seasons is greater than 4°C, mainly concentrated on the central and western subcontinent. During the SON season, drastic temperature increases will be experienced largely over the interior of Botswana, extending towards central South Africa even reaching Gauteng, during this season (SON). Over the before mentioned specified areas, temperature increases will be at over 8°C during the spring season. The decrease of temperatures towards the coast will also be a common phenomenon during this period similar to the near-term and medium-term periods.

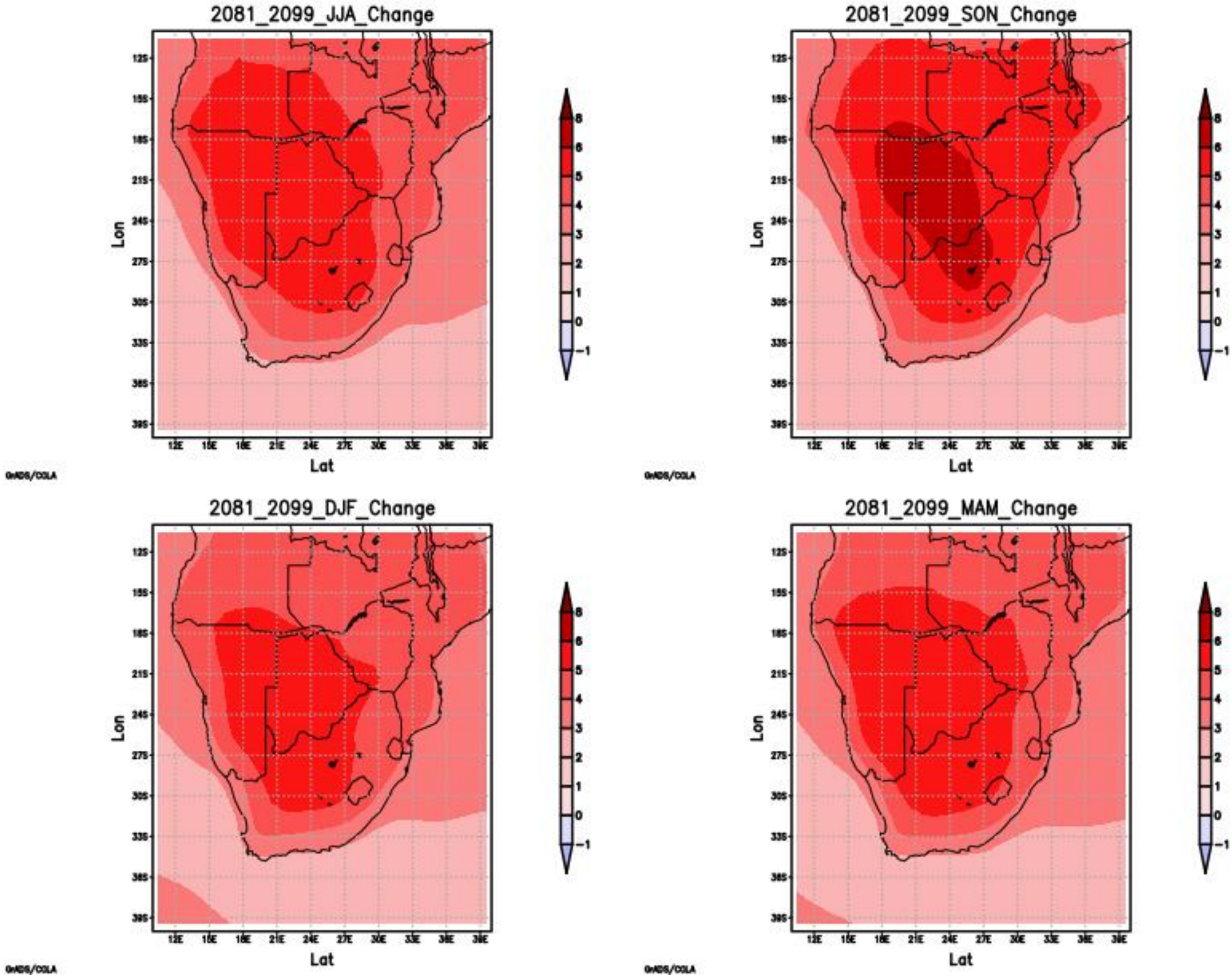

Figure 4.20: Projected change in seasonal average temperatures (°C) in the long-term (2081-2099) relative to 1979-2014 across southern Africa.

4.4.3 Regional temperature change

The following figures display the projected changes in temperature (°C) across the different southern African sub regions of (Engelbrecht et al., 2009) and Chapter 3, for the near-term (orange), mid-term (grey) and long-term (yellow) relative to the 1979-2014 (blue), under low climate change mitigation (SSP5-8.5).

4.4.3.1 Cape south coast

The Cape south coast has a similar projected temperature trend as the south Western Cape (Figure 4.21). Simulated CMIP6 temperatures for the reference period peak at above 20°C. In the long term, this maximum is projected to become 25°C.

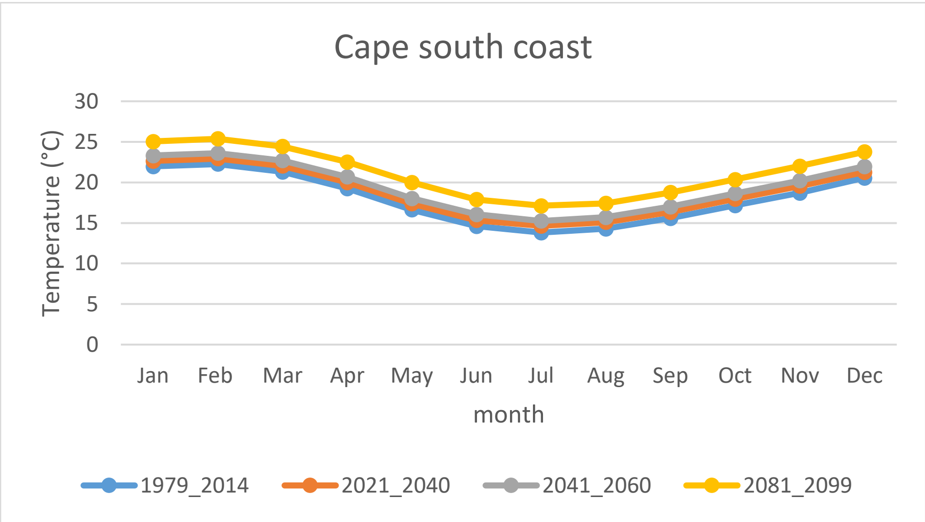

Figure 4.21: Monthly temperature climatology for the present day climate (blue), near –term (orange), medium term (grey) and long term (yellow) for Cape south coast in ^{0}Celsius.

4.4.3.2 Eastern South Africa

The historical CMIP6 dataset outlines the rainfall peak of this region to be slightly above 20°C in January (figure 4.22). Temperature increases are projected to increase from the near-term to the long-term, with the January peak reaching 25°C in the long-term.

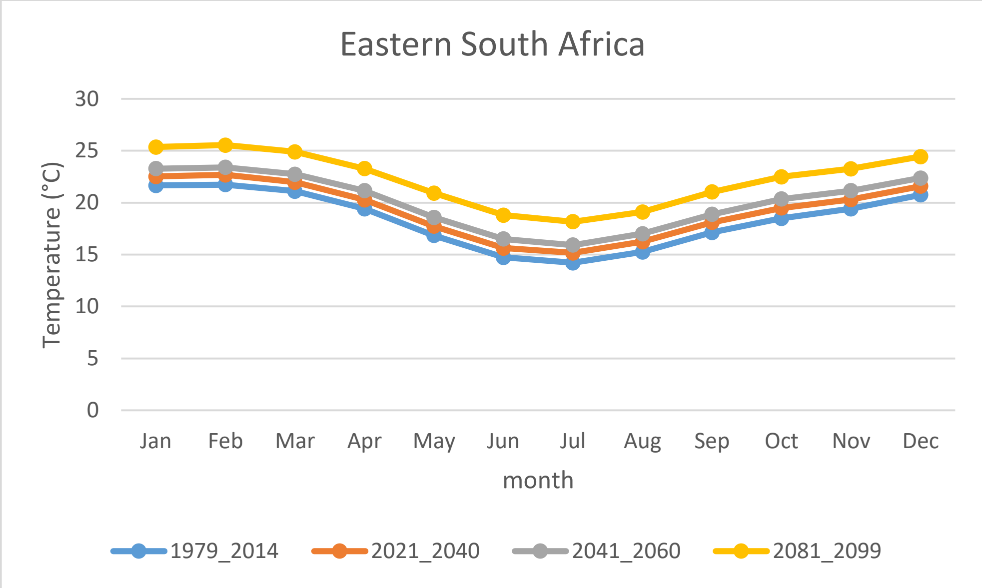

Figure 4.22: Monthly temperature climatology for the present day climate (blue), near –term (orange), medium-term (grey) and long-term (yellow) for eastern South Africa in ^{0}Celsius.

4.4.3.3 Northern subcontinent

The northern subcontinent is a consistently hot region (Figure 4.23). Simulated historical temperatures over the northern subcontinent are slightly below 20°C for all the months. According to future CMIP6 climate projections under low mitigation measures, there is a constant temperature increase over this region. During the long-term period, the temperatures over this region will be slightly be 30°C.

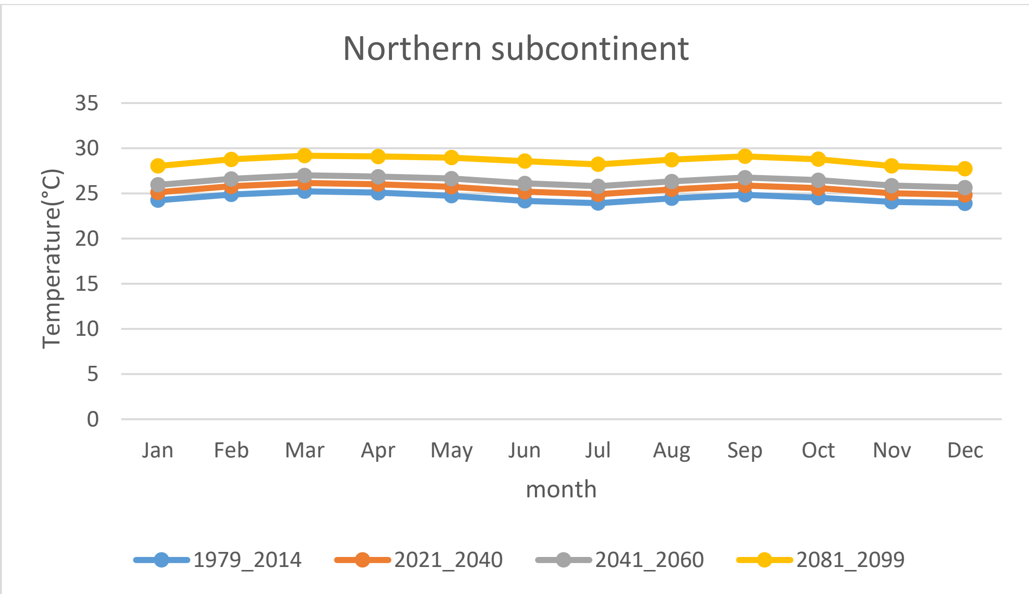

Figure 4.23: Monthly temperature climatology for the present day climate (blue), near –term (orange), medium term (grey) and long term (yellow) for northern subcontinent in Celsius

4.4.3.4 North-eastern South Africa, S Zimbabwe, and S Mozambique

The NESA region is also hot (Figure 4.24). The historical CMIP6 dataset simulates the maximum present-day monthly-means temperature over this region to be 25°C in January. The graph below indicates sharp increases in temperature over the NESA region, under low mitigation scenarios. The January temperature peak for the long-term period will be 30°C. Moving further and further into the future, this region is projected to become hot.

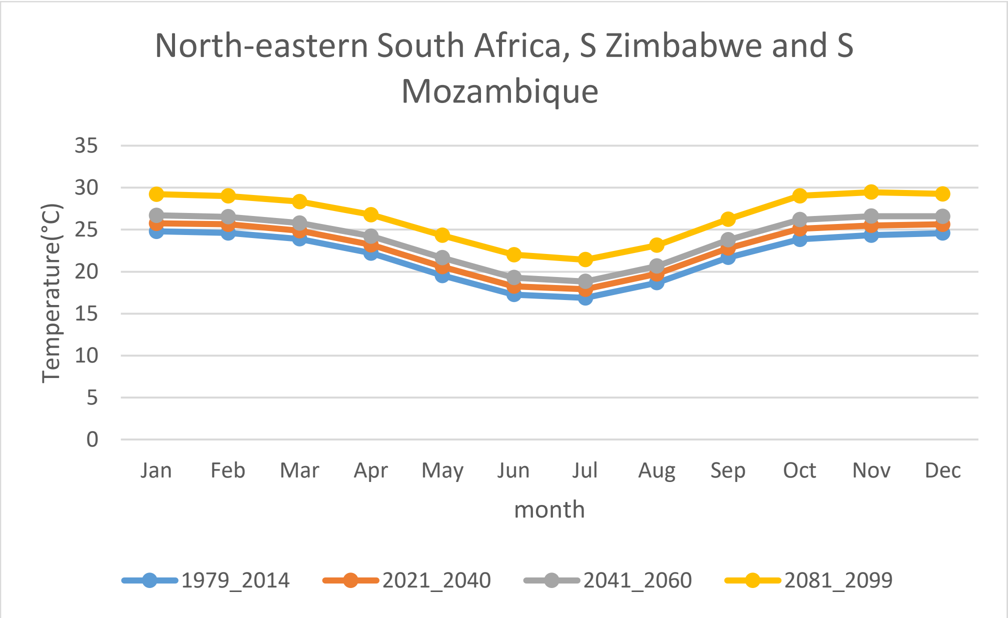

Figure 4.24: Monthly temperature climatology for the present day climate (blue), near –term (orange), medium term(grey) and long term (yellow) for north eastern South Africa, south Zimbabwe and south Mozambique in ^{0}Celsius.

4.4.3.5 Western subcontinent

The western subcontinent is hotter than all the other regions in the southern African subcontinent (Figure 4.25). According to CMIP6 simulation for the historical period the temperature peak for the western subcontinent is slightly below 25°C. The projected future periods will experience increased temperature over this region. The long-term period simulates the present-day reference temperature peak to be slightly increase to just below 30°C.

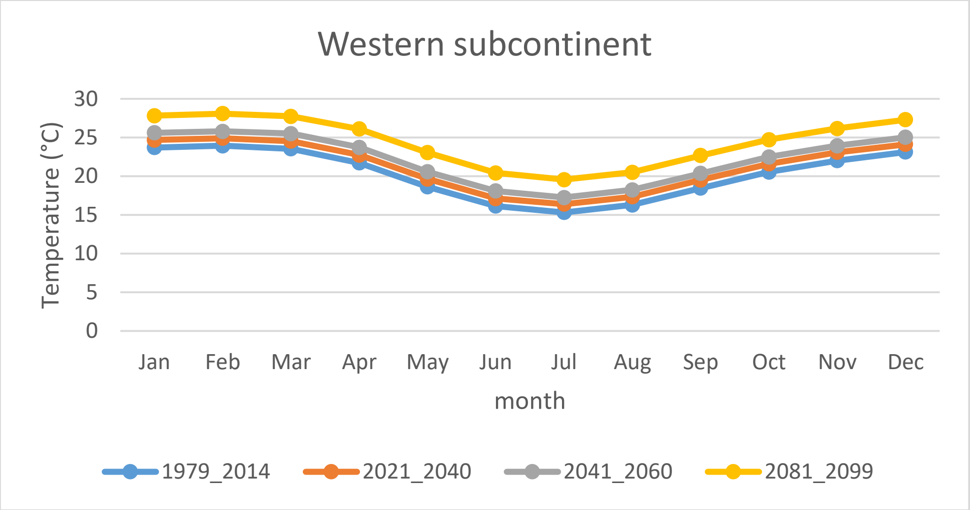

Figure 4.25: Figure 4.24: Monthly temperature climatology for the present day climate (blue), near –term (orange), medium term (grey) and long term (yellow) for the western subcontinent in ^{0}Celsius.

4.4.3.6 South Western Cape

Figure 4.26 illustrates that the CMIP6 simulation for the historical period defines the monthly average temperature maximum of the south Western Cape to be slightly above 20°C. Systematic temperature increases are projected for the south Western Cape over time, so that January temperatures will eventually be above 25°C, under low mitigation scenarios in the long-term.

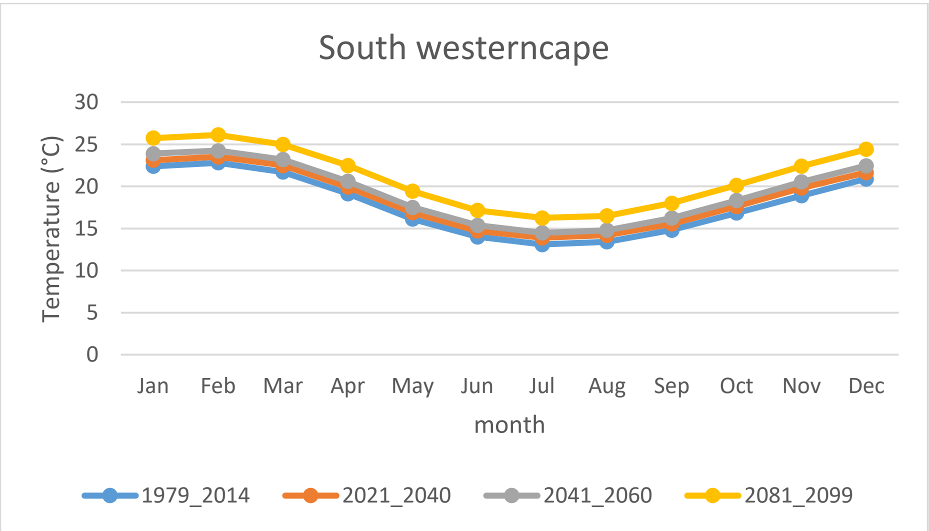

Figure 4.26: Monthly temperature climatology for the present day climate (blue), near –term (orange), medium term (grey) and long term (yellow) for south Western Cape in ^{0}Celsius.

4.4.3.7 N Mozambique and Tanzania

Northern Mozambique and Tanzania experience hot temperatures (Figure 4.27). The simulated historical temperature peak is 25°C in January. The CMIP6 ensemble projections under SSP5-8.5, simulates the temperature peak to be slightly above 31°C during summer in the long-term.

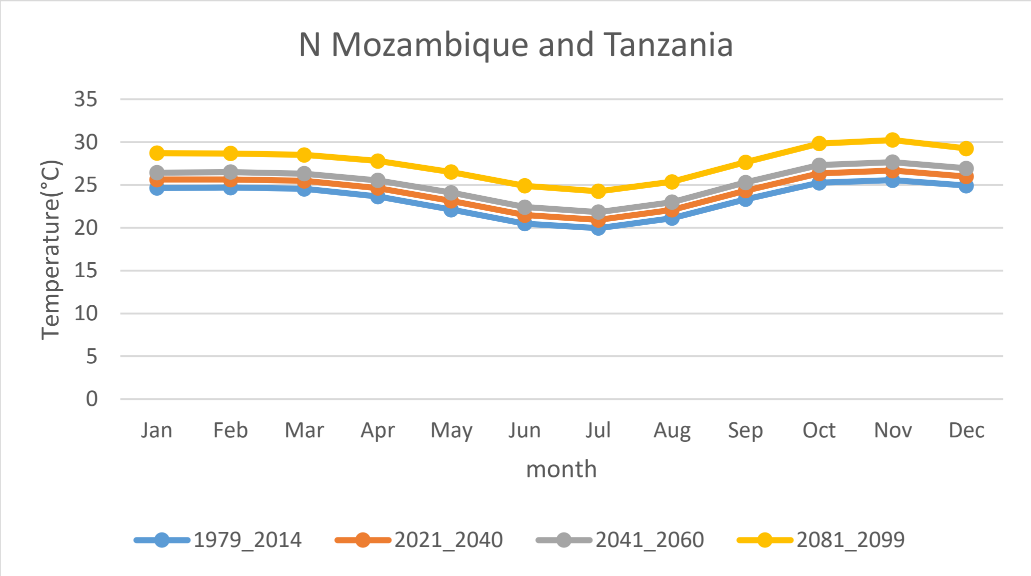

Figure 4.27: Monthly temperature climatology for the present day climate (blue), near –term (orange), medium term (grey) and long term (yellow) for northern Mozambique and Tanzania in ^{0}Celsius.

4.4.3.8 Central subcontinent

The central subcontinent is also a hot region. According to CMIP6 simulations for the present-day period, the temperature peak for this region is exactly 25°C in January (Figure 4.28). Future model projections at different periods under low mitigation scenarios simulate high-temperature increases. For the long-term period, the temperature peak will be 30°C, and this increasing trend in temperatures is prevalent across all the months and increases as we move further into the future under no mitigations structures.

.

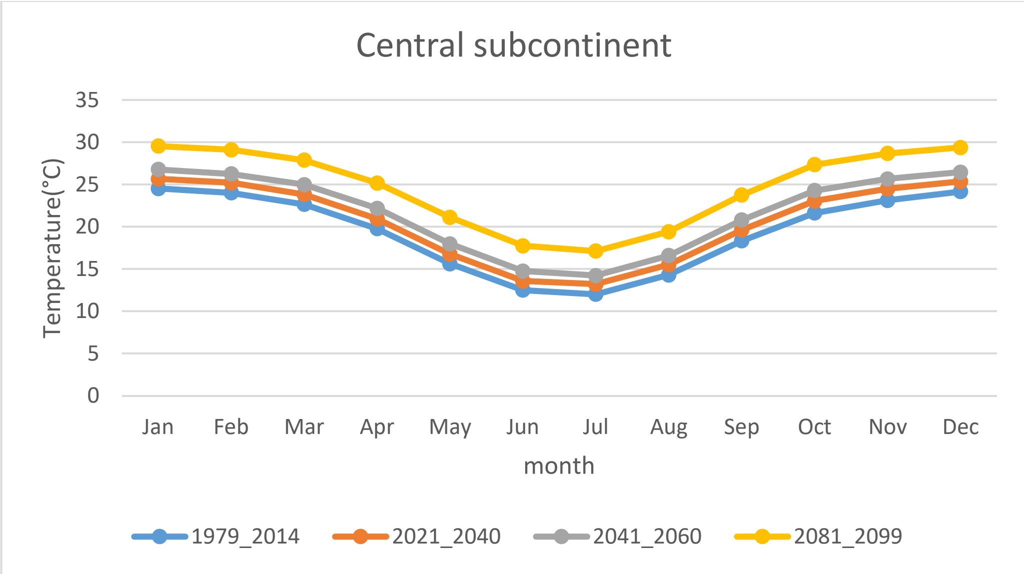

Figure 4.28: Monthly temperature climatology for the present day climate (blue), near –term (orange), medium term (grey) and long term (yellow) for the central subcontinent in ^{0}Celsius.

4.5 Discussion

CMIP6 ensemble simulates rainfall patterns over southern Africa realistically (compared to the observed reference dataset CRU). A general positive bias is present across southern Africa in terms of the representation of annual rainfall totals. The strongest rainfall reductions are projected for the western subcontinent and Mozambique. Rainfall increases are projected over the norther subcontinent, in association with the southern expansion of the tropical belt in a warmer world.

Seasonal temperature change indicates an intensely increased temperature pattern, more intense than in the previous periods during the long-term period, under low mitigation measures. The general rate of temperature increase throughout all the seasons is greater than 4°C. Temperature will continue to rise in-between seasons, all seasons experience the continued temperature increases, all inland/central areas for all the seasons experience a 2°C temperature increase, and coastal areas between all the seasons experience a 1°C temperature, besides the west coast during JJA. However, Mozambique, in almost all the seasons experiences a lower degree of increase compared to all the countries in the southern Africa region.

4.6 Conclusion

In closing, the eastern and western regions of southern Africa will experience different climate extremes as far as climate change is concerned. The eastern parts of southern Africa tend to be generally hot with variable rainfall (ENSO cycle), but with high rainfall totals compared to the western parts of southern Africa. These regions are projected to become drastically hotter and generally drier, except for the eastern escarpment areas that are projected to become wetter. The western regions of the subcontinent are hot and dry under present-day climate, and are not only projected to become drastically hotter, but simultaneously also drier.

CHAPTER 5: CONCLUSIONS AND RECOMMENDATIONS

The single most prominent characteristic feature of southern African climate is its pronounced dry-wet seasonality, as opposed to the hot-cold seasonality that dominates climate of the high latitudes of the Northern Hemisphere. The bulk of southern Africa's climatological rainfall occurs during a short period of about three months, during the austral summer, when precipitation is larger or more or less equal to potential evaporation. The dry season can be up to nine months long, in the sense of potential evaporation outweighing precipitation. Dry-wet seasonality has been the dominant modelled feature of southern Africa's climate for about 10 million years, but its origins are unknown. It is thought however, that the African savannahs, the dominant biome in southern and East Africa, evolved in the presence of fire and dry-wet seasonality during this period.

Global warming is already impacting on southern African climate, with the interior regions recording a rate of temperature increase almost twice the rate of global warming, over the last several decades. The main aim for undertaking this research project was to assess how future climate change may impact dry-wet seasonality in Southern Africa under low mitigation (high emissions) scenarios, through the use of objective model projections of future climate change. This research sought to answer two questions, which are first, the impact of climate change on the seasonal cycle of temperature, and the impact of climate change on the seasonal cycle in rainfall over southern Africa using the multi-model ensemble of projections of future climate change from CMIP6

As a preceding step, the study also had the objective of verifying how realistically the CMIP6 ensemble simulates present-day seasonality in southern Africa. This involved a comparative analysis between model simulations and observations, not only undertaken for the CMIP6 ensemble, but also for ETA-interim reanalysis. Reanalysis represents the type of climate simulation that theoretically should represent reality the closest, given that observed data is assimilated into the model simulations. Indeed, the verification results obtained revealed that reanalysis models are capable to simulate intra-annual variability (that is, the seasonal cycle) of both rainfall and temperature in southern Africa with great realism. This holds true for regions with diversely different climatic regimes: the winter-rainfall region of South Africa, the larger summer rainfall region of southern Africa, and the bimodal rainfall region of East Africa. There is a single exception, namely the narrow all-year rainfall region of the Cape south coast of South Africa, where the correlation between ERA-interim data and observations in terms of intra-annual rainfall variability is substantially weaker than for other regions in southern Africa. In general, across the different climate regions considered, the CMIP6 ensemble qualitatively performs similarly to ERA-interim simulations, in the sense that it realistically simulates the intra-annual variability in both rainfall and temperature. For most regions, the CMIP6 scaled standard deviation for the rainfall variable is less than 1 and also smaller than that of ERA-interim, implying that the CMIP6 models with their lower spatial resolution underestimates the month-to-month variability of rainfall totals (or, stated alternatively, the amplitude of seasonality). CMIP6 data exhibits a general positive bias in simulating rainfall totals over southern Africa. The temperature bias is consistently cold, with the exception of autumn, which has a heat bias. Overall, the representation of present-day seasonality by the CMIP6 ensemble generates confidence in its projections of future climate change.

A consequence of southern Africa's location in the subtropics and wet-dry seasonality, is that it is generally a hot and dry region. In fact, about half of the southern African region's climate is semi-arid (annual rainfall totals less than 500 mm). The climate of the region displays pronounced inter-annual variability in relation to ENSO, and it is often during the El Niño phase of the cycle that brings enhanced water-stress to parts of southern Africa. It is against this background that the CMIP6 ensemble projects general reductions in rainfall over southern Africa under low mitigation, with corresponding drastic increases in temperature. These results from CMIP6 confirm the 2018 classification by the IPCC SR1.5 report, of the southern African region being a climate change hotspot: when a hot and dry region becomes even hotter and likely also drier, the options for adaptation are limited. Another important point is that over large parts of eastern and central southern Africa, the largest indication of drier and hotter future conditions (largest rainfall deficits coupled with largest temperature increases) is in the spring period.

There are some important exceptions, in terms of the general pattern of change projected by the CMIP6 ensemble. The first is the northernmost parts of southern Africa, located in the tropical savannah zone, where increases in rainfall are projected. This pattern of change relates to the expansion of the humid tropical belt in a hotter climate. The second is the eastern escarpment areas of South Africa where general increases in rainfall are projected. This signal has been detected before, in projections of regional climate models and the CMIP5 ensemble, which preceded CMIP6. It is not a signal associated with strong agreement across individual climate models, however, as shown in the recent AR6 report. Conversely, there is strong model agreement and high confidence in the general pattern of drying projected for the southern African region. This drying scales over time under low mitigation futures, or in other words, with the level of global warning. That is, the pattern of drying projected for southern Africa for the near-term, amplifies over time, and so does the pattern of regional warming being strong compared to the level of global warming.

In closing, the eastern and western regions of southern Africa are projected to experience climate change futures that in some aspects may be different. The eastern parts of southern Africa tend to be generally hot with variable rainfall (ENSO cycle), but with high rainfall totals compared to the western parts of southern Africa. These regions are projected to become drastically hotter and generally drier, except for the eastern escarpment areas that may become wetter. The western regions of the subcontinent are hot and dry under present-day climate, and are not only projected to become drastically hotter, but simultaneously also drier.

Climate change in eastern southern Africa may pose a unique set of risks to communities and government in a changing climate. Although the region is projected to become generally drier, summers are projected to be generally wetter in the east. This implies an increase in the nature of rainfall – namely more intense rainfall events in summer. Wetter and hotter summers pose many risks, starting with more damaging heavy precipitation events, heat-waves impacting on human health, and the possibility of diseases and pests spreading more easily in the more humid climate. On the other hand, the western subcontinent is projected to experience increasingly hot and dry conditions from the southwest coast towards the north of Angola. This effectively renders these regions a climate-change hotspot, since when climates that a naturally hot and dry become hotter and drier, the options for adaptation are limited.

It should finally be noted that the CMIP6 ensemble projects staggeringly large temperature increases over the interior regions of southern Africa under low mitigation relative to 1979-2014. Over large regions of the interior, and across all seasons, this change is in the order of 5 °C. Temperature increases of this magnitude may well be devastating to aspects of southern African agriculture and biodiversity, and will also impact directly on human health. In eastern southern Africa general reductions in rainfall but increases in summer rainfall effectively implies an increase in the amplitude of wet seasonality. Across the southern African region, drastically increase in temperature, which translates to enhanced evaporation from soils, in combination with projected reductions in rainfall effectively suggests a longer burning season, and a shorter growing season (through reductions in soil moisture).

Although South Africa needs to contribute its fair share to climate change mitigation as per the Paris Agreement on Climate Change, it should be realised that avoiding low mitigation futures is not in South Africa’s hands. Should the international action on mitigation fails, this research is indicative of major and far-reaching risks for southern Africa. The region should thus focus strongly on adaptation action, in addition to its efforts on mitigation.

CHAPTER 6: REFERENCES

Africa's Climate Report. (2016). Helping Decision-makers make sense of Climate Information.https://www.futureclimateafrica.org/wp-content/uploads/2016/11/africas-climate-final-report-4nov16.pdf.

Akinsanola, A.A. Ajayi, V.O. Adejare, A.T. Adeyeri, O.E. Gbode, I.E. Ogunjobi, K.O. Nikulin, G. & Abolude, A.T. (2017). Theory of Applied Climatology: *Evaluation of rainfall simulations over West Africa in dynamically downscaled CMIP5 global circulation models.* DOI 10.1007/s00704-017-2087-8.

Archer, E.M. Landman, W.A. c, Mark Alexander, M. Tadross, M.A. Malherbe, J. Weepener, H. Maluleke, P. Marumbwa, F.M. (2017). Climate Risk Management: *Understanding the evolution of the 2014–2016 summer rainfall seasons in southern Africa: Key lessons.* 16, 22–28.

Archibald, S. Roy. D. Van Wilgen, B. & Scholes R.J. (2009). Global Change Biology: *What limits fire? An examination of drivers of burnt area in Southern Africa.* doi: 10.1111/j.1365-2486.2008. 01754.

Balfour, D. & Howison, O. (2001). African Journal of Range & Forage Science: *Spatial and temporal variation in a mesic savanna fire Regime: responses to variation in annual rainfall*. 19, 45-53.

Bates, B. Kundzewicz, Z.W. Wu, S. & Palutikof, J. (2008). Climate change and water. IPCC Tech. Paper 6, 200.

Bowman, D. Zhang, Y. Walsh, A. & Williams, R. (2003). International journal for Wildlife Fire: *Experimental comparison of four remote sensing techniques to map tropical savanna fire-scars using Landsat-TM imagery*. 12,341–348. https://doi.org/10.1071/WF03030.

Cook, C. Reason, C.J. & Hewitson, B.C. (2004). Climate Research: *Wet and dry spells within particularly wet and dry summers in the South African summer rainfall region.* 26(1), 17– 31.

Cook, K. H. & Vizy, E.K. (2013). International journal of Climatology: *Projected changes in East African rainy seasons.* 26, 5931–5948. https://doi.org/10.1175/JCLI-D-12-00455.1.

Cook, K.H. (2001). Journal of the Atmospheric Sciences: *A Southern Hemisphere wave response to ENSO with implications for Southern Africa precipitation*. 58(15), 2146– 2162.

Crétat, J. Richard, Y & Pohl, B. (2012). International journal of Climatology: *Recurrent daily rainfall patterns over South Africa and associated dynamics during the core of the austral summer.* 32,261–273. https ://doi.org/10.1002/joc.2266.

D'Aberton, P.C & Tyson, P.D. (1996). Water SA: *Three-dimensional kinematic trajectory modelling of water vapour transport over Southern Africa*. 22, 297–305.

Davis, C. L. & Vincent, K. (2017). Climate risk and vulnerability: A handbook for SouthernAfrica.https://www.csir.co.za/sites/default/files/Documents/SADC%20Handbook_Second%20Edition_full%20report.pdfhttp://hdl.handle.net/10204/10066.

Dedekind, Z. Engelbrecht, F.A & Van der Merwe, J. (2016). Water SA*: Model simulations of rainfall over southern Africa and its eastern escarpment.* 42, 129-143.

Dedekind, Z. Engelbrecht, F.A. & Van der Merwe, J. (2015). Water SA: *Model simulations of rainfall over southern Africa and its eastern escarpment.* 42, 1.

Dieppois B, Rouault M &· New M. (2015). Climate Dynamics: *The impact of ENSO on Southern African rainfall in CMIP5 ocean atmosphere coupled climate models*. 45,2425–2442. DOI 10.1007/s00382-015-2480-x.

Engelbrecht, C. J. Engelbrecht, F.A. & Dyson, L.L. (2013). International journal of Climatology: *High resolution model-projected changes in mid-tropospheric closed lows and extreme rainfall events over southern Africa. 33, 173-187.*

Engelbrecht, C.J. & Engelbrecht, F.A. (2016). Theoretical and applied climatology: *Shifts in Köppen-Geiger climate zones over southern Africa in relation to key global temperature goals.* 123, 247-261. DOI 10.1007/s00704-014-1354-1.

Engelbrecht, C.J. & Landman, W.A. (2015). Climate Dynamics: *Inter-annual variability of seasonal rainfall over the Cape south coast of South Africa and synoptic type association.* 47, 295–313.

Engelbrecht, C.J. Landman, W.A., Engelbrecht, F.A. & Malherbe, J. (2015a). Climate Dynamics: *A synoptic decomposition of rainfall over the Cape south coast of South Africa.* 44,2589-2607. doi: 10.1007/s00382-014-2230-5.

Engelbrecht, C.J., Engelbrecht, F.A. & Dyson, L.L. (2013). International Journal of Climatology: *High-resolution model-projected changes in mid-tropospheric closed-lows and extreme rainfall events over southern Africa.* 33, 173-187. DOI: 10/1002/joc.3420.

Engelbrecht, F. Adegoke, J. Bopape, M-J. Naidoo, M. Garland, R. Thatcher, M. McGregor, J. Katzfey, J. Werner, M. Ichoku, C. & Gatebe, C. (2015b). Environmental Research Letters: *Projections of rapidly rising surface temperatures over Africa under low mitigation.* (10)085004.

Engelbrecht, F.A. Landman, W.A. Engelbrecht, C. Landman, S. Bopape, M., Roux, B. McGregor, J. & Thatcher, M. (2011). Water SA: *Multi-scale climate modelling over Southern Africa using a variable-resolution global model.* 37 (5), 647–658.

Engelbrecht, F.A. McGregor, J.L. & Engelbrecht, C.J. (2009). International Journal of Climatology: *Dynamics of the conformal-cubic atmospheric model projected climate-change signal over southern Africa.* 29, 1013-1033. DOI: 10/1002/joc.1742.

Engelbrecht, F.A. Rautenbach, C.J. McGregor, J.L. & Katz, J.J. (2002). Water SA: *January and July climate simulations over the SADC region using the limited-area model DARLAM*. 28, 361-374.

Eyring, V. Bony, S. Meehl, G.A. Senior, C.A. Stevens, B. Stouffer, R.J. & Taylor K.E. (2016). Geoscience Model Development: *Overview of the Coupled Model Intercomparison Project Phase 6 (CMIP6) experimental design and organization.* 9, 1937–1958.

Fauchereau, N. Pohl, B. Reason, C.J.C. Rouault, M. & Richard, Y. (2009). Climate Dynamics: *Recurrent daily OLR patterns in the Southern Africa/Southwest Indian Ocean region, implications for South African rainfall and teleconnections.* 32(4), 575– 591.

Fauchereaun, N. Trzaska, S. Rouaul, M. & Richard, Y. (2003). Natural Hazards: *Rainfall Variability and Changes in Southern Africa during the 20th Century in the Global Warming Context.* 29, 139–154.

Favre, A. Hewitson, B. Lennard, C. Cerezo-Mota, R. & Tadross, M. (2013). Climate Dynamics: *Cut-off Lows in the South Africa region and their contributionto precipitation.* 41, 2331–2351.

Gore, M. Abiodun, B.J. & Kucharski, F. (2020). Climate Dynamics: *Understanding the influence of ENSO patterns on drought over southern Africa using SPEEDY*. 54, 307–327.

Harrison, M. S. J. (1984). International journal of Climatology: A generalized classification of South African summer rain-bearing synoptic systems. 4, 547-560. https://doi.org/10.1002/joc.3370040510.

Hart, N. C. G. Reason, C. J. C. & Fauchereau, N. (2013). Climate Dynamics: *Cloud bands over southern Africa: Seasonality, contribution to rainfall variability and modulation by the MJO*.41, 1199–1212. https://doi.org/10.1007/s00382-012-1589-4.

Hewitson, B.C. & Crane, R.G. (2002). Climate Research: *Self-organizing maps: applications to synoptic climatology*. 22, 13–26.

Hoegh-Guldberg O. Jacob, D. Taylor,M. Guillén Bolaños, T. Bindi, M. S. Brown, S. Camilloni, I.A. Diedhiou, A. Djalante, R. Engelbrecht, F. Guiot, J. Hijioka, Y. Mehrotra, S. Hope, C.W. Payne, A.J. Pörtner, H.O. Seneviratne, S.I. Thomas, A. Warren, R. Zhou, G. (2019). Science: *The human imperative of stabilizing global climate change at 1.5°C*. 1-8.

Hoell, A. Funk, C. Zinke, J. & Harrison, L. (2017). Climate Dynamics: *Modulation of the Southern Africa precipitation response to the El Niño Southern Oscillation by the subtropical Indian Ocean Dipole.* 48, 2529–2540.

IPCC (Intergovernmental Panel on Climate Change). (2007). Climate Change 2007: The Physical Science Basis. Contribution of Working Group I to the Fourth Assessment Report of the Intergovernmental Panel on Climate Change, S. Solomon, D. Qin, M. Manning, Z.Chen, M. Marquis, K. B. Averyt, M. Tignor and H. L. Miller, Eds.

IPCC (Intergovernmental Panel on Climate Change). (2021). The Physical Science Basis. Contribution of Working Group I to the Fourth Assessment Report of the Intergovernmental Panel on Climate Change, S. Solomon, D. Qin, M. Manning, Z.Chen, M. Marquis, K. B. Averyt, M. Tignor and H. L. Miller, Eds.

James, J. Munday, C. & Reason, C. (2020). Journal of Climate: *Coupled Climate Model Simulation of Tropical–Extratropical Cloud Bands over Southern Africa.* 33(19),1-66 10.1175/JCLI-D-19-0731.1.

Jury M.R. (2013). South African Journal of Science: *Climate trends in Southern Africa.* 109,12.

Klutse, N.A.B. Abiodun, B.J. Hewitson, B.C. Gutowski, W.J. & Tadross, M.A. (2016). Theoretical and Applied Climatology: *Evaluation of two GCMs in simulating rainfall inter-annual variability over Southern Africa.* 123(3–4), 415– 436.

Kriegler, E. Edmonds, J. Hallegatte, S. Ebi, K. Kram, T. Riahi, K. Winkler, H. & Van Vuuren, D. (2014a). Climate Change: *A new scenario framework for climate change research: the concept of shared climate policy assumptions*.122 (3), 401-414.

Kriegler, E. O'Neill, B.C. Hallegatte, S. Kram, T. Lempert, R.J. Moss, R.H. & Wilbanks, T. (2012) Global Environmental Change: *The need for and use of socio-economic scenarios for climate change analysis: a new approach based on shared socio-economic pathways.* 22, 807-822. doi: 10.1016/j.gloenvcha.2012.05.005, 2012.

Kruger, A.C. & Nxumalo, M.P. (2016). International journal of Climatology: *Surface temperature trends from homogenized time series in South Africa: 1931–2015*. 37, 2364–2377.

Landman, W.A. & Beraki, A. (2012). International journal of Climatology: *Multi-model forecast skill for mid-summer rainfall over southern Africa.* 32 (2), 303–314.

Lazenby, M. J. Chadwick, R. & Wang, Y. (2018). International journal of Climatology: *Future precipitation projections over central and southern Africa and the adjacent Indian Ocean: What causes the changes and the uncertainty.* 31, 4807–4826, https://doi.org/10.1175/JCLI-D-17-0311.1.

Lee, J. Marotzke, G. Bala, L. Cao, S. Corti, J.P. Dunne, F. Engelbrecht, E. Fischer, J.C. Fyfe, C. Jones, A. Maycock, J. Mutemi, O. Ndiaye, S. Panickal, T. Zhou. (2021). Future Global

Climate: Scenario-Based Projections and Near-Term Information. In: Climate Change 2021: *The Physical Science Basis. Contribution of Working Group I to the Sixth Assessment Report of the Intergovernmental Panel on Climate Change.* Cambridge University Press.

Lee, C. C. (2017). International journal of Climatology: *Reanalysing the impacts of atmospheric teleconnections on cold-season weather using multivariate surface weather types and self-organizing maps.* 37, 3714–3730. https://doi.org/10.1002/joc.4950.

Mahlobo D.D. Ndarana Y. Grab S. & Engelbrecht F. (2018). International journal of Climatology: *Integrated climatology and trends in the subtropical Hadley cell, sunshine duration, and cloud cover over South Africa.* https://doi.org/10.1002/joc.5917.

Malherbe, J. Dieppois, B. Maluleke, P. Van Staden, M. & Pillay D.L. (2016). Natural Hazards: *South African droughts and decadal variability.* 80, 657–681.

Malherbe, J. Engelbrecht, F.A. & Landman, W.A. (2013). Climate Dynamics: *Projected changes in tropical cyclone climatology and landfall in the Southwest Indian Ocean region under enhanced anthropogenic forcing.* 40, 1267-1286. DOI 10.1007/s00382-012-1635-2.

Marumbwa, F.M. Cho-Paxie, M.A. & Chirwa, W. (2019). Physics and Chemistry of the Earth: *Analysis of spatio-temporal rainfall trends across southern African biomes between 1981 and 2016*. https://doi.org/10.1016/j.pce.2019.10.004.

Maslin, M.A., & Trauth, M.H. (2006). The first human origin and early evolution of the genus homo: Plio-Pleistocene East African Pulsed Climate Variability and Its Influence on Early Human Evolution. Springer publishers.

Micheels, A. Angela, &A. Bruchab, D. (2007). Paleoecology Paleogeography, Palaeoclimatology: *A Late Miocene climate model simulation with ECHAM4/ML and its quantitative validation with terrestrial proxy data.* 253, 251-270.

Morishima, W. & Akasaka, I. (2010). African Study Monographs: *Seasonal trends of rainfall and surface temperature over southern Africa.* 40,67–76.

Munday, C. & Washington, R. (2018). International journal of Climatology: *Systematic climate model rainfall biases over Southern Africa: Links to moisture circulation and topography*. 31, 7533–7548. https://doi.org/10.1175/JCLI-D-18-0008.1.

Muthige, M. Malherbe, J. Engelbrecht, F. Grab, S. Beraki, A. Maisha, R. & Van der Merwe J. (2018). Environmental research Letters: *Projected changes in tropical cyclones over the southwest Indian Ocean under different extents of global warming*. (13) 065019.

New, M. Hewitson, B. & Stephenson, D.B. (2006). Geophysical Research Letter: *Evidence of trends in daily climate extremes over southern and west Africa.* 111.

Niang, I. (2014). Climate Change 2014: Impacts, Adaptation, and Vulnerability. Part B: Regional Aspects. Contribution of Working Group II to the Fifth Assessment Report of the Intergovernmental panel for climate change.

Nicholson, S. (2000). Global and Planetary Change: *The nature of rainfall variability over Africa on time scales of decades to millenia*. 26, 137-158.

Nicholson, S.E. & Kim, J. (1997). International Journal of Climatology: *The relationship of the El Niño–southern oscillation to African rainfall.* 17(2), 117– 135.

Nicholson, S.E. (1997). International Journal of Climatology: *A Journal of the Royal Meteorological Society, An analysis of the ENSO signal in the tropical Atlantic and western Indian Oceans.* 17(4), 345– 375.

Nicholson, S.E. (2020). Bulletin of the American Meteorological Society: *The ITCZ and the seasonal cycle over equatorial Africa.* 337-248.

Nikulin, G. C. Jones, F. Giorgi, G. Asrar, M. Buchner, R. Cerezo-Mota, O. B. Christensen,M. D. (2012). Journal of Climate: *Precipitation climatology in an ensemble of CORDEX-Africa regional climate simulations*. 25, 6057-6078.

Nikulin, G. Jones, C. Giorgi, F. Asrar, G. Büchner, M. Cerezo-Mota, R. Christensen, O. B. Déqué, M. Fernandez, J. Hänsler, A. Van Meijgaard, E. Samuelsson, P. Sylla, M. B. & Sushama, L. (2012). Journal of Climate: *Precipitation Climatology in an Ensemble of CORDEX-Africa Regional Climate Simulations.* 25(18), 6057-6078.

O'Neill, B.C. Kriegler, E. Riahi, K. Ebi, K. Hallegatte, S. Carter, T.R. Mathur, R. & Van Vuuren, D.P. (2016). Climate change: *A new scenario framework for climate change research: The concept of shared socio-economic pathways*.122, 387-400.

Pinto, I. Jack, C. & Hewitson, B. (2018). International journal of Climatology: *Process-based model evaluation and projections over southern Africa from Coordinated Regional Climate Downscaling Experiment and Coupled Model Intercomparison Project Phase 5 models*. 38, 4251–4261. DOI: 10.1002/joc.5666.

Pohl, B. Richard, Y. & Fauchereau, N. (2007). International journal of Climatology: *Influence of the Madden–Julian oscillation on southern African summer rainfall.* J. 20, 4227–4242.

Preston-Whyte, R.A. & Tyson, P.D., (1988). The weather and climate of southern Africa. Cape Town; New York. Published by Oxford University Press.

Quaraine, K.A. Hewitson, B.Jack, C. Wolski, P. Pinto, I. &Lennard, C. (2019). American Meteorological Society: *Using Co-Behavior Analysis to Interrogate the Performance of CMIP5 GCMs over Southern Africa.* 2891-2905. DOI: 10.1175/JCLI-D-19-0472.1.

Ratnam, S.B. Behera, S. & Ratnam, J.V. (2013a). Climate Dynamics: *An index for tropical temperate troughs over southern Africa*. 41,421–441. https ://doi.org/10.1007/s0038 2-012-1540-8.

Ratnam, J.V. Behera, S.K. Masumoto, Y. & Yamagata, T. (2014). International journal of Climatology: *Remote effects of El Niño and modoki events on the Austral summer precipitation of Southern Africa*. 27,3802–3815. https://doi.org/10.1175/JCLI-D-13-00431.

Reason, C.J.C. Landman, W. & Tennant, W. (2005). Bulletin of the American Meteorological Society: *Seasonal to decadal prediction of southern African climate and its links with variability of the Atlantic Ocean.* 87(7), 941– 955.

Riahi, K. Van Vuuren, D.P. Kriegler, E. Edmonds, & J. O'Neill, B.C. (2016). The Shared Socioeconomic Pathways: An Overview, Global Environmental Change (submitted).

Richard, Y. Fauchereau, N. Poccard, I. Rouault, M. Trzaska, S. (2001). International journal of Climatology: *20th century droughts in southern Africa: Spatial and temporal variability, teleconnections with oceanic and atmospheric conditions*. 21, 873–895. http://dx.doi.org/10.1002/joc.656.

Roffe, S.J. Fitchett, J.M. & Curtis,C.J. (2019). South African Geographical Journal: *Classifying and mapping rainfall seasonality in South Africa*: *a review*. 2-17.

Roffe, S.J. Fitchett, J.M. & Curtis,C.J. (2020). International *Journal of Climatology: Investigating changes in rainfall seasonality across South Africa: 1987–2016.* 1-20.

Rouault, M. & Richard, Y. (2003). Geophysical Research letters: *Intensity and spatial extent of droughts in southern Africa*. (32)15702. doi:10.1029/2005GL022436.

Schreck, C.J. & Semazzi, F.H.M. (2004). International journal of Climatology: *Variability of the Recent Climate of Eastern Africa* 24, 681-701. https://doi.org/10.1002/joc.1019.

Shongwe, M. Oldenborgh, G. Van den Hurk, B. De Boer, B. & C. Coelho, C. (2009). International journal of Climatology: *Projected changes in mean and extreme precipitation in Africa under global warming. Part I: Southern Africa*. 22, 3819–3837.

Stocker, T. F. Edmonds, J. Thomson, A. Nakicenovic, N. Kram, T. Berkhout, F. Swart, R. Janetos, A. Rose, S.K. (2013). Technical summary. Climate Change 2013: The Physical Science Basis. Cambridge University Press. 33–115.

Tadross, M. Jack,C. & Hewitson, B. (2005). Geophysical Research Letters: *On RCM-based projections of change in southern African summer climate.*

https://doi.org/10.1029/

2005GL024460.

Taljaard, J. J. (1996). Atmospheric Circulation Systems, Synoptic Climatology and Weather Phenomena of South Africa: Rainfall in South Africa, Part 6. South Africa. Weather Bureau. Government Printer.

Taylor, J., K. Norris, M. A. C. Nicoll, E. Black, P. L. Vidale, C. M. Dunning, V. Tatayah, & C. G. Jones. (2001). Nature Ecology and Evolution: *Shifting seasonal windows: a novel climate change mechanism in a tropical wild bird population.*

Tennant, W. (2004). Geophysical Research Letters: *Considerations when using pre-1979 NCEP/NCAR reanalyses in the southern hemisphere.* (31)11112. doi:10.1029/2004GL019751.

Tennant, W.J. & Hewitson, B.C. (2002). International Journal of Climatology: *Intra-seasonal rainfall characteristics and their importance to the seasonal prediction problem.* 22(9), 1033–1048.

Todd, M. & Washington, R. (1999). Climate Dynamics: *Circulation anomalies associated with tropical-temperate troughs in southern Africa and the southwest Indian Ocean*. 15(12), 937–951.

Tyson, P.D & Whyte, R.A. (2000). The Weather and Climate of South Africa. Oxford University Press Southern Africa, Cape Town.

Tyson, P.D. (1986). Climatic Change and Variability over Southern Africa. Oxford University Press, Cape Town.

Van Vuuren, D.P. Riahi, K. Moss, R. Edmonds, J. Thomson, A. Nakicenovic, N. Kram, T. Berkhout, F. Swart, R. Janetos, A. Rose, S.K. and Arnell, N. (2012). Global Environmental Change: *A proposal for a new scenario framework to support research and assessment in different climate research communities.* 22 (1) 21–35.

Van Wilgen, B.W. & Scholes, R.J. (1997). The vegetation and fire regimes of southern hemisphere Africa. In: Fire in Southern African Savannas: Ecological and Atmospheric Perspectives. 27–46. Witwatersrand University Press, Johannesburg, South Africa.

Van Wilgen, B.W. Govender, N. Biggs, H.C. Ntsala, D. & Funda, X.N. (2004). Conservation Biology: *Response of savannah fire regimes to changing fire-management policies in a large African national park*. 18, 1533-1540.

Wolski, P. Jack, C. Tadross, M. Lennard, C. Van Ardenne, L. & Hewitson, B. (2018). Climate Dynamics: *Interannual rainfall variability and SOM-based circulation classification*. 50, 479–492.